8-9-2014

Synthesis, Characterization and Optical Properties of Conjugated Boronate-Linked Materials and Their Applications in Optical Sensing of Lewis Bases

Min Cai
University of South Carolina - Columbia

SYNTHESIS, CHARACTERIZATION AND OPTICAL PROPERTIES OF CONJUGATED BORONATE-LINKED MATERIALS AND THEIR APPLICATIONS IN OPTICAL SENSING OF LEWIS BASES

by

Min Cai

Bachelor of Science
Huazhong Normal University, 2005

Master of Science
Wuhan University, 2007

Submitted in Partial Fulfillment of the Requirements

For the Degree of Doctor of Philosophy in

Chemistry

College of Arts and Sciences

University of South Carolina

2014

Accepted by:

John J. Lavigne, Major Professor

Ken D. Shimizu, Committee Member

Stephen L. Morgan, Committee Member

Guiren Wang, Committee Member

Lacy Ford, Vice Provost and Dean of Graduate Studies

DEDICATION

This dissertation is dedicated to my family and friends. Thanks for all their help and support.

ACKNOWLEDGEMENTS

My Ph.D. life in U.S. is like an adventure, full of happiness, tears, excitement and anxiety. During this process, I would like to thank all my professors, lab-mates, friends and family members. It is their unlimited love, help and encouragement that have supported me to overcome difficulties and finish my study.

First, I would like to thank my advisor Dr. John J. Lavigne, who has given me a lot of guidance in both of my academic and personal life. For research, he gave me freedom to choose projects and taught me how to think independently, present data and write papers. For teaching, he allowed me to teach undergraduate courses and be a research mentor for undergraduates. The research and teaching experience are rewarding for my academia development. Besides, he is so considerate and has given a lot of support and help to me and my family.

Except Dr. John J. Lavigne, other committee members and professors have given me guidance and support. For instance, Dr. Ken D. Shimizu, Dr. Stephen L. Morgan and Dr. Guiren Wang, listened to my plan, proposal and dissertation defense and revised my writing. Especially, Dr. Shimizu motivated me to think and helped me calculate binding constant. During my last year, I had the opportunity to work for Dr. Sheryl L. Wiskur, while I learned computational calculations from Dr. Vitaly Rassolov in USC and Dr. Osvaldo Gutierrez in University of Pennsylvania. I would also thank Dr. Thomas A. Bryson, allowed me to teach for him for several years, which motivate my interests in undergraduate teaching.

It is so grateful to be a member in Lavigne group, because of the lovely group members. Thanks to Dr. Theppawut Israsena, Dr. Kevin L. Bicker, Dr. Laura M. Lanni, Dr. Jie Liu, Kevin Sapp, Hao Jing, and Vincenzo DiSantis, they gave me a lot of valuable suggestions for group meetings and research. I give special thanks to my great lab-mates and friends, Dr. Jing Sun and Dr. Xiaoning Li. The current members of Shakena Daniel, Matthew DiCarmine, Anna Veldkamp, Dr. Kathleen O'Connell, Erin E. Gatrone, and Tanya Hundal, are so nice and help me a lot. The undergraduate Anthony Minh Le help me with research. I really enjoy the group parties and activities with all group members.

Other friends also deserve my thanks. During my early years in USC, Dr. Yuewen Xu, Dr. Qingbiao Zhao, and Dr. Jing Du helped me adjust to the Ph.D. life in U.S. Yan Zhang, Rui Tan and his wife Lanlan Meng gave me a lot of help during my last year. Besides, I really enjoy the fun time with Dr. Jing Sun, Dr. Xiaoning Li, Chunxue Wang, and other friends. I would also thank Dr. Yan Lin, Dr. Ying Tan, Yan Zhang and Chunyan Yang. They were not in USC, but we shared our thoughts and happy moments.

I would like to thank my family, which is the most important part in my life. My dad has been dead for four years because of cancer, but I love and miss him so much. I want to thank my great mom, who has taken care of my dad for a long time. Even though she was not in U.S., she still gave me a lot of support during my study. I am really appreciated that my husband Wenjun Jiang has entered my life during my most difficult time. He gives me a lot of love and encouragement. And I will thank my boy, Alex Jiang, who is a gift that totally changes my life.

Last, I will thank the Royal Society of Chemistry. Part of Chapter 2 is reproduced by permission of The Royal Society of Chemistry.

ABSTRACT

Organoboron compounds, with Lewis acidic boron centers, have been emerged as an important class of materials, especially in the area of chemical sensors. Herein, boranes and boronate esters in the sensing perspective were overviewed in Chapter 1. Examples of synthesis and sensing applications of boron-containing conjugated polymers were highlighted.

Boronate ester formation provides the advantages of facile synthesis, tunable optical properties, enhanced stability and planar geometry. Thus, boronate esters, especially dioxaboroles, were proposed to use as alternatives of boranes to design better sensors for Lewis bases. Based on the previous investigation of fluorenyl bis- and poly-dioxaboroles by our group, the binding mechanism of dioxaborole based sensors for Lewis bases were discussed in Chapter 2. The binding between dioxaboroles and fluoride was tunable, sensitive, reversible and cross-reactive. The selected fluorenyl bis(dioxaborole)s were employed in cross-reactive sensor arrays for anion differentiation in Chapter 3.

Inspired by the extensive research of donor-π-acceptor (D-π-A) boranes, triphenylamino group was attached to borole moiety to form two families of D-π-A boronate esters. Synthesis, characterization, structure and opto/electronic property relationship and sensing applications were investigated in Chapter 4 and 5.

Based on the previous work of boronate ester-linked materials in sensors, the future directions were predicted in Chapter 6. The new fluorenyl boroles, D-π-A boroles, cruciform and metal-chelated boronate esters were explored.

TABLE OF CONTENTS

LIST OF TABLES

LIST OF FIGURES

CHAPTER 1

OVERVIEW OF ORGANOBORON MATERIALS IN CHEMICAL SENSORS

1.0 INTRODUCTION

With regard to sensing applications in industry, medicine and the environment, the need for better sensory materials is urgent.[1-3] Efforts have been made to develop materials, which can be easily synthesized with tuned properties and can also detect analytes with a high selectivity and sensitivity.[4] Among the π-conjugated compounds, conjugated polymers with the recognition motif in the main-chain may provide a possibility as better sensory materials.[5-11]

Organoboron compounds, with Lewis acidic boron centers, extend π-conjugation. These compounds, including boranes and boronate esters, have emerged as an important class of materials, especially in the area of chemical sensors.[12] Among them, boranes are relatively well-studied and used to detect Lewis bases, based on the hard Lewis acid-base interactions.[13-27] Their sensing modes can be easily tuned by charge transfer, geometric changes, and metal chelation.[17-27] Boronic acid is known to detect sugars, based on covalent but reversible boronate ester formation.[28-35] This interaction has recently been used to detect hydrogen peroxide[36] and Lewis bases[37-39].

Herein, organoboron materials from the sensing perspective will be overviewed. Before that, the background of chemical sensors, especially the optical sensors will be briefly introduced. Conjugated polymers as the optical transducers in sensors will be

discussed. Then, organoboron compounds of boranes and boronate esters will be discussed in detail. Interesting examples of synthesis and sensing applications of boron-containing conjugated polymers will be highlighted.

1.1 Chemical Sensors

Chemical sensors are analytical devices that convert chemical information such as composition and/or concentration into a physical signal.[1] Sensors usually consist of two units: recognition motifs and signal transducers. Recognition motifs bind with and/or recognize analytes, while signal transducers transform the recognized information into an optical, electrochemical or electric signal (**Figure 1.1**). Due to their simple operation, low cost, and compact size, chemical sensors have drawn great attention from both academic and practical usage, including industry, medicine and environmental monitoring.[2]

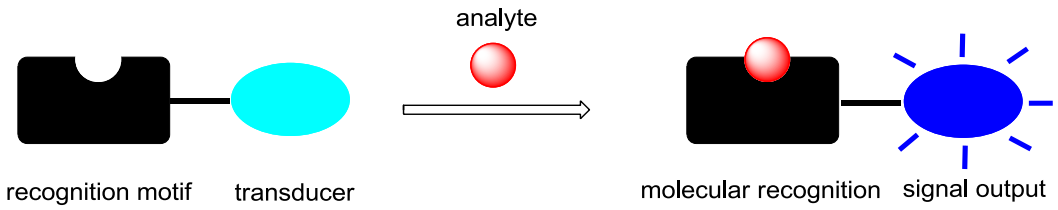

Figure 1.1 Principle and composition of chemical sensors.

As a branch of chemical sensors, optical sensors employ transduction techniques based on absorbance and fluorescence.[3] These optical sensing methods have the good attributes, including fast response, low cost, and high selectivity and sensitivity, making them ideal for use in chemical sensors.[4] In these sensors, sensory materials as the

recognition motif and/or transduction platform have drawn great attention. Efforts have been made to discover better materials with the following attributes: (1) easy to synthesize; (2) optical properties can be easily tuned; and (3) can be used to detect the analyte with a high selectivity and sensitivity.[4]

1.2 Conjugated Polymers

Conjugated polymers (CPs) have attributes that make them better sensing materials in optical sensors.[5,6] For instance, CPs have excellent optical properties, which can be easily tuned by modification of their repeat units. Moreover, these optical properties are quite sensitive to external stimuli, including solvent, temperature, and charge changes. Thus, CPs can act as transducers in sensors, transferring a chemical event into optical (fluorescent or colorimetric) signal with a high sensitivity.

As early as 1995, the Swager group explored the origins of highly sensitive CPs.[7] They found that the fluorescence of poly(*p*-phenylene ethynylene) **1.1** with a dibenzocrown ether repeat unit could be easily quenched by the cationic paraquat **1.2**. The quenching efficiency of polymer was 65 times that of monomer. They attributed the enhanced fluorescence quenching to the "molecular wire effect" (**Figure 1.2**). In CPs, photons are excited to generate electron-hole pairs, which migrate along the main chain of polymer. The cationic paraquat traps an electron-rich dibenzocrown ether unit by an electrostatic interaction. Due to the fast energy migration, the fluorescence of the polymer is quenched by electron transfer, amplifying the quenching efficiency.

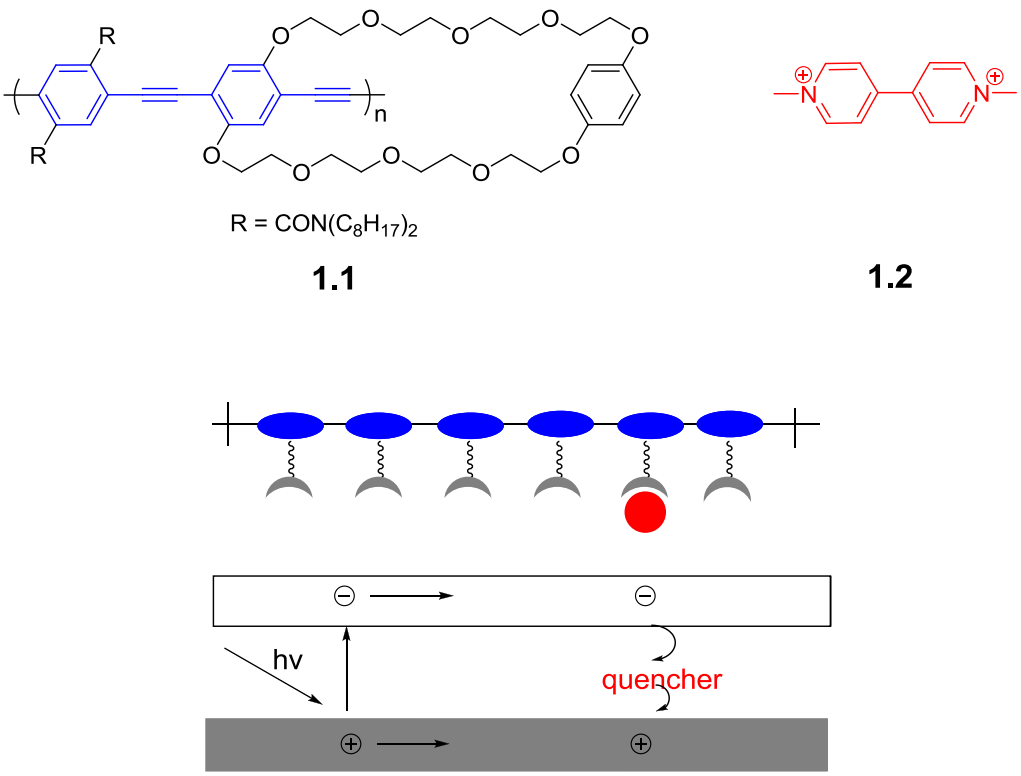

Figure 1.2 "Molecular wire effect" of conjugated polymers.[7]

Based on the above features, CPs have been used as signal transducers in chemical sensors.[5,6] Within these sensors, recognition motifs can be incorporated into the side-chains or embedded in the main-chains of polymers. In the peripheral side-chain approach (**Figure 1.3a**),[8] the electronic properties and/or main-chain conformation are perturbed when a target binds to the recognition motifs, resulting in optical change.[9] For instance, the Lavigne group attached a carboxylic acid recognition unit to the side chains of poly(thiophene) **1.3**. The added diamine analytes (such as 1,2-ethylenediamine **1.4**) had an interaction with the carboxylic acid, leading to the main-chain twisting, leading to a color change. Since each diamine or polyamine had a unique chromic response, the

cross-reactive poly(thiophene) polymers could identify structurally similar amines or biogenic amines, creating a colorimetric sensor for food spoilage.[10]

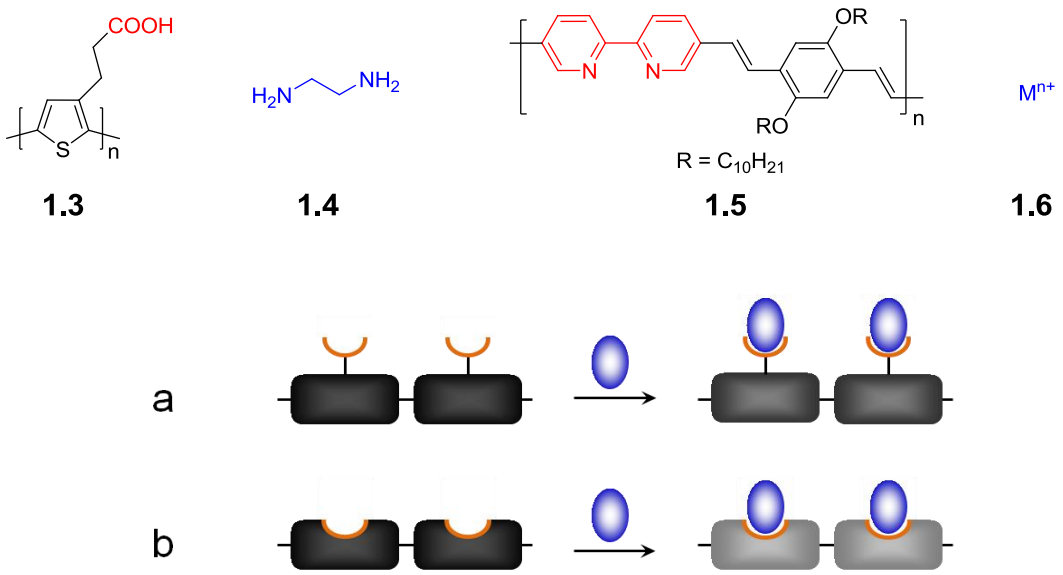

Figure 1.3 Conjugated polymer-based chemical sensors in (a) side-chain and (b) main-chain approaches (black: π-conjugation system, red: recognition motif, blue: analyte, gray: π-conjugation system interrupted by analytes binding).[8] Reproduced by permission of The Royal Society of Chemistry.

In the main-chain approach (**Figure 1.3b**),[8] the binding sites are embedded in the polymer backbone. The binding of analytes changes the π-conjugation of the polymer backbone. For example, the recognition motif of 2,2'-bipyridine was incorporated into the main-chain of a phenylene-vinylene-based polymer **1.5**. The metal ions analytes **1.6** that bound to 2,2'-bipyridine forced the polymer to be planar and highly ionochromic. Thus, this polymer could be used as a promising ion-responsive material.[11] Although the side-chain approach is common, the main-chain approach has a direct impact on π-conjugation, yet is rarely studied. It would be anticipated that analyte binding directly to

the signal transducer would afford an enhanced signal generation, thus providing a more sensitive sensing strategy.

1.3 BORANES

Organoboron compounds, especially boranes, have recently emerged as an important class of materials due to their interesting optical and electronic properties.[12] With an empty p orbital, the electron-deficient boron center can act as a Lewis acid or electron acceptor, which shares the electrons from neighboring π systems and extends π-conjugation. When connected to an electron donor, a borane can form a donor-π-acceptor system, resulting in intramolecular charge transfer. Thus, boranes have wide applications in several areas, including chemical sensors for Lewis bases, blue emitters and charge-transporters in organic light-emitting devices (OLEDs), non-linear optics and two-photon emitting materials.[12] Herein, sensing applications of borane-based small molecules and polymers will be discussed in detail.

1.3.1 BORANES IN SENSORS

Boranes with a Lewis acidic boron center extend π-conjugation by interaction of its vacant p orbital with the electrons from the neighboring π-systems, such as aryl rings. Sensing applications of boranes are usually based on Lewis acid-base interactions between boron centers and Lewis bases. As shown in **Figure 1.4**, the added Lewis base or nucleophile coordinates with the boron and interrupts π-conjugation, resulting in a geometric change of the boron moiety from trigonal planar to tetrahedral. The optical properties are accordingly altered, including a blue shift in absorption wavelength,

decrease in absorbance and/or quenching of fluorescence.[12b] Based on this, sensors of borane-based small molecules as well as polymers have been developed and will be discussed below.

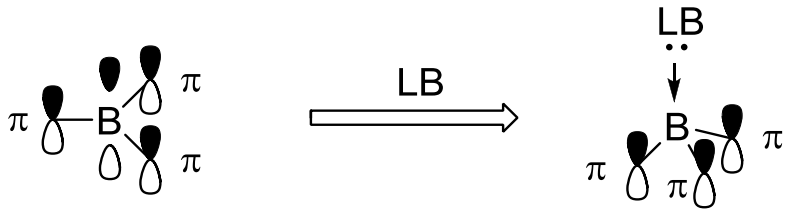

Figure 1.4 Principle of boranes sensing Lewis bases (π refers to π-conjugated system and LB refers to Lewis base).[12b]

1.3.1.1 BORANE-BASED SMALL MOLECULES

The sensing applications of boranes started with fluoride detection, which took advantage of the well-known Lewis acid-base interactions between boron and fluoride. The seminal work by the Yamaguchi group developed a colorimetric fluoride sensor based on trianthrylborane.[13] Tri(9-anthryl)borane **1.7** was synthesized from the organometallic reaction between 9-anthryllithium and BF_3. When fluoride was added, the extended π-conjugation through the p orbital on boron was interrupted. Thus, the absorption band of borane blue shifted from 470 nm to 360-410 nm. The color changed accordingly from orange to colorless, which was visible to the naked eye. Upon the addition of water, the resultant fluoroborate was returned to the borane, which confirmed the binding reversibility of this system. Tri(9-anthryl)borane showed a selective binding to fluoride with a binding constant of $(2.8 \pm 0.3) \times 10^5$ M^{-1}, while it showed a smaller binding constant for AcO^- and OH^- of 10^3 M^{-1} and no binding response to larger anions such as Cl^-, Br^-, I^-, ClO_4^- and BF_4^-.

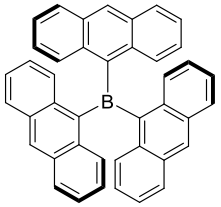

1.7

Figure 1.5 Structure of borane used for sensing fluoride.[13]

1.3.1.2 POLY(BORANE)S

Conjugated polymers have been emerged as important sensory materials, mostly due to their signal amplification from the molecular wire effect.[7] Incorporation of boron centers in the main-chain, poly(borane)s have been investigated in sensing Lewis bases, such as fluoride, cyanide and amines. The first poly(borane) **1.8** was reported by the Chujo group to sense fluoride.[14] The polymer (**Figure 1.6**) was synthesized by the hydroboration polymerization of diyne. The resultant polymer in chloroform showed an absorption maximum at 377nm, which showed a blue-shift upon the addition of fluoride. However, the polymer did not response to large anions, including Cl^-, Br^- and I^-, indicative of the strong hard Lewis acid-base interaction between boron and fluoride. The addition of 0.5 equiv. of fluoride could quench fluorescence of the blue emissive polymer, confirming its signal amplifying ability.

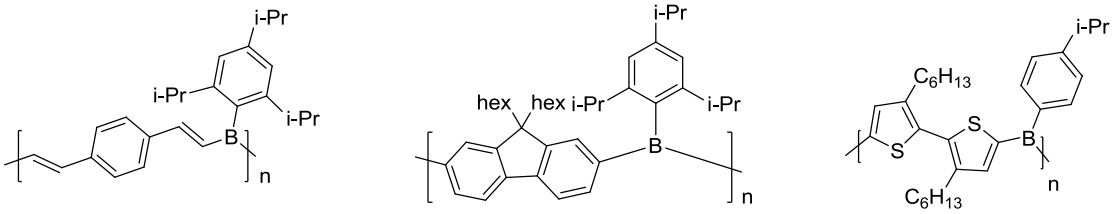

1.8 **1.9** **1.10**

Figure 1.6 Structures of poly(borane)s[14-16] used for sensing Lewis bases.

Apart from fluoride, poly(borane)s can be used to detect other anions, such as cyanide.[15] For example, poly(fluorenylborane) **1.9** (**Figure 1.6**) was cross-reactive to fluoride and cyanide.[15] The polymer was synthesized by an organometallic polycondensation between fluorenyl dibromoborane and fluorenyl ditin, followed by post-modification with an arylcopper. Upon the addition of fluoride or cyanide, the absorption maxima of the polymer blue-shifted and the fluorescence intensity at 403 and 425 nm decreased while a new band at 475 nm developed, due to the intramolecular charge transfer from the electron-rich borate to the electron-deficient borane.

In addition to anions, poly(borane)s can be used to detect amines.[16] For example, the thiophene functionalized poly(borane) **1.10** (**Figure 1.6**) was developed by the Jäkle group.[16] The polymer was synthesized by an organometallic polycondensation between aryl boron dibromide and distannylated bithiophene. Complexation of pyridine to the polymer gave an upfield chemical shift in the ^{11}B NMR spectra, confirming the geometric change of boron moiety from a trigonal planar to tetrahetral. The coordinated pyridine was removed by the addition of $B(C_6F_5)_3$, which demonstrated the reversible binding between boron and pyridine. The absorption and fluorescence titrations of pyridine to the

polymer showed a blue-shift of the absorption maximum and fluorescence quenching. Interestingly, sterics and electronics influenced the sensing behaviors.

1.3.2 DONOR-Π-ACCEPTOR BORANES

Boranes with electron-deficient boron centers can also act as electron acceptors. By linking with electron donors such as amino groups, boranes can form donor-π-acceptor (D-π-A) systems. These systems are highly polarized when excited with light, leading to intramolecular charge transfer.[12] Upon the binding of Lewis base analytes to the boron centers, the optical properties, especially fluorescence, is changed. Thus, D-π-A boranes have promising applications as chemical sensors for Lewis bases.

According to the relative positions of donor and acceptor, these systems have three general structures.[12] As shown in **Figure 1.7**, the donor and acceptor can be located at the terminals of a π-system to form a linear or a curved U-shaped structure. The donor and acceptor can also be at the lateral positions of a π-system to form a cruciform structure. Due to their diverse structures, optical properties and sensing abilities of D-π-A boranes are easily tuned. Herein, some interesting examples of sensors based on D-π-A boranes will be highlighted.

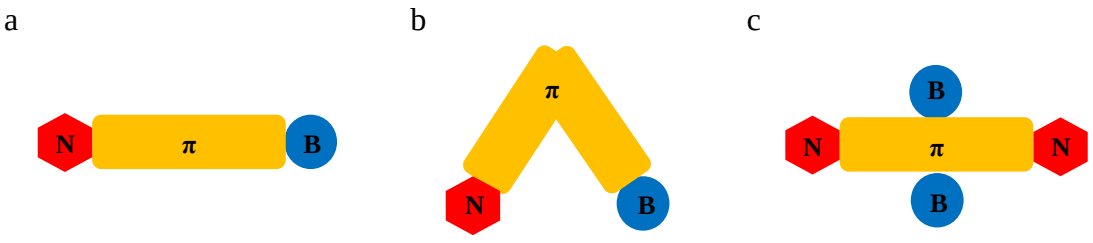

Figure 1.7 D-π-A boranes with a (a) linear structure, (b) U-shaped structure, and (c) cruciform structure.[12]

1.3.2.1 LINEAR D-π-A BORANES

A typical example of linear D-π-A triarylboranes was reported by the Wang group.[17] In D-π-A borane **1.11** (**Figure 1.8**), triarylamine acts as an electron donor and mesitylborane acts as an electron acceptor. These groups are linked by a biphenyl group. The donor was attached by Ullmann condensation, while the acceptor was attached by organolithium chemistry.[18] The resultant borane showed a fluorescent solvent response, due to the intramolecular charge-transfer from the amine to the boron moiety. Upon fluoride binding, the fluorescence of the borane was quenched. Fluoride coordination increased the electron-density on the boron center and turned off charge-transfer. The binding was selective to fluoride, because the bulky mesityl groups around boron blocked large analytes, such as chloride or bromide. Similar sensors based on D-π-A boranes were also designed by modification of linkers and electron donors. For instance, stilbene[19] or pentaphenylene[20] were used as linkers. Porphyrin[21] or tetrathiafulvalene[22] were used as electron donors.

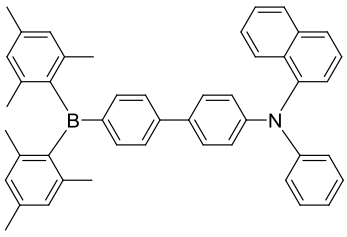

1.11

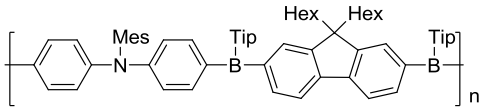

1.12

Figure 1.8 Structures of linear D-π-A borane[17] and poly(borane)[23] for sensing fluoride.

Linear D-π-A borane can also be incorporated in conjugated polymers. For example, the Jäkle group reported D-π-A poly(borane) **1.12**.[23] The polymer (**Figure 1.8**) was synthesized by the organometallic polycondensation of an arylamino- ditin monomer

and a fluorenyl- diboron monomer. Then, the bulky triisopropylphenyl group on boron was post-modified for protection. The resultant polymer had a relatively high molecular weight (M_w = 13,000). Moreover, it showed an intense emission depending on the solvent polarity, due to intramolecular charge-transfer. The addition of small anions, such as fluoride or cyanide, allowed the absorption maximum to be blue-shifted and the fluorescence quenched. However, large anions such as chloride, bromide or nitrate did not result in any optical change to the polymer.

Interestingly, the titration of cyanide showed a distinct two-step binding to the polymer. First, one equiv of cyanide bound to borons with a higher Lewis acidity. The absorption maximum blue-shifted from 422 nm to 405 nm, indicating a charge-transfer with a higher energy. During this process, the fluorescence of the polymer at 459 nm was quenched when $\leqslant$ 0.3 equiv of cyanide was added. After that, a new emmisive band appeared at 550 nm and then blue-shifted to 510 nm, due to the charge-transfer from the formed tetracoordinate boron to the neighboring tricoordinate boron. Second, more than one equiv of cyanide bound to the other boron. The new absorption bands appeared in the region from 270 to 325 nm and fluorescence at 510 nm was quenched, indicating that the intramolecular charge-tranfer was turned off.

The Lewis-base sensing modes of D-π-A boranes can be easily tuned by incorporation of linker chelating metals.[24] For instance, the Wang group[24] designed the Pt(II)-borane complex **1.13** (**Figure 1.9**). The complex was synthesized from the organometallic reaction between 2,2'-bipy lithium salt and $BMes_2F$, then the resultant ligand coordinated with Pt(II). After metal chelation, the Lewis acidity of the borons was

enhanced, which was confirmed by electrochemical methods. The complex showed a red color, due to the metal-to-ligand charge transfer (MLCT).

The fluoride titration showed a two-step binding to the boron sites in **1.13**. The addition of ~1 equiv of fluoride changed the color from red to orange, while the addition of ~2.5 equiv of fluoride changed the color further to light yellow. The absorption maxmium was accordingly blue-shifted, because fluoride binding increased the LUMO energy of the ligand and turned off MLCT. Binding constants of $K_1 \geqslant 10^9\ M^{-1}$ and $K_2 = 10^6\ M^{-1}$ were measured by absorption titration. Although **1.13** was not fluorescent, complex **1.14** (**Figure 1.9**) with one boron center changed to amine showed "turn-on" fluorescent response to fluoride.

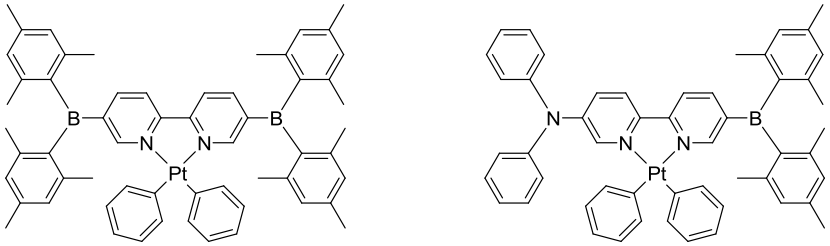

1.13 **1.14**

Figure 1.9 Structures of metal chelated D-π-A boranes[24] for sensing fluoride.

1.3.2.2 U-SHAPED D-ΠΠ-A BORANES

Apart from the linkers and donor-acceptor pairs, charge-transfer is also dependent on the molecular geometry, which can be used to tune the sensing modes. For example, the Wang group[17] synthesized the U-shaped D-π-A borane **1.15** (**Figure 1.10**). It showed solvatochromism by fluorescence, resulting from the intramolecular charge-transfer from amine to boron moiety through-space. Upon the addition of fluoride, the emission

wavelength blue-shifted from 504 to 453 nm, while fluorescent intensity was enhanced. The emissive color was accordingly changed from green to blue, making it an unusual "turn-on" sensor for fluoride. This occurred because the fluoride binding to boron interrupted the charge-transfer and activated the highly emissive amine moiety. ^{19}F NMR spectrum showed the binding ratio between boron and fluoride was 1:1. Fluorescent titration indicated that the binding constant was $> 4.0 \times 10^4$ M^{-1}. Large ions, such as chloride, bromide or iodide, did not compete with the fluoride sensing. The sensor also showed reversibility, when water was used to extract fluoride. In addition to U-shaped D-π-A boranes, V-shaped systems[25] were also developed to sense fluoride.

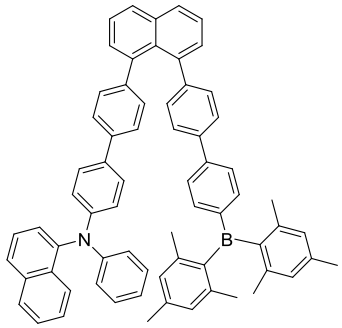

1.15

Figure 1.10 Structure of U-shaped D-π-A borane[17] used to sense fluoride.

1.3.2.3 CRUCIFORM D-Π-A BORANES

Cruciforms, possessing spatially separated molecular obitals, have recently been developed as a new class of sensing materials. When analytes bind, either the HOMO or LUMO of cruciforms will change, leading to a dramatic optical change, especially in their emission properties. Pioneered by the Bunz group, cruciforms have been studied as a sensing platform to detect acids, metal ions, anions, and amines.[26]

As mentioned before, nitrogen and boron are an excellent electron donor-accepter pair. The Zhao group[27] put the LUMO located boron moiety and HOMO located amine moiety in a perpendicular position to form a cruciform-type D-π-A borane **1.16** (**Figure 1.11**). The borane cruciform was synthesized by a Sonogashira coupling reaction, followed by a Suzuki coupling reaction. The resultant borane showed an emission dependant on the solvent polarity, due to intramolecular charge-transfer from the amine to the borane moiety. Upon the addition of fluoride, the fluorescence at 540 nm decreased, while the fluorescence at 442 nm increased. Accordingly, the emissive color changed from yellow to blue. The large blue-shift of the emission wavelength (up to 100 nm) was because the fluoride binding increased the LUMO energy and turned off charge-transfer. The binding constant was calculated to be 3.27×10^{10} M^{-2}. The cruciform also showed a response to fluoride in the solid-state.

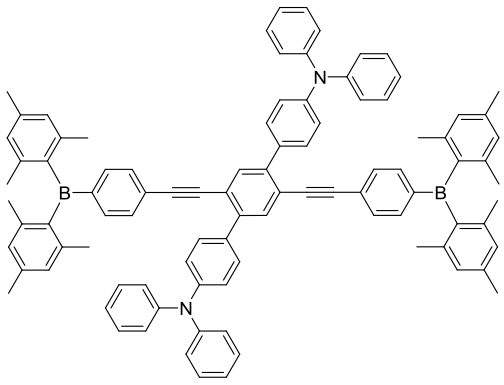

1.16

Figure 1.11 Structure of cruciform D-π-A borane for sensing fluoride.

1.3.3 CONSIDERATIONS

Boranes, with Lewis acidic boron centers, have emerged as an important class of optoelectronic materials. The optical and/or electronic properties of these materials can easily be tuned by the modification of their π-systems. When attached to an electron-donor such as an amine, boranes form D-π-A systems resulting in intramolecular charge-transfer.[12] The structures of D-π-A boranes can be altered by modification of linkers, metal chelation, and molecular geometry, leading to intriguing optical and/or electronic properties, including absorbance, fluorescence, phosphorescence, and/or electrochemistry.[12] These properties can be utilized to develop versatile optical sensors for Lewis bases, based on the Lewis acid-base interactions.[13-27]

However, boranes are usually synthesized by organometallic chemistry, under stringent conditions without water and oxygen and require tedious workup procedures using column chromatography. Moreover, these materials are relatively unstable toward water and oxidation, because of their highly electron-deficient boron centers.[12] Thus, bulky substituents, such as 2,4,6-trimethylphenyl (Mes) groups are often incorporated at the ortho- position on arylboranes to prevent nucleophilic attack. The employed bulky groups limit sensing to small Lewis bases, such as fluoride and cyanide. However, they prevent access to larger Lewis bases and lower the sensing abilities. Thus, better materials other than boranes are required to develop sensors for Lewis bases.

1.4 BORONATE ESTERS

Boronic acid reacts with diols to form boronate esters.[28] This reaction, with its covalent yet reversible nature, provides a tool to detect sugars.[35] It has recently drawn

great attention in the building of boronate-linked complex materials, such as polymers[29-32] and covalent organic frameworks[33,34]. Compared with the previously mentioned boranes, boronate esters have the advantages of facile synthesis, tuned optoelectronic properties, enhanced stability and planar structures. Thus, boronate esters have been explored as the sensory materials for detecting hydrogen peroxide[36] and Lewis bases[37-39]. In this section, some interesting examples of boronate-linked materials will be highlighted. Optical sensors based on boronate esters will also be discussed.

1.4.1 BORONATE-LINKED MATERIALS

Boronic acids reacts with 1,2- or 1,3- diols to produce boronate esters (**Figure 1.12**).[28] The resultant water is usually removed to push the reversible reaction to completion. The formation of boronate esters has been used to assemble complex materials, such as polymers and colavent organic frameworks, which will be discussed in detail herein.

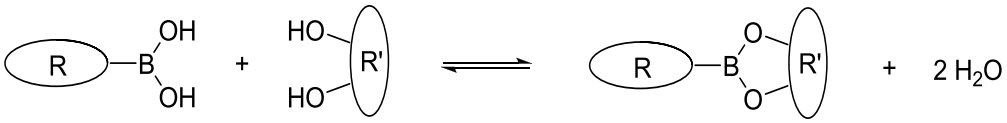

Figure 1.12 Formation of boronate esters from boronic acid and diol.[28]

1.4.1.1 BORONATE-LINKED LINEAR POLYMERS

After intensively researching oligomeric boronate esters,[29] the Lavigne group incorporated the boronate ester moiety into the main-chain of a linear polymer poly(dioxaborolane) **1.17**. The dioxaborolane repeating unit refers to the non-aromatic

six-membered cyclic boronate ester.[30] As shown in **Figure 1.13**, polymer **1.17** was synthesized by a condensation reaction between fluorenyl diboronic acid and pentaerythritol in toluene, with the removal of water by a Dean-Stark trap. It was soluble in aprotic solvents, such as toluene, dichloromethane and hexane. Gel permeation chromatography (GPC) determined that the polymer had an M_w of 28,000 with 58 repeat units and was stable for days in dry dichloromethane. The polymer could be easily modified by changing the ratio of diboronic acids and diols, reaction time, or post-polymeriztion process. The polymer was shortened under hydrolytic conditions, while it was self-repaired by storage under reduced pressure.

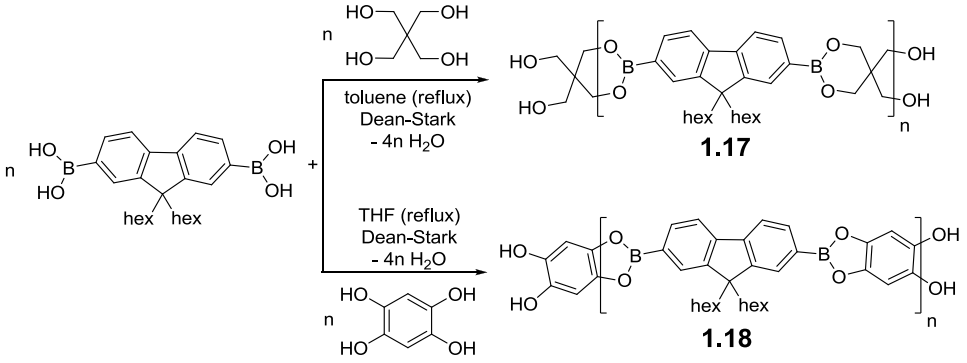

Figure 1.13 Synthesis of poly(dioxaborolane)[30] and poly(dioxaborole)[31].

Apart from the self-repairing poly(dioxaborolane), poly(dioxaborole) **1.18** was also reported by the Lavigne group.[31] The dioxaborole repeating unit refers to the aromatic five-membered cyclic boronate ester. As shown in **Figure 1.13**, polymer **1.18** was synthesized by a facile condensation between fluorenyl diboronic acid and 1,2,4,5-tetrahydroxybenzene. After the azeotropic removal of water, the polymer was obtained with a high yield of ~ 90% in 30 min. It was soluble in non-polar solvents, including chloroform, dichloromethane, and THF. GPC analysis showed that the polymer had an

M_w of ~25,000 and PDI of 2.4. Polymers with higher molecular weights could easily be synthesized by lengthening the reaction times. However, the resultant polymers had limited solubility in organic solvents. Compared to the diester or the non-conjugated poly(dioxaborolane), the conjugated poly(dioxaborole) had a red-shifted absorption and emission wavelengths. These results indicated that there was an extended π-conjugation through the backbone of the polymer, due to the overlap of the vacant p orbital on boron with the lone pairs on the neighboring oxygen atoms. The effective conjugation length was calculated to be 3-5 bridging repeat units. This polymer had potential applications as a blue-emissive material in OLEDs.

1.4.1.2 BORONATE-LINKED COORDINATION POLYMERS

Based on the coordination between boron and amine, the boronate-linked coordination polymer **1.19** was developed by the Severin group.[32] The polymer was synthesized by a three-component one-pot reaction (**Figure 1.14**). Substituted phenyl boronic acid, 1,2,4,5-tetrahydroxybenzen and 1,2-bis(4-pyridyl)ethylene were mixed in a 2:1:1 ratio and heated in benzene. After the reaction mixture was cooled down, the dark-purple self-assembled polymer precipitated. The polymer was dissolved in hot chloroform, but it fell apart to give the pyridyl linker and boronate diester, due to the weak dative B-N bond. However, if it was cooled down, it went back to the precipitated polymer, indicating the reversibility of the process. Computational studies showed that the intense color was the result of the intramolecular charge-transfer from tetraoxobenzene to the pyridyl linker.

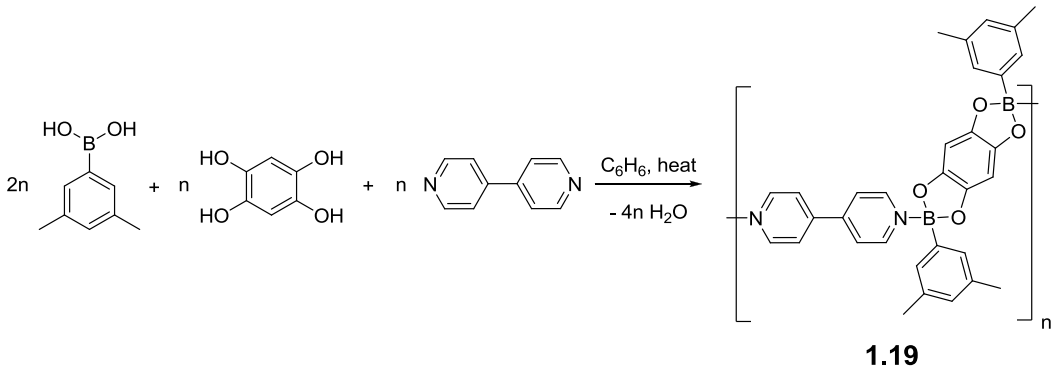

1.19

Figure 1.14 Synthesis of coordinated poly(boronate).[32]

1.4.1.3 COVALENT ORGANIC FRAMEWORKS

Apart from polymers, boronate ester formation can be used to build larger systems, such as covalent organic frameworks (COFs). COFs are porous materials, which have potential applications in gas storage, catalysis, and separation. The Yaghi[33] and Lavigne group[34] did seminal work in the COF area. For example, the Lavigne group synthesized COF-18Å **1.20** with pores of 18 Å diameters. The compound was obtained by the dehydration reaction of benzene-1,3,5-triboronic acid and 1,2,4,5-tetrahydroxybenzene which were refluxed in 2 % methanol/THF for three days (**Figure 1.15**). After workup, the product was obtained with a yield of 85-95%. COF-18Å showed a highly crystalline network, with thermal stable pores (> 500 ℃), high surface areas (1260 cm^2/g) and a microspore volume (0.29 cm^3/g).

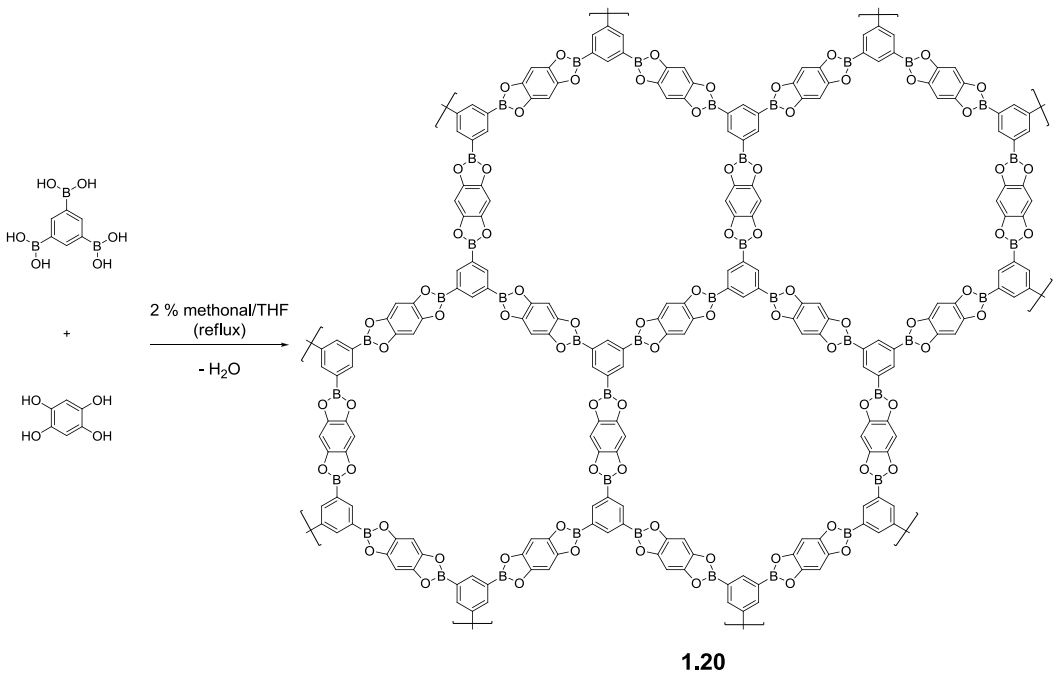

Figure 1.15 Synthesis of COF-18 Å.[34]

1.4.2 BORONATE ESTERS IN CHEMICAL SENSORS

Apart from use as building blocks for complex materials, the formation of boronate esters can be applied in the sensing area. Well-known examples are to sense sugars, using the covalent but reversible interaction between boronic acids and *cis*-diols.[35] Recently, boronate esters have been used to detect hydrogen peroxide, due to the oxidative deprotection of boronates by hydrogen peroxide.[36] Similar to boranes, boronate esters are also reported to detect Lewis bases, because of the Lewis acidic boron centers.[37-39] In this section, interesting examples of boronate esters in chemical sensors will be highlighted.

1.4.2.1 SENSING SUGARS

The formation of boronate esters provides a sensing tool for saccharides, which are difficult to detect in aqueous solutions.[35] The first fluorescent sensor for sugars was reported by the Czarnik group (**Figure 1.16**).[35] Anthrylboronic acid **1.21** was emissive at 416 nm, due to the fluorescent anthracene moiety. When fructose was added, fructose bound to the boronic acid, lowering its pK_a from 8.8 to 5.9. In aqueous solution (pH = 7.4), the boronate anions were dominant The boronate anions were non-fluorescent, due to photoinduced electron-transfer (PET) quenching. Thus, anthrylboronic acid could be used to detect fructose by the fluorescent turn-off mechanism.

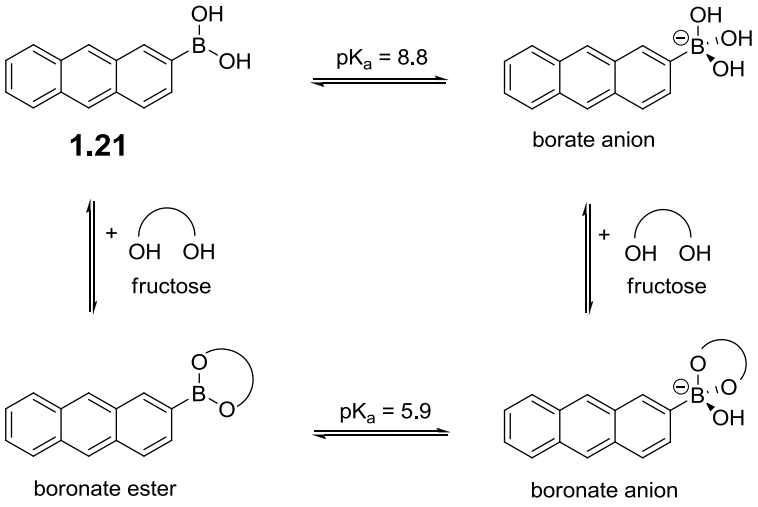

Figure 1.16 Principle of the first fluorescent sensor for sugars based on anthrylboronic acid.[35]

1.4.2.2 SENSING HYDROGEN PEROXIDE

Apart from sugars, boronate esters can be used to detect hydrogen peroxide, which can be produced from peroxide explosives by UV or acid-catalyzed decomposition.[36] The Trogler group[36] reported the use of functionalized poly(boronate)

1.22 to detect vapor and liquid H_2O_2. The polymer was synthesized by the transesterification polymerization between 3',6'-bis(pinacolatoboron)fluoran and pentaerythritol in MeOH-H_2O at 50 °C for two days (**Figure 1.17**). After workup, the polymer was obtained in a good yield of 75%. Molecular weight was determined to be 10,000 by GPC with a PDI of 1.5. As a thin-film, the polymer was non-fluorescent. When exposed to 2.9 ppm of H_2O_2 vapor for 3.5 h, the fluorescent intensity at 510 nm increased eight-fold, due to the oxidative deprotection of boronate ester by hydrogen peroxide and the release of fluorescent fluorescein. The detection limit was 3 ppb after 8 h of exposure to hydrogen peroxide. In addition, the polymer could also detect 30 ppm of H_2O_2 in water by the solution spot test after 3s.

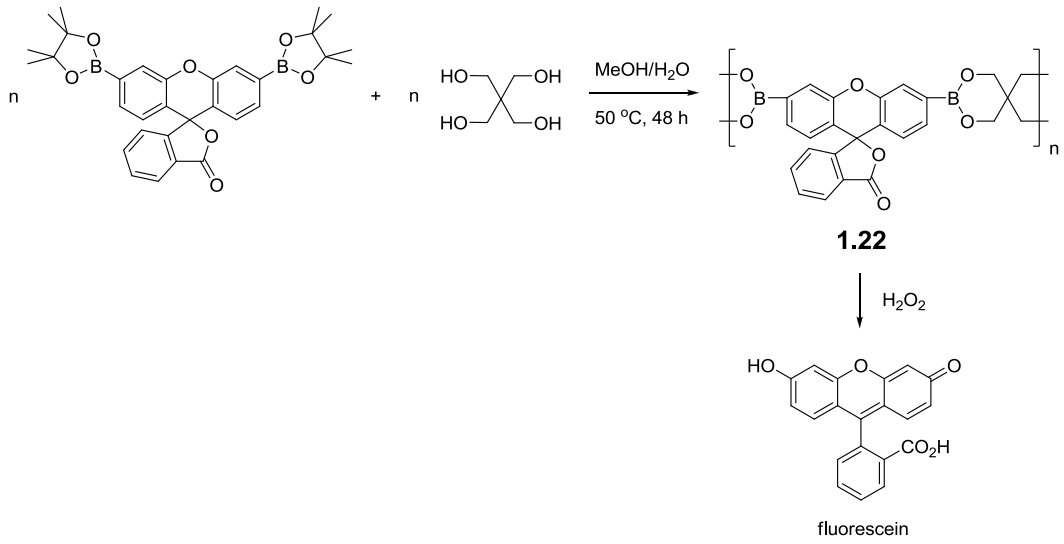

Figure 1.17 Synthesis of the functionalized poly(boronate)[36] used for sensing hydrogen peroxide.

1.4.2.3 SENSING LEWIS BASES

Similar to boranes, boronate esters have been reported as sensory materials for Lewis bases. For example, the James group developed bis(bora)calixarene **1.23** (**Figure 1.18**) as a fluorescent fluoride sensor.[37] The compound was synthesized by an organometallic reaction between tetralithiated calixarene and dichlorophenylborane. Calixarene was a rigid scaffold, providing the bidentate boron centers for fluoride. Thus, the addition of fluoride quenched the fluorescence of 10^{-2} M bis(bora)calixarene in chloroform. However, chloride or bromide made no significant optical change to bis(bora)calixarene, indicating the selective binding with fluoride. The binding constant for the fluoride complex was calculated as $\log K = 6.3 \pm 0.4$.

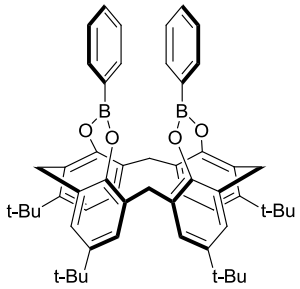

1.23

Figure 1.18 Structure of bis(bora)calixarene[37] for sensing fluoride.

Similarly, the Baumgartner group[38] developed bis(boryl)dithienophosphole **1.24** as a sensory material for fluoride. As shown in **Figure 1.19**, dithienophosphole was lithiated by LDA and borated, followed by an oxidation by tert-butylhydroperoxide. The generated phosphole showed absorption maximum at 398 nm and emission maximum at 452 nm. The addition of fluoride made the absorption and emission maximum red shift to 415 nm and 485 nm, respectively. Chloride, bromide and iodide did not make

significant response to phosphole, indicating the binding selectivity of fluoride. Fluorescence titration showed the binding constants of $\log K_1$ = 4.02(8) and $\log K_2$ = 3.79(8). Fluoride at a low concentration as ppm could be detected by the fluorescent phosphole, while fluoride as low as 10^{-5} M could be recognized by the naked eye, upon the irradiation at 366 nm. A similar example can also be found in literature.[39]

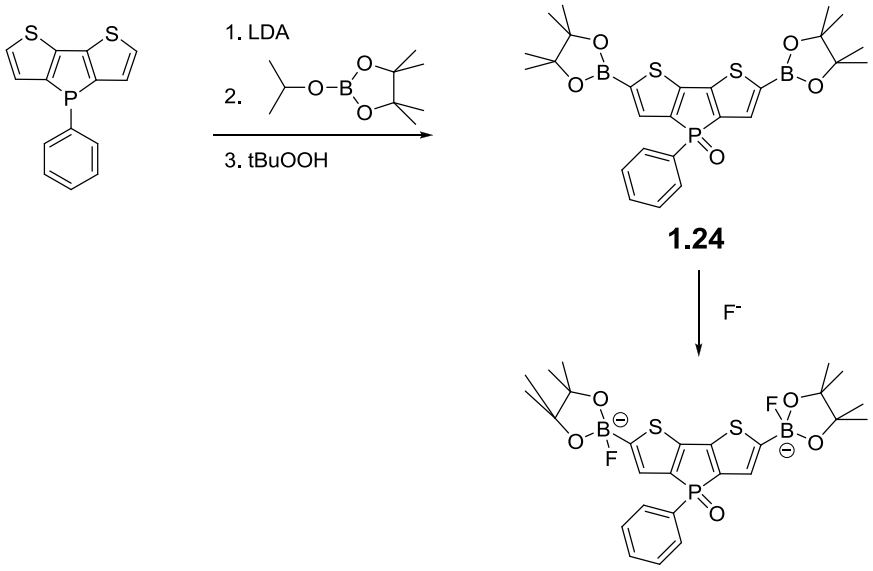

Figure 1.19 Synthesis of bis(boryl)dithienophosphole[38] for sensing fluoride.

1.4.3 CONSIDERATIONS

Boronate esters are formed between boronic acids and *cis*-diols.[28] As early as 1992, the formation of boronate esters was used to detect sugars.[35] Moreover, boronate esters have been investigated as the building blocks to construct complex materials, including polymers[29-32] and covalent organic frameworks[33,34]. These materials have potential applications as self-healing, blue-emissive or porous materials.[29-34] Boronate

esters are also used for hydrogen peroxide detection, using the oxidative deprotection of boronate esters.[36]

As mentioned before, borane-based small molecules and polymers have been well-studied in sensing Lewis bases.[12] However, boranes suffer from disadvantages, including complicated syntheses, instability toward water and oxidation, and crowded structure.[12] Compared to boranes, boronates can be synthesized by the catalyst-free dehydration between boronic acids and 1,2- or 1,3- *cis*-diols, under mild conditions with high yields.[29-31] The optical or electronic properties can be easily tuned by modification of the boronic acid and diol moieties. In addition, boron centers can be incorporated into five- or six- membered heterocyclic ring to form dioxaborolane or dioxaborole, which have enhanced stability toward air and moisture. Although a few boronate esters have been reported to sense fluoride, the incomplete π-conjugation through boronates may limit their sensing abilities.[37-39]

1.5 Cross-reactive Sensor Arrays

Traditional sensors use a single variable to read and analyze transduction signals.[40] For instance, the previously discussed examples of fluoride sensing by boranes are "lock and key" type sensors. However, these sensors cannot differentiate multiple structurally and/or chemically similar analytes or meet the demand of complex analytical problems in environmental, industrial, biological or medical processes.[41]

Inspired by the nature's use of mammalian olfactory and gustatory systems, cross-reactive sensor arrays were developed to differentiate multiple analytes. Each sensor has selectivity for different analytes and produces different signals. The signals can be based

on one, two or multiple dimensions. These dimensions form the fingerprint patterns of sensor arrays, which can be differentiated using statistical techniques.[40]

1.5.1 STATISTICAL TECHNIQUES FOR PATTERN RECOGNITION

The applications of statistical techniques to deal with multivariate analysis for pattern recognition dated back to 1971.[42] Several statistical methods were commonly used in cross-reactive sensor arrays, including principal component analysis (PCA) and linear discriminate analysis (LDA). LDA minimizes the variation in the patterns within each analyte group, while it maximizes the differences in the patterns between different groups.

1.5.2 SINGLE/MULTIPLE DIMENSIONAL RROSS-REACTIVE SENSOR ARRAYS

The simplest sensor arrays are based on one sensor, providing a pattern for each target by one wavelength response. For example, the Chang group reported a colorimetric sensor array to differentiate cations.[43] This array used 47 commercially-available dyes as one sensor called New York Tongue 1: (NYT-1) to test 47 cations including 44 metal cations. The recognition pattern of each analyte was formed by one wavelength response at the absorption maxima of each dye. By grouping the alkali-metal ions as one analyte, cations were identified with the accuracy of 99.4 % and quantified with the accuracy of 96.8 % by PCA analysis.

The dimensions of sensor arrays can easily be increased using multiple wavelength response. For example, the Lavigne group developed a sensor using carboxylic acid functionalized poly(thiophene) **1.25** (**Figure 1.20**) to distinguish

structurally similar diamines. The response was based on electrostatic and hydrogen-bonding interactions between the analytes and the polymer, which were coupled to π-π interactions between polymer chains and analyte-induced polymer aggregation. LDA was used to classify the patterns and differentiate the diamines by multiple wavelengths response in the entire spectra. In an organic solution,[9a] nine wavelengths or dimensions were selected to identify and quantify six diamines by LDA with the accuracy over 99%. In the aqueous solution,[9c] 36 wavelengths were chosen to identify and differentiate 22 biologically relevant amines by LDA with 97% accuracy. A multi-layered analysis was further developed to enhance accuracy, categorize analytes and determine concentration.[9b]

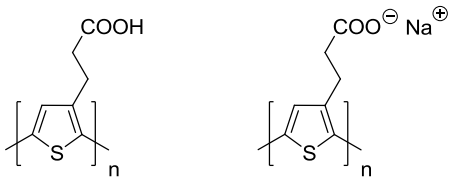

1.25 **1.26**

Figure 1.20 Structures of poly(thiophene)s[9,44] for differentiation of amines.

Dimensions of cross-reactive sensor arrays can be increased further by using multiple sensors. For instance, the Lavigne group[44] used poly(thiophene) **1.26** (**Figure 1.20**) to sense soft metal ions in a competitive two-step approach. Metal ions were added to precipitate the polymer, then a competitive ligand of diamine was used to re-dissolve the assembly of metal ions and polymer. 36 wavelengths and 2 diamines were selected to form a 72 (36×2) dimensional sensor array to distinguish seven soft metal ions with an accuracy of 100 %.

1.5.3 CONSIDERATIONS

Cross-reactive sensor arrays have interactions with analytes and produces different signals based on one, two or multiple dimensions. The generated recognition patterns are differentiated by using statistical techniques.[40] Sensor arrays have been developed to differentiate multiple analytes, including ions[43], organic small molecules[9,44] or biologically relevant analytes[9].

1.6 CONCLUSION

In summary, chemical sensors especially optical sensors, were briefly introduced. In those optical sensors, conjugated polymers as transduction or/and recognition motif were also discussed. Organoboron compounds, including boranes and boronate esters were overviewed in detail, from the perspective of synthesis and sensing applications.

1.7 REFERENCES

[1] Hulanicki, A.; Glab, S.; Ingman, F. Chemical sensors definitions and classification. *Pure & App. Chem.*, **1991**, *63* (9), 1247-1250.

[2] Vlasov, Yu. G.; Ermolenko, Yu. E.; Legin, A. V.; Rudnitskaya, A. M.; Kolodnikov,V. V. Chemical sensors and their systems. *J. Anal. Chem.*, **2010**, *65* (9), 880–898.

[3] McDonagh, C.; Burke, C. S.; MacCraith B. D. Optical chemical sensors. *Chem. Rev.*, **2008**, *108* (2), 400-422.

[4] Yuan, M. J.; Li, Y. J.; Liu, H. B.; Li, Y. L. Chemical sensors based on π-conjugated organic molecules and gold nanoparticles. *Sci. China Ser. B Chem.*, **2009**, *52* (6), 715-730.

[5] Liu, Y.; Ogawa, K.; Schanze K. S. Conjugated polyelectrolytes as fluorescent sensors. *J. Photochem. Photobiol. C: Photochem. Rev.*, **2009**, *10*, 173-190.

[6] Thomas III, S. W.; Joly, G. D.; Swager, T. M. Chemical sensors based on amplifying fluorescent conjugated polymers. *Chem. Rev.*, **2007**, *107* (4), 1339-1386.

[7] Zhou, Q.; Swager, T. M. Fluorescent chemosensors based on energy migration in conjugated polymers: the molecular wire approach to increased sensitivity. *J. Am. Chem. Soc.*, **1995**, *117*(50), 12593-12602.

8 Cai, M.; Daniel, S. L.; Lavigne, J. J. Conjugated bis and poly(dioxaborole)s for optical sensing of Lewis bases based on main-chain perturbations. *Chem. Commun.*, **2013**, *49*, 6504-6506. Reproduced by permission of The Royal Society of Chemistry. http://pubs.rsc.org/en/content/articlelanding/2013/CC/c3cc41189c#!divAbstract

[9] Lee, K.; Povlich, L. K.; Kim, J. Recent advances in fluorescent and colorimetric conjugated polymer-based biosensors. *Analyst*, **2010**, *135*, 2179-2189.

[10] (a) Nelson, T. L.; O'Sullivan C.; Greene, N. T.; Maynor, M. S.; Lavigne, J. J. Cross-reactive conjugated polymers: analyte-specific aggregative response for structurally similar diamines. *J. Am. Chem. Soc.*, **2006**, *128*(17), 5640-5641. (b) Nelson, T. L.; Tran, I.; Ingallinera, T. G.; Maynor, M. S.; Lavigne, J. J. Multi-layered analyses using directed partitioning to identify and discriminate between biogenic amines. *Analyst*, **2007**, *132*, 1024-1030. (c) Maynor, M. S.; Nelson, T. L.; O'Sullivan C.; Lavigne, J. J. A food freshness sensor using the multistate response from analyte-induced aggregation of a cross-reactive poly(thiophene). *Org. Lett.*, **2007**, *9*(17), 3217-3220.

[11] Wang, B.; Wasielewski, M. R. Design and synthesis of metal ion-recognition-induced conjugated polymers: an approach to metal ion sensory materials. *J. Am. Chem. Soc.*, **1997**, *119*(1), 12-21.

[12] (a) Hudson, Z. M.; Wang, S. Impact of donor-acceptor geometry and metal chelation on photophysical properties and applications of triarylboranes. *Acc. Chem. Res.*, **2009**, *42*(10): 1584-1596. (b) Jäkle, F. Advances in the synthesis of organoborane polymers for optical, electronic, and sensory applications. *Chem. Rev.*, **2010**, *110*(7), 3985-4022. (c) Mou, X.; Liu, S. J.; Dai, C. L.; Ma, T. C.; Zhao, Q.; Ling, Q. D.; Huang, W. A class of fascinating optoelectronic materials: triarylboron compounds. *Sci. China Chem.*, **2010**, *53*(6): 1235-1245. (d) Hudnall, T. W.; Chiu, C.-W.; Gabbai, F. P. Fluoride ion recognition by chelating and cationic boranes. *Acc. Chem. Res.*, **2009**, *42*(2): 388-397. (e) Wade, C. R.; Broomsgrove, A. E. J.; Aldridge, S.; Gabbai, F. P. Fluoride ion complexation and sensing using organoboron compounds. *Chem. Rev.*, **2010**, *110*(7), 3958-3984. (f) Galbraith, E.; James, T. D. Boron based anion receptors as sensor. *Chem. Soc. Rev.*, **2010**, *39*, 3831-3842. (g) Hudson, Z. M.; Wang, S. Metal-containing triarylboron compounds for optoelectronic applications. *Dalton Trans.*, **2011**, *40*: 7805-7816.

[13] (a) Yamaguchi, S.; Akiyama, S.; Tamao, K. Colorimetric fluoride ion sensing by boron-containing π-electron systems. *J. Am. Chem. Soc.*, **2001**, *123*(46), 11372-11375. (b) Yamaguchi, S.; Akiyama, S.; Tamao, K. Tri-9-anthrylborane and its derivatives: new boron-containing π-electron systems with divergently extended π-conjugation through boron. *J. Am. Chem. Soc.*, **2000**, *122*(26), 6335-6336.

[14] Miyata, M.; Chujo, Y. π-Conjugated organoboron polymer as an anion sensor. *Polym. J.*, **2002**, *34*(12), 967-969.

[15] Li, H.; Jäkle, F. Universal scaffold for fluorescent conjugated organoborane polymers. *Angew. Chem., Int. Ed*., **2009**, *48*, 2313-2316.

[16] Sundararaman, A.; Victor, M.; Varughese, R.; Jäkle, F. A family of main-chain polymeric Lewis acids: synthesis and fluorescent sensing properties of boron-modified polythiophene. *J. Am. Chem. Soc.*, **2005**, *127*(40), 13748-13749.

[17] Liu, X. Y.; Bai, D. R.; Wang, S. Charge-transfer emission in nonplanar three-coordinate organoboron compounds for fluorescent sensing of fluoride. *Angew. Chem. Int. Ed.*, **2006**, *45*, 5475-5478.

[18] Jia, W. L.; Feng, X. Dong.; Bai, D. R.; Lu, Z. H.; Wang, S.; Vamvounis, G. Mes_2B(*p*-4,4'-biphenyl-NPh(1-naphthyl)): a multifunctional molecule for electroluminescent devices. *Chem. Mater.*, **2005**, *17*(1), 164-170.

[19] Liu, Z.-Q.; Shi, M.; Li, F.-Y.; Fang, Q.; Chen, Z.-H.; Yi, T.; Huang, C.-H. Highly selective two-photon chemosensor for fluoride derived from organic boranes. *Org. Lett.*, **2005**, *7*(24), 5481-5484.

[20] Zhou, G.; Baumgarten, M.; Müllen, K. Mesitylboron-substituted ladder-type pentaphenylenes: charge-transfer, electronic communication, and sensing properties. *J. Am. Chem. Soc.*, **2008**, *130*(37), 12477-12484.

[21] Kubo, Y.; Yamamoto, M.; Ikeda, M.; Takeuchi, M.; Shinkai, S.; Yamaguchi, S.; Tamao, K. A colorimetric and ratiometric fluorescent chemosensor with three emission changes: fluoride ion sensing by a triarylborane-porphyrin conjugate. *Angew. Chem. Int. Ed.*, **2003**, *42*, 2036-2040.

[22] Li, J.; Zhang, G.; Zhang, D.; Zheng, R.; Shi, Q.; Zhu, D. Boron-containing monopyrrolo-annelated tetratriafulvalene compounds: synthesis and absorption spectral/electrochemical responsiveness toward fluoride ion. *J. Org. Chem.*, **2010**, *75*(15), 5330-5333.

[23] Li, H.; Jäkle, F. Donor-π-acceptor polymer with alternating triarylborane and triphenylamine moieties. *Macromol. Rapid Commun.*, **2010**, 915-920.

[24] (a) Sun, Y.; Ross, N.; Zhao, S.-B.; Huszarik, K.; Jia, W.-L.; Wang, R.-Y.; Macartney, D.; Wang, S. Enhancing electron accepting ability of triarylboron via π-conjugation with 2,2'-bipy and metal chelation: 5,5'-bis($BMes_2$)-2,2'-bipy and its metal complexes. *J. Am. Chem. Soc.*, **2007**, *129*(24), 7510-7511. (b) Sun, Y.; Wang, S. Conjugated triarylboryl donor-acceptor systems supported by 2,2'-bipyridine: metal chelation impact on intraligand charge transfer emission, electron accepting ability, and "turn-on" fluoride sensing. *Inorg. Chem.*, **2009**, *48*(9), 3755-3767.

[25] (a) Bai, D.-R.; Liu, X.-Y.; Wang, S. Charge-transfer emission involving three-coordinate organoboron: V-shape versus U-shape and impact of the spacer on dual emission and fluorescent sensing. *Chem. Eur. J.*, **2007**, *13*, 5713-5723. (b) Cao, D.; Liu, Z.; Zhang, G.; Li, G. The synthesis, photophysical properties and fluoride anion recognition of a novel branched organoboron compound. *Dyes Pigm.*, **2009**, *81*, 193-196. (c) Pan, H.; Fu, G.-L.; Zhao, Y.-H.; Zhao, C.-H. Through-space charge-transfer emitting biphenyls containing a boryl and an amino group at the o,o'-positions. *Org. Lett.*, **2011**, *13*(18), 4830-4833.

[26] (a) Zucchero, A. J.; Mcgrier, P. L.; Bunz, U. H. F. Cross-conjugated cruciform fluorophores. *Acc. Chem. Res.*, **2010**, *43*(3): 397-408. (b) Wilson, J. N.; Bunz, U. H. F. Switching of intramolecular charge transfer in cruciforms: metal ion sensing, *J. Am. Chem. Soc.*, **2005**, *127*(12), 4124-4125. (c) Zucchero, A. J.; Wilson, J. N.; Bunz, U. H. F. Cruciforms as functional fluorophores: response to protons and selected metal ions. *J. Am. Chem. Soc.*, **2006**, *128*(36), 11872-11881. (d) Tolosa, J.; Zucchero, A. J.; Bunz, U. H. F. Water-soluble cruciforms: response to protons and selected metal ions. *J. Am. Chem. Soc.*, **2008**, *130*(20), 6498-6506. (e) Brombosz, S. M.; Zucchero, A. J.; Phillips, R. L.; Vazquez, D.; Wilson, A.; Bunz, U. H. F. Terpyridine-based cruciform-Zn^{2+} complexes as anion-responsive fluorophores. *Org. Lett.*, **2007**, *9*(22), 4519-4522. (f) Hauck, M.; Schönhaber, J.; Zucchero, A. J.; Hardcastle, K. I.; Müller, T. J. J.; Bunz, U. H. F. Phenothiazine cruciforms: synthesis and metallochromic properties. *J. Org. Chem.*, **2007**, *72*(18), 6714-6725. (g) McGrier, P. L.; Solntsev, K. M.; Schönhaber, J.; Brombosz, S. M.; Tolbert, L. M.; Bunz, U. H. F. Hydroxy-cruciforms. *Chem. Commun.*, **2007**, 2127-2129. (h) McGrier, P. L.; Solntsev, K. M.; Miao, S.; Tolbert, L. M.; Miranda, O. R.; Rotello, V. M.; Bunz, U. H. F. Hydroxycruciforms: amine-responsive fluorophores. *Chem. Eur. J.*, **2008**, *14*, 4503-

4510. (i) Carroll, C. N.; Coombs, B. A.; McClintock, S. P.; Johnson II, C. A.; Berryman, O. B.; Johnson, D. W.; Haley, M. M. Anion-dependent fluorescence in bis(anilinoethynyl)pyridine derivatives: switchable ON-OFF and OFF-ON responses. *Chem. Commun.*, **2011**, *47*, 5539-5541. (j) Davey, E. A.; Zucchero, A. J.; Trapp, O.; Bunz, U. H. F. Discrimination of organic acids using a three molecule array based upon cruciform fluorophores. *J. Am. Chem. Soc.*, **2011**, *133*, 7716-7718. (k) Lim, J.; Nam, D.; Miljanić, O. Š. Identification of carboxylic and organoboronic acids and phenols with a single benzobisoxazole fluorophore. *Chem. Sci.*, **2012**, *3*, 559-563.

[27] Zhao, Y.-H.; Pan, H.; Fu, G.-L.; Lin, J.-M.; Zhao, C.-H. A highly emissive cruciform triarylborane as a ratiometric and solid state fluorescence sensor for fluoride ions. *Tetrahedron Lett.*, **2011**, *52*, 3832-3835.

[28] Severin, K. Boronic acids as building blocks for molecular nanostructures and polymeric materials. *Dalton Trans.*, **2009**, 5254-5264.

[29] (a) Niu, W. J.; Rambo, B.; Smith, M. D.; Lavigne, J. J., Substituent effects on the structure and supramolecular assembly of bis(dioxaborole)s. *Chem. Commun.* **2005**, (41), 5166-5168. (b) Niu, W.; Rambo, B. M.; Smith, M. D.; Lavigne, J. J., Self-assembling polymeric and oligomeric borole materials. *Polym. Mater. Sci. Eng.* **2005**, *91*, 147-148. (c) Niu, W. J.; Smith, M. D.; Lavigne, J. J., Substituent effects on the structure and supramolecular assembly of bis(dioxaborole)s derived from 1,2,4,5-tetrahydroxybenzene. *Cryst. Growth & Des.* **2006**, *6*(6), 1274-1277. (d) Rambo, B. M.; Lavigne, J. J., Defining self-assembling linear oligo(dioxaborole)s. *Chem. Mater.* **2007**, *19*(15), 3732-3739.

[30] Niu, W.; O'Sullivan, C.; Rambo, B. M.; Smith, M. D.; Lavigne, J. J. Self-repairing polymers: poly(dioxaborole)s containing trigonal planar boron. *Chem. Commun.*, **2005**, 4342-4344.

[31] Niu, W.; Smith, M. D.; Lavigne, J. J. Self-assembling poly(dioxaborole)s as blue-emissive materials. *J. Am. Chem. Soc.*, **2006**, *128*(51), 16466-16467.

[32] Christinat, N.; Croisier, E.; Scopelliti, R.; Cascella, M.; Röthlisberger, U.; Severin, K. Formation of boronate ester polymers with efficient intrastrand charge-transfer transitions by three-component reactions. *Eur. J. Inorg. Chem.*, **2007**, 5177-5181.

[33] Côté, A. P.; Benin, A. I.; Ockwig, N. W.; Matzger, A. J.; O'Keeffe, M.; Yaghi, O. M. Porous, crystalline, covalent organic frameworks, *Science*, **2005**, *310*, 1166-1170.

[34] Tilford, R. W.; Gemmill, W. R.; zur Loye, H.-C.; Lavigne, J. J. Facile synthesis of a highly crystalline, covalently linked porous boronate network. *Chem. Mater.*, **2006**, *18*(22), 5296-5301.

[35] Yoon, J.; Czarnik, A. W. Fluorescent chemosensors of carbohydrates, a means of chemically communicating the binding of polyols in water based on chelation-enhanced quenching. *J. Am. Chem. Soc.*, **1992**, *114*, 5874-5875.

[36] Sanchez, J. C.; Trogler, W. C. Polymerization of a boronate-functionalized fluorophore by double transferification: applications to fluorescence detection of hydrogen peroxide vapor. *J. Mater. Chem.*, **2008**, *18*, 5134-5141.

[37] Arimori, S.; Davidson, M. G.; Fyles, T. M.; Hibbert, T. G.; James, T. D.; Kociok-Köhn, G. I. Synthesis and structural characterization of the first bis(bora)calixarene: a selective, bidentate, fluorescent fluoride sensor. *Chem. Commun.*, **2004**, 1640-1641.

[38] Neumann, T.; Dienes, Y.; Baumgartner, T. Highly sensitive sensory materials for fluoride ions based on the dithieno[3,2-b:2',3'-d]phosphole system. *Org. Lett.*, **2006**, *8*(3), 495-497.

[39] Liu, W.; Pink, M.; Lee, D. Conjugated polymer sensors built on π-extended borasiloxane cages. *J. Am. Chem. Soc.*, **2009**, *131*(24), 8703-8707.

[40] Li, X. Development of conjugated boronate ester-linked materials for optical sensing applications targeting small molecules. Ph.D. Thesis, University of South Carolina, Columbia, SC, 2012.

[41] Nishiyabu, R.; Palacios, M. A.; Dehaen, W.; Anzenbacher, Jr. P. Synthesis, structure, anion binding, and sensing by calix[4]pyrrole isomers. *J. Am. Chem. Soc.*, **2006**, *128*, 11496-11504.

[42] Beebe, K. R.; Pell, R. J.; Seasholtz, M. B. *Chemometrics: A Practical Guide*, Wiley, 1998.

[43] Lee, J. W.; Lee, J.-S.; Kang, M.; Su, A. I.; Chang, Y.-T. Visual artificial tongue for quantitative metal-cation analysis by an off-the-shelf dye array. *Chem. Eur. J.*, **2006**, *12*, 5691-5696.

[44] Maynor, M. S.; Deason, T. K.; Nelson, T. L.; Lavigne, J. J. Multidimensional response analysis towards the detection and identification of soft divalent metal ions. *Supramolecular Chemistry*, **2009**, *21*(3-4), 310-315.

CHAPTER 2

SYNTHESIS, CHARACTERIZATION AND SENSING APPLICATIONS OF CONJUGATED BIS- AND POLY- DIOXABOROLES[1]

2.0 INTRODUCTION

Conjugated polymers have been investigated as signal transducers for sensing applications, due to their signal amplification[2] and versatile design[3]. Within these sensors, the recognition motifs can be pendent on the side-chain or embedded in the main-chain of polymers (**Figure 2.1**). In the first approach (**Figure 2.1a**), the targets bind to the pendent motifs and indirectly perturb the electronic properties or conformation of main-chain, resulting in the optical change.[4] In the latter approach (**Figure 2.1b**), the binding sites are embedded in the main-chain, where the analytes binding directly changes the π-conjugation along the backbone. For example, the partially conjugated polymer containing 2,2'-bipyridine binds metals ions, effectively forcing the planarization of polymer.[5]

The main-chain approach has been rarely studied, however, it is predicted that the direct binding can generate the amplified signal. Moreover, the electronic or optical properties can be easily tuned by introduction of versatile groups. Thus, the main-chain approach provides a more sensitive and smart sensing strategy. Herein, we report the

signal transduction and utility of dioxaborole containing oligomers and polymers for sensing of Lewis bases.

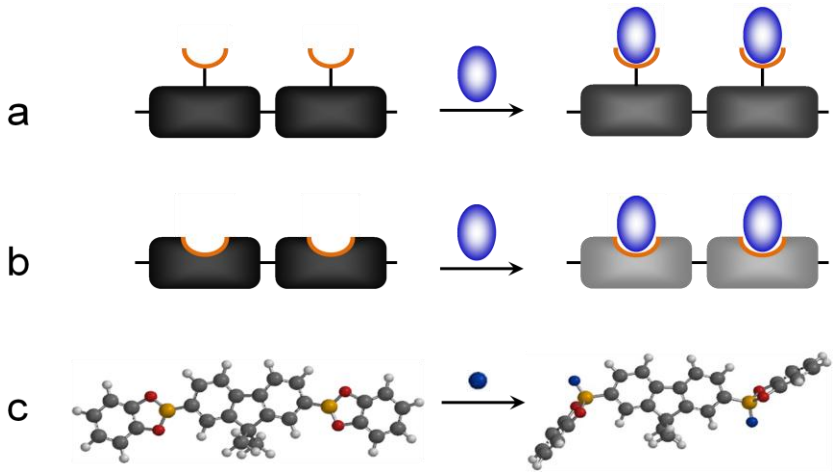

Figure 2.1 Schematic representation of chemosensors based on conjugated polymers with (a) side-chain and (b) main-chain recognition motifs. Black: π-conjugation system, red: recognition motif, blue: analyte, gray: π-conjugation system interrupted by the analytes binding. (c) Molecular modeling of fluoride binding to bis(dioxaborole) by using a DFT B3LYP-6-31G* package in a computational software of Spartan 08.

As one class of conjugated polymers, poly(borane)s with Lewis acidic boron centers in the main-chain have recently been applied to detect Lewis bases, including fluoride[6,7,8], cyanide[7,8] as well as amines[9]. However, these sensory materials are often difficult to synthesize using organometalic chemistry. And they are instable toward hydrolysis and oxidation. In order to protect and stabilize the boron centers, bulky substituents are usually incorporated. [10] Thus, the conjugated main-chain of poly(borane)s is twisted and the access of analytes blocked, reducing the effective response from the analyte binding.

Boronate ester formation, with its covalent yet reversible nature, provides the attributes for sensory materials. For example, boronates can be synthesized by the

dehydration reaction between boronic acid and 1,2- or 1,3- *cis*-diol, which is facile with high yields (>90 %).[11a] In addition, boron centers can be incorporated into the five-membered heterocyclic ring to form dioxaborole, allowing stability toward hydrolysis.[12] Moreover, boronate esters provide planar geometries with extended π-conjugation. Thus, boronate esters are considered as alternative conjugated organoboron-based sensors.

The Lavigne group has intensively researched conjugated boronate esters, including oligomeric and polymeric dioxaboroles.[11] Herein, we investigate whether dioxaboroles can be incorporated into the main-chain of conjugated polymers and used as novel optical sensor for Lewis bases. Due to the novelty of sensing applications, it is of importance to understand the sensing mechanisms of the smaller model molecules as well as polymer for Lewis bases. Thus, a series of bis- and poly- dioxaboroles **2.1**-**2.6** (**Figure 2.2**) were designed, synthesized, characterized and evaluated to elucidate the sensing mechanism toward the conjugated polymer-based sensor.

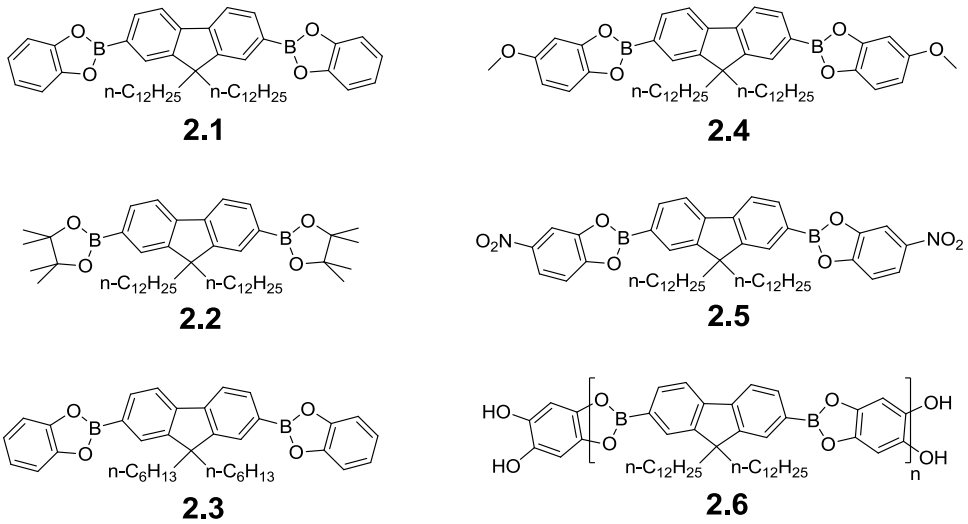

Figure 2.2 Structures of bis- and poly- dioxaboroles **2.1**-**2.6**.

Bis(dioxaborole) **2.1(-H)** was designed as a conjugated model for poly(dioxaborole) **2.6**. Non-conjugated bis(dioxaborole)s **2.2** was used as a control to study how π-conjugation affected binding. The control, bis(dioxaborole) **2.3** with hexyl groups was designed to study the impact of remote sterics. Electron-rich **2.4(-OCH_3)** and electron-deficient **2.5(-NO_2)** were selected to study how electronic properties affect binding. The sensing mechanism and signal transduction, studied by absorption, fluorescence and NMR spectroscopy and computational calculation, are detailed below.

2.1 Results and Discussion

2.1.1 Synthesis and characterization

Before starting with the sensing studies, a series of bis- and poly- dioxaboroles **2.1-2.6** were synthesized. All the starting materials were commercially available except for 3-methoxycatechol [13] and 1,2,4,5-tetrahydroxybenzene (THB) [14], which were synthesized by some modifications of procedures available in literature. The decision to use 9,9-didodecylfluorene-2,7-diboronic acid as a starting material to synthesize bis(dioxaborole)s was based on two reasons: (1) Dodecyl groups can increase the solubility of diboronic acids and products in organic solvents, allowing the following characterization and sensing applications, and (2) Fluorenyl ring has interesting optical properties, resulting from its rigid structure and large π-conjugation system.

Bis- and poly- dioxaboroles **2.1-2.6** were generated by dehydration reactions between fluorenyl diboronic acid and a *cis*-1,2-diol or THB (**Figure 2.3**).[11a] The starting materials were refluxed in toluene or THF and the resultant water was removed by a Dean-Stark trap. After removing the excess solvent and 1,2-diol or THB, products were

obtained in yields greater than 36%. The resultant bis(dioxaborole)s **2.1**-**2.5** showed good solubility in organic solvents, such as THF, toluene and dichloromethane, while poly(dioxaborole) **2.6** showed a decent solubility in THF and toluene.

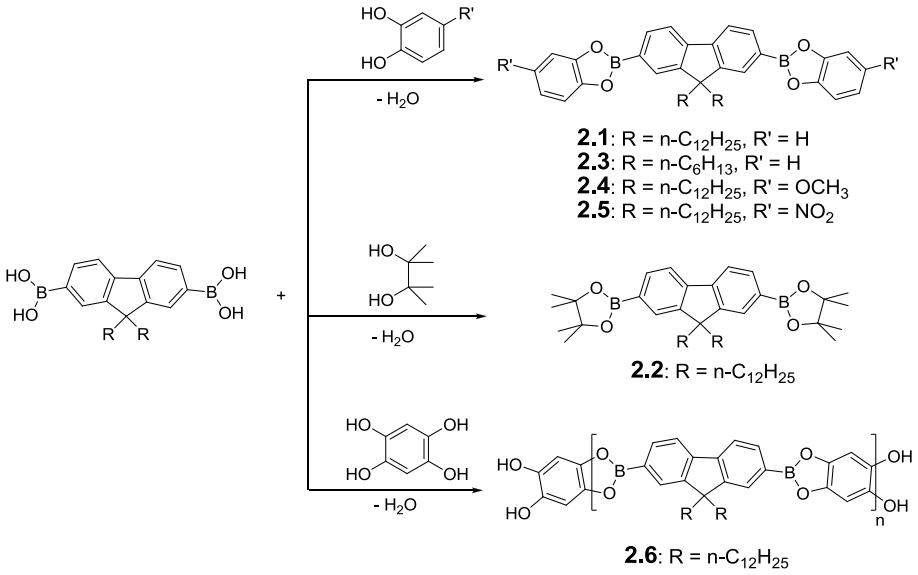

Figure 2.3 Synthesis of bis- and poly- dioxaboroles by dehydration reactions.

The formation of boronate ester linkage was easily characterized by FT-IR and ^{1}H NMR spectroscopy.[11e] In FT-IR spectra, the attenuation of the broad peak in the range of 3200-3400 cm^{-1} suggests the disappearance of the hydroxyl groups in 1,2-diols or THB. The diagnostic bands in the 1300-1350 cm^{-1} and 1000-1050 cm^{-1} range indicate the formation of boronate esters. The peak at 688 cm^{-1} indicates the THB linked boronate ester of **2.6**.[9d] In ^{1}H NMR spectra, the attenuation of the peak in 4.5-5.5 ppm suggests the disappearance of the hydroxyl moieties in *cis*-1,2-diols or THB. The peaks in the downfield of 7.8-8.2 ppm suggest the protons on the fluorenyl ring ortho to the boron centers, due to the extended π-conjugation through the vacant p-orbital of borons.[11d] Bis- and poly- dioxaboroles **2.1**-**2.6** were also characterized by ^{13}C NMR and mass

spectroscopy. The synthetic routes and characterization data are detailed listed in Experimental section.

2.1.2 Optical property studies

To study the sensing mechanism and signal transduction in these bis(dioxaborole)-based sensors, fluoride was used to maximize the signal response, based on the hard Lewis acid-hard Lewis base interaction between boron and fluoride. Tetra-n-butylammonium fluoride (TBAF) was selected as the fluoride source, due to its excellent solubility in organic solvent, such as THF and CH_2Cl_2. For the following studies, two equivalents of TBAF were added to bis(dioxaborole)s **2.1-2.5**, providing a 1:1 fluoride to boron ratio. The fluoride binding studies were investigated by absorption and fluorescence spectroscopy, due to the optical fluorenyl ring on bis(dioxaborole)s.

2.1.2.1 Effect of π-conjugation

To investigate the effect of π-conjugationon fluoride binding, non-conjugated **2.2** bis(dioxaborole) was used as a control for **2.1**. The absorption and fluorescence spectra in **Figure 2.4a** show that bis(dioxaborole)s **2.1** and **2.2** have multiple strong bands, resulting from the rigid fluorenyl ring.[8] Bis(dioxaborole) **2.1** shows the absorption maxima at 331 nm and the emission maxima at 352 nm. Compared to the non-conjugated **2.2**, bis(dioxaborole) **2.1** have the maximum wavelengths red-shifted by approximate 15 nm, due to its extended π-conjugation through the vacant p-orbital of boron.

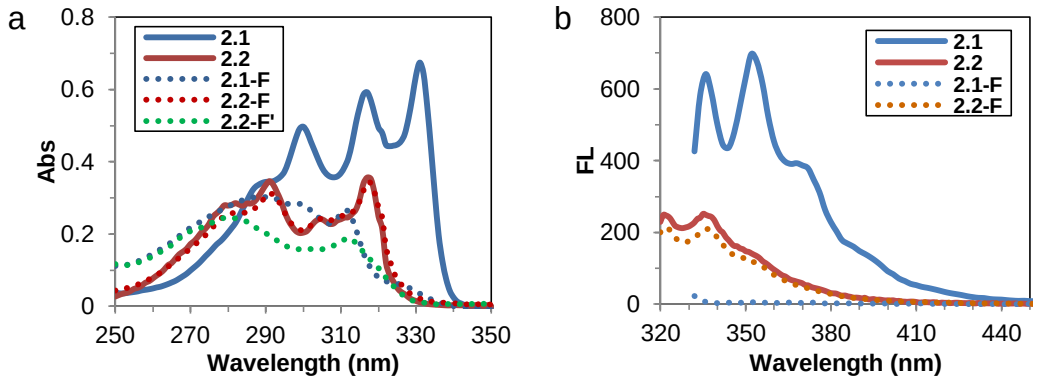

Figure 2.4 (a) Absorption spectra of bis(dioxaborole)s **2.1** and **2.2** (1×10^{-5} M), and (b) fluorescence spectra of bis(dioxaborole)s **2.1** and **2.2** (1×10^{-6} M) in the absence and presence of fluoride in CH_2Cl_2.

Upon the addition of TBAF, bis(dioxaborole) **2.1** gave a blue shift of the absorption maxima from 331 nm to 311 nm and a complete decrease in absorbance at 331 nm (**Figure 2.4a, 2.1-F**). Its fluorescence at 352 nm was accordingly quenched (**Figure 2.4b, 2.1-F**). The following computational calculation and ^{1}H NMR study displayed the similar effects. These results indicate that the fluoride coordination to bis(dioxaborole) **2.1** changes the boron from a trigonal planar to a tetrahedral geometry, thereby interrupting π-conjugation along the backbone (**Figure 2.1c**).

However, the addition of TBAF to the non-conjugated **2.2** made no obvious change to the spectra (**Figure 2.4, 2.2-F**). Even when 300 equivalents of TBAF (3×10^{-3} M) was added to the non-conjugated **2.2**, the absorption maxima of **2.2** blue-shifted from 317nm to 312 nm and absorbance at 317 nm decreased a little (**Figure 2.4a, 2.2-F'**). Thus, π-conjugation along the borole is important to the sensitive response of bis(dioxaborole) **2.1** to Lewis base binding.

2.1.2.2 EFFECT OF REMOTE STERICS

To investigate the effect of remote sterics on fluoride binding, bis(dioxaborole) **2.3** with hexyl groups was designed. As shown in **Figure 2.5**, bis(dioxaborole) **2.3** has the same optical properties and identical response to fluoride as **2.1**. These results suggest that remote sterics on the side arm of fluorenyl ring have little impact on fluoride binding.

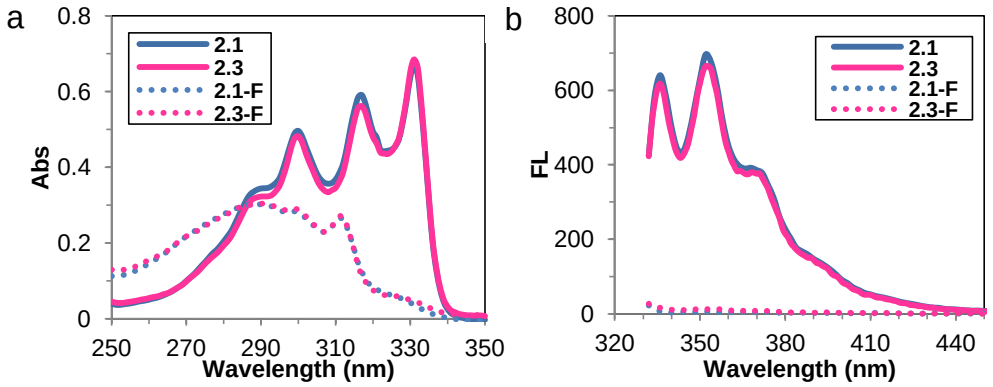

Figure 2.5 (a) Absorption spectra of bis(dioxaborole)s **2.1** and **2.3** (1×10^{-5} M), and (b) fluorescence spectra of bis(dioxaborole)s **2.1** and **2.3** (1×10^{-6} M) in the absence and presence of fluoride in CH_2Cl_2.

2.1.2.3 EFFECT OF ELECTRONICS

Electron-rich **2.4(-OCH_3)** and electron-deficient **2.5(-NO_2)** were designed to investigate the impact that borole electronics have on Lewis base binding. As shown in **Figure 2.6a**, bis(dioxaborole)s **2.4(-OCH_3) and 2.5(-NO_2)** show the absorption maxima at 336 nm, 5 nm longer than the absorption maxima of **2.1(-H)**. As shown in **Figure 2.6b**, bis(dioxabrole) **2.4(-OCH_3)** shows the emission wavelength at 432 nm, with a large Stock's shift of 109 nm. However, the fluorescence of **2.5(-NO_2)** was not detected, because the nitro groups enhance internal conversion, thereby quenching fluorescence.[15]

Upon the addition of fluoride, bis(dioxaborole) **2.4(-OCH_3)** and **2.5(-NO_2)** showed a similar optical response to fluoride as **2.1(-H)** (**Figure 2.6**). The absorption maxima blue shifts and fluorescence quenches. Interestingly, the addition of fluoride to **2.5(-NO_2)** made the colorless solution turn yellow. The resultant fluoride complex **2.5-F** has a new absorption peak centered at 403 nm, studied by computational calculations.

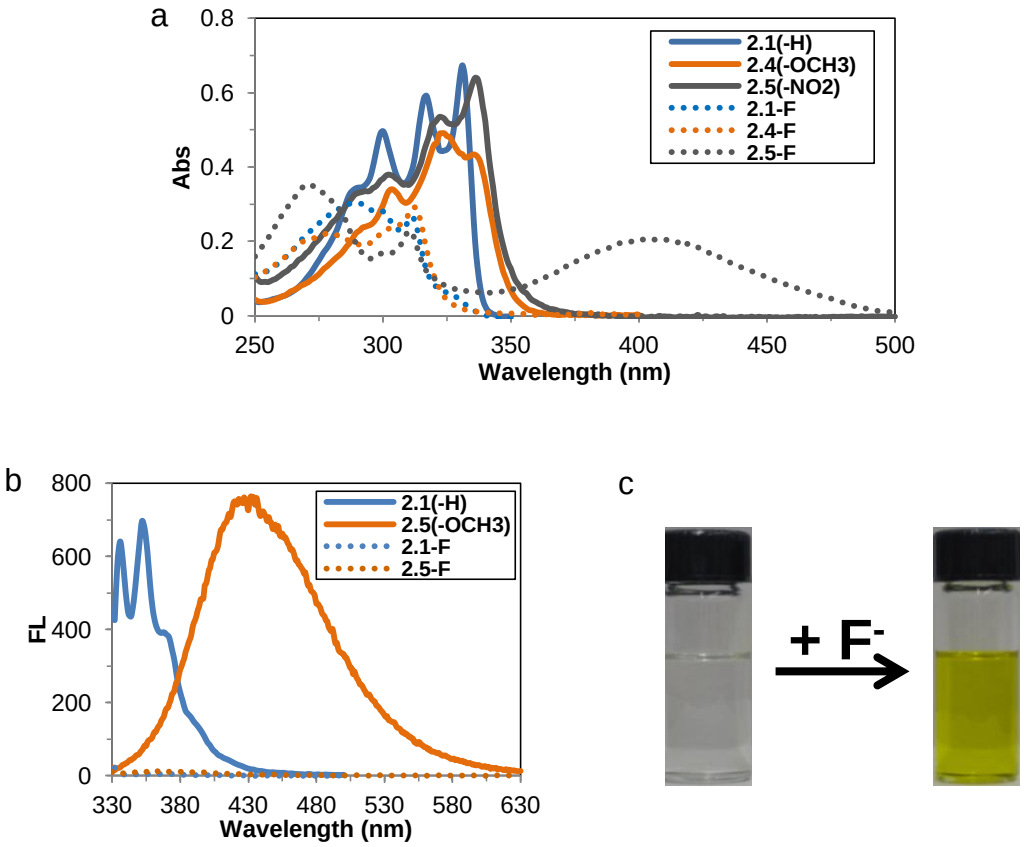

Figure 2.6 (a) Absorption spectra of bis(dioxaborole)s **2.1(-H)**, **2.4(-OCH_3)** and **2.5(-NO_2)** (1×10^{-5} M), and (b) fluorescence spectra of bis(dioxaborole)s **2.1(-H)**, **2.4(-OCH_3)** and **2.5(-NO_2)** (1×10^{-6} M) in the absence and presence of fluoride in CH_2Cl_2. (c) The color formation for bis(dioxaborole) **2.5(-NO_2)** (1×10^{-3} M) with added fluoride (2×10^{-3} M).

2.1.3 COMPUTATIONAL CALCULATIONS

Computational calculations can provide theoretical information about electronic/optical properties of molecules. Thus, computational calculations for bis(dioxaborole)s and their fluoride complexes were performed on the basis of DFT (B3LYP 6-31G*) in software Spartan 08. Methyl groups, instead of dodecyl groups, on fluorenyl ring were used to save calculation time. The calculated and experimental band gaps and optical wavelengths are listed in **Table 2.1**. And the computed geometries and energies of molecular orbitals are summarized in **Table 2.2**.

Table 2.1 Calculated and experimental band gaps and optical wavelengths.

Compound	E_{cal} (eV)	E_{exp} (eV)	λ_{cal} (nm)	λ_{exp} (nm)	λ_{em} (nm)	Stock's shift (nm)
2.1(-H)	4.15	3.75	299	331	352	21
2.1-F	4.41	3.99	281	311	-	-
2.2	4.47	3.91	278	317	335	18
2.2-F	4.79	3.98	259	312	-	-
2.4(-OCH_3)	3.93	3.70	316	335	432	109
2.4-F	4.41	3.98	281	312	-	-
2.5(-NO_2)	3.88	3.69	320	336	-	-
2.5-F	3.63	3.08	342	403	-	-

2.1.3.1 EFFECT OF Π-CONJUGATION

To investigate the effect of π-conjugation on fluoride binding, computational calculations of bis(dioxarbole)s **2.1**, **2.2** and their fluoride complexes were performed. As shown in **Table 2.1**, HOMO of **2.1** localizes on fluorenyl ring and catechol moieties, a larger system than HOMO of **2.2**. While LUMOs of bis(dioxaborole)s **2.1** and **2.2** show significant contributions from boron centers, the p orbitals of which overlap with their neighboring fluorenyl ring and oxygen atoms, thereby extending π-conjugation. The

calculated band gap of **2.1** is 4.15 eV, 0.32 eV smaller than band gap of **2.2**, which is consistent with the experimental decreasing band gap (**Table 2.2**).

Table 2.2 Computed geometries and energies of molecular orbitals.

Compound	HOMO	LUMO
2.1(-H)	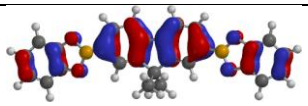 -5.79 eV	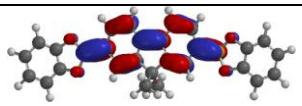 -1.64 eV
2.1-F[a]	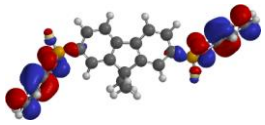 0.14 eV	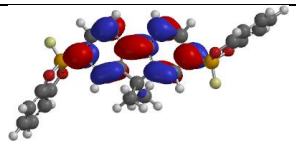 4.55 eV
2.2	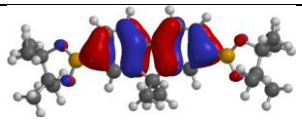 -5.63 eV	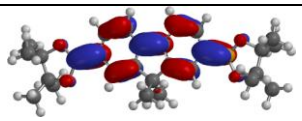 -1.16 eV
2.2-F	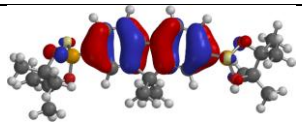 0.32 eV	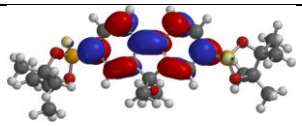 5.11 eV
2.4(-OCH_3)	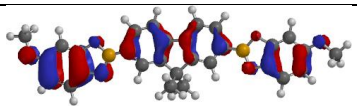 -5.50 eV	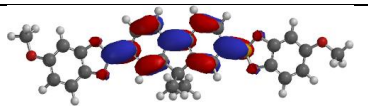 -1.57 eV
2.4-F	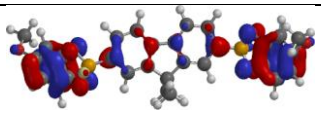 0.11 eV	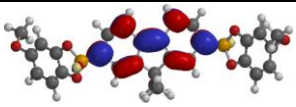 4.52 eV
2.5(-NO_2)	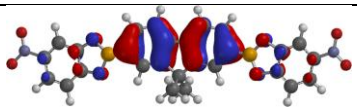 -6.36 eV	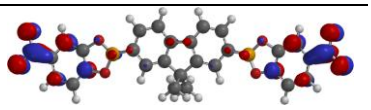 -2.48 eV
2.5-F[a]	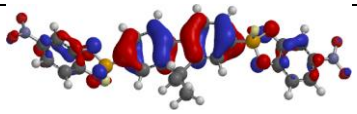 -0.71 eV	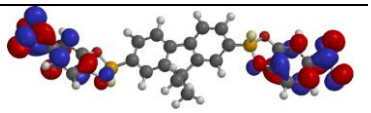 2.92 eV

[a] HOMO is located on the left diol moiety and HOMO(-1) is centered on the right part.

Upon binding fluoride, the fluoride complex **2.1-F** changes the geometry of boron and interrupts the extended π-conjugation (**Table 2.1**). The interruption prevents boron making contribution to LUMO. Thus, band gap of **2.1-F** increases to 4.41 eV, approaching the calculated band gap of the non-conjugated bis(dioxaborole) **2.2**. The calculated increasing band gap is consistent with the hypsochromic shift of absorption maxima.

2.1.3.2 EFFECT OF ELECTRONICS

To understand the effect of borole electronics on fluoride binding, computational calculations of bis(dioxaborole)s **2.1(-H)**, **2.4(-OCH_3)**, **2.5(-NO_2)** and their fluoride complexes were performed. Compared to bis(dioxaborole) **2.1(-H)**, **2.4(-OCH_3)** shows a similar HOMO and LUMO distribution. However, **2.4(-OCH_3)** has a smaller band gap and longer absorption maxima, due to the electon-donating methoxy groups increasing HOMO energy, 0.22 eV more than LUMO energy. Upon binding fluoride, complex **2.4-F** shows an increasing band gap to 4.41 eV, explaining the hypsochromic shift of absorption maxima.

Different from bis(dioxaborole) **2.1(-H)**, HOMO of **2.5(-NO_2)** is centered on fluorenyl ring, while LUMO is located on the terminal diol moieties due to the strong electron-withdrawing ability of nitro groups. Bis(dioxaborole) **2.5(-NO_2)** shows a calculated band gap of 3.88 eV, 0.27 eV smaller than band gap of **2.1(-H)**, explaining the fact that **2.5(-NO_2)** has a longer absorption maximum than **2.1(-H)**. Upon fluoride binding, electron-withdrawing nitro groups stabilize LUMO more efficiently than HOMO, thereby HOMO energy increases more than LUMO energy. Thus, fluoride binding

lowers band gap from 3.88 eV to 3.63 eV, consistent with a new longer absorption peak at 403 nm of complex **2.5-F**.

2.1.4 ABSORPTION TITRATIONS

To further investigate the binding interactions between bis(dioxaborole)s and Lewis bases, absorption titrations were conducted by the sequential addition of fluoride to bis(dioxaborole)s. Binding properties of bis(dioxaborole)s toward fluoride were listed in **Table 2.3**. Absorption spectra upon the addition of fluoride to bis(dioxaborole)s were depicted in **Figure 2.7**.

Table 2.3 Binding properties of bis(dioxaborole)s toward fluoride in CH_2Cl_2.

Compound	**Dynamic range[a] (M)**	**|Slope|[b]**	**Ratio[c]**	**K_1 (M^{-1})**	**K_2 (M^{-1})**
2.1(-H)	$0\text{-}2.10 \times 10^{-5}$	0.3120	2.02	3.53×10^5	3.43×10^4
2.4(-OCH_3)	$0\text{-}1.59 \times 10^{-5}$	0.4049	1.52	4.14×10^6	8.45×10^4
2.5(-NO_2)	$0\text{-}1.96 \times 10^{-5}$	0.2515	1.84	8.07×10^4	8.07×10^4

[a,b] Dynamic range of the concentration of fluoride and absolute slope was determined from the linear regression part of calibration curves (**Figure 2.8**)
[c] Mole ratio of fluoride to bis(dioxaborole)

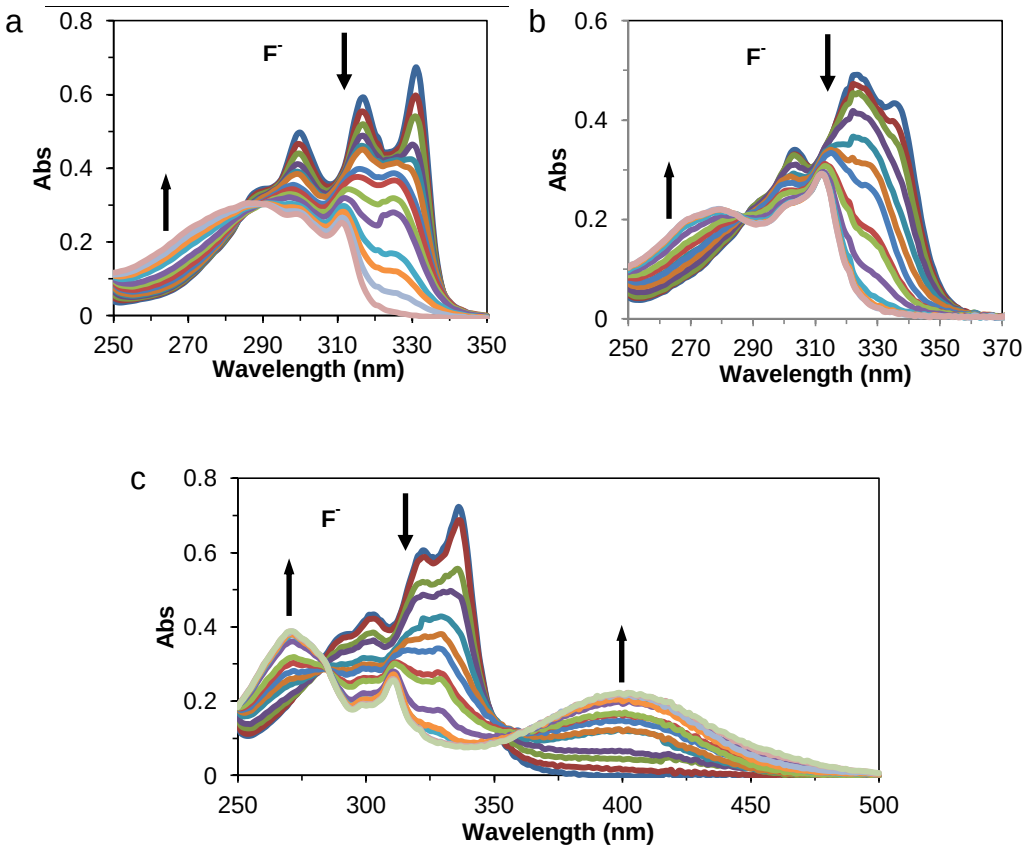

Figure 2.7 Absorption titration of 1×10^{-5} M bis(dioxaborole)s (a) **2.1(-H)**, (b) **2.4(-OCH_3)**, and (c) **2.5(-NO_2)** upon TBAF addition in CH_2Cl_2.

2.1.4.1 BINDING SENSITIVITY

The hypsochromic shift and decreased absorbance previously discussed for bis(dioxaborole)s **2.1(-H)**, **2.4(-OCH_3)** and **2.5(-NO_2)** is dependent on the concentration of added fluoride (**Figure 2.8**). The absorbance response is linearly proportional to the concentration of fluoride in the range of $0\text{-}2\times10^{-5}$ M.

In the dynamic range, the absolute slope of bis(dioxaborole) **2.4(-OCH_3)** is 0.2515, 0.0608 smaller than that of **2.1(-H)**, which means **2.4(-OCH_3)** is 20% less responsive to fluoride than **2.1(-H)**. This is because that the electron- donating methoxy groups decrease the Lewis acidity of boron centers, allowing **2.4(-OCH_3)** less sensitive to

fluoride. In contrast, the electron-withdrawing nitro groups increase the Lewis acidity of boron, making bis(dioxaborole) **2.5(-NO_2)** 30% more sensitive to fluoride than **2.1(-H)**. As shown in **Figure 2.8**, the absolute slope of **2.5(-NO_2)** is 0.4049, 0.0929 larger than that of **2.1(-H)**.

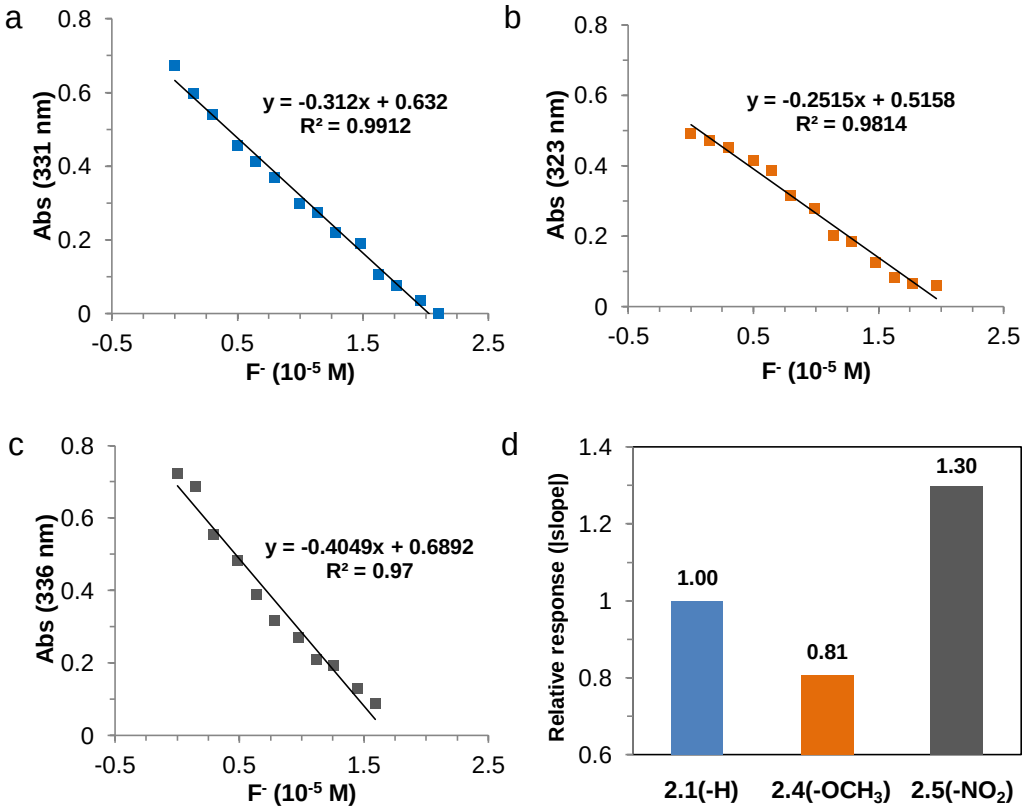

Figure 2.8 Plots of the change in absorbance at the specific absorption maxima vesus the concentration of fluoride (linear regression analysis data presented) for (a) **2.1(-H)**, (b) **2.4(-OCH_3)** and (c) **2.5(-NO_2)**. (d) Relative response of bis(dioxaborole)s to fluoride.

2.1.4.2 BINDING STOICHIOMETRY

Stoichiometric ratios of fluoride to bis(dioxaborole)s were studied by mole ratio plot. The intercept of the two straight lines in the plot indicates binding ratio (**Figure 2.9**). [16] For bis(dioxaborole)s **2.1(-H)**, **2.4(-OCH_3)** and **2.5(-NO_2)**, their fluoride complexes show the binding stoichiometry of 2:1. This is consistent with the hypothesis

that one fluoride binds to each of the two boron binding sites on bis(dioxaborole)s, affording a 1:1 ratio of fluoride to boron.

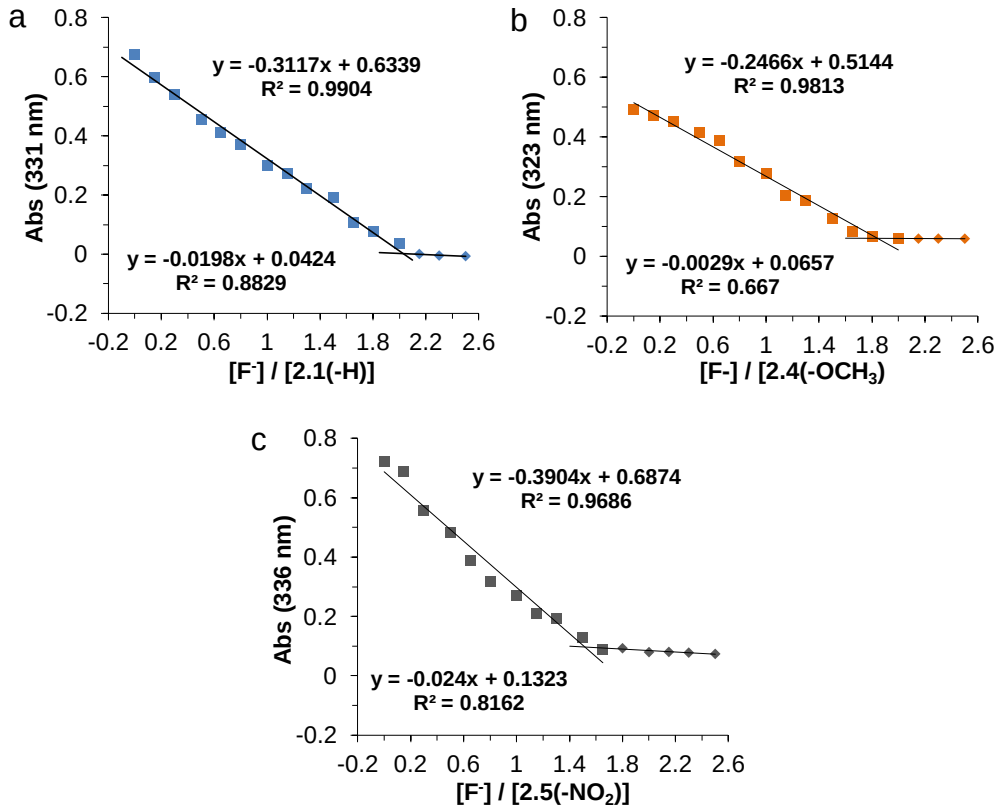

Figure 2.9 Mole ratio plots of 1×10^{-5} M bis(dioxaborole)s (a) **2.1(-H)**, (b) **2.4(-OCH_3)** and (c) **2.5(-NO_2)** upon TBAF addition in CH_2Cl_2.

2.1.4.3 BINDING AFFINITY

Binding stoichiometry for fluoride-bis(dioxaborole) complexes was the same, however, the binding affinity differed. Binding constants were calculated by using a 2:1 (guest:host) binding isotherm (**Figure 2.10**).[17] The calculated first binding constant K_1 followed the same trend as binding sensitivity.

Bis(dioxaborole) **2.4(-OCH_3)** shows a K_1 of 8.07×10^4 M^{-1}, indicating a lower affinity to fluoride as 0.2 times as **2.1(-H)**. This is because that the electron-donating

methoxy groups make boron atoms less Lewis acidic, thereby decreasing the affinity to fluoride. To the contrary, the calculated K_1 of bis(dioxaborole) **2.5(-NO$_2$)** is 4.14×10^6 M^{-1}, suggesting that **2.5(-NO$_2$)** binds fluoride as 11.7 times tightly as **2.1(-H)**. This increased affinity of **2.5(-NO$_2$)** is because that the electron-withdrawing nitro groups make borons more Lewis acidic, allowing more affinity to fluoride.

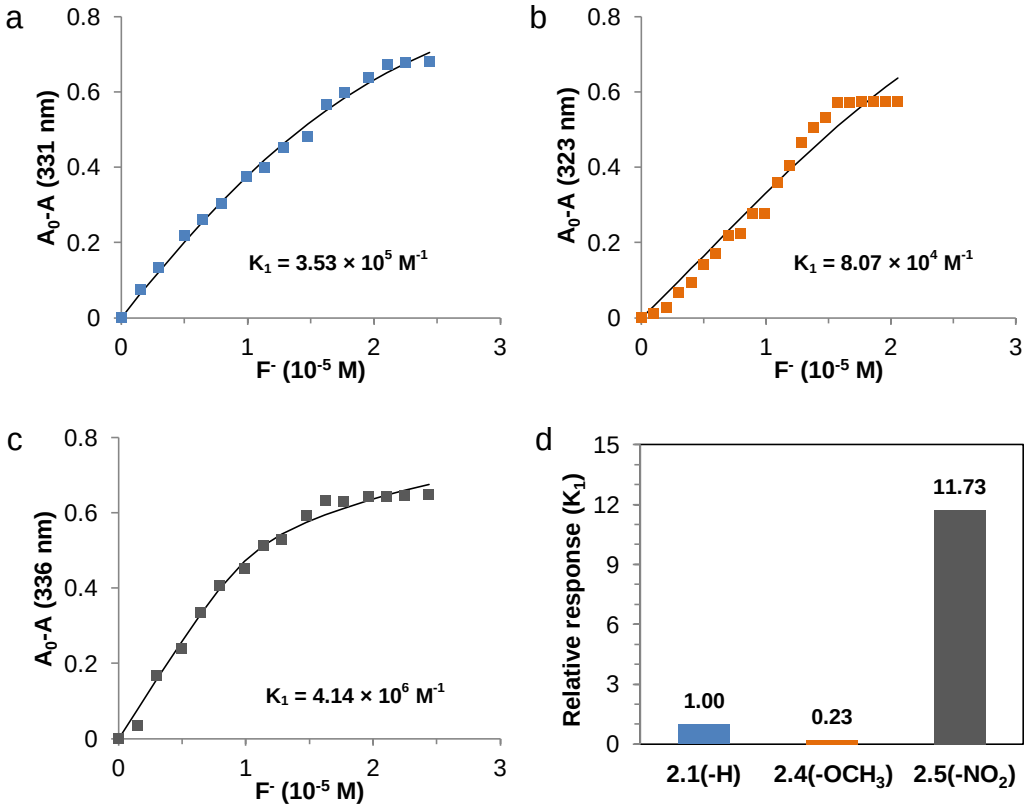

Figure 2.10 Binding isotherms of 1×10^{-5} M bis(dioxaborole)s (a) **2.1(-H)**, (b) **2.4(-OCH$_3$)** and (c) **2.5(-NO$_2$)** upon TBAF addition in CH_2Cl_2. (d) Relative response of bis(dioxaborole)s to fluoride.

2.1.5 FLUORESCENCE TITRATIONS

The titration process was also monitored by fluorescence spectroscopy. Fluorescence emission spectra upon the addition of fluoride to bis(dioxaborole)s **2.1(-H)** and **2.4(-OCH$_3$)** are displayed in **Figure 2.11**. As the concentration of fluoride

increasing, fluorescence of **2.1(-H)** and **2.4(-OCH$_3$)** at emission maxima quenches, indicating the non-fluorescent bis(dioxaborole)-fluoride complexes. Fluoride can be detected as low as 0.15×10^{-6} M by **2.1(-H)** or **2.4(-OCH$_3$)**, lower than the data reported by using other boronates.[18] Thus, bis(dioxaborole)s **2.1(-H)** and **2.4(-OCH$_3$)** may be promising materials to sensitively detect fluoride by fluorescence spectroscopy.

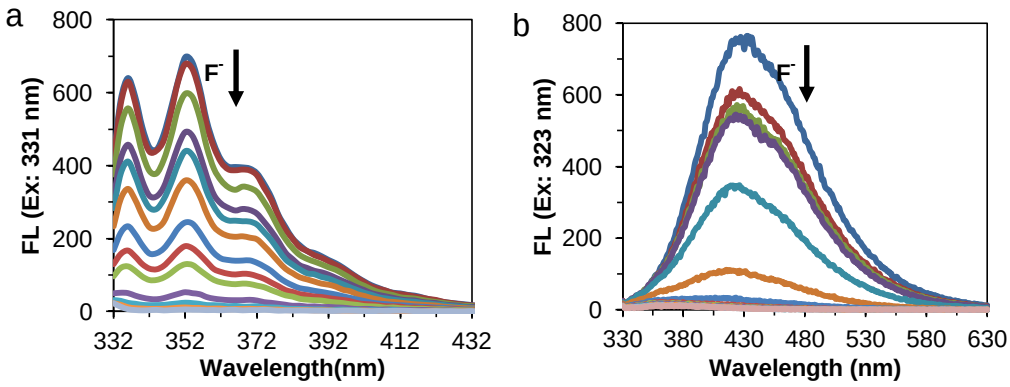

Figure 2.11 Fluorescence titration of 1×10^{-6} M bis(dioxaborole)s (a) **2.1(-H)** and **2.4 (-OCH$_3$)** upon TBAF addition in CH_2Cl_2.

2.1.6 BINDING STABILITY

Boronate ester is formed by a covalent yet reversible bond, which is sensitive to water. Since the commercially-available TBAF dissolves in 1M THF with 5 wt% H_2O, the impact of water on binding stability was investigated by absorption and ^{1}H NMR spectroscopy. Bis(dioxaborole) **2.1** was used as a representative compound for study. The addition of 5 wt% (2.5×10^{-5} M) of water does not change absorbance of bis(dioxaborole) **2.1**. After 45 min, the absorption spectrum has no obvious change. In addition, the complex **2.1-F** is not responsive to 5 wt% of water, either (**Figure 2.12**). Thus, bis(dioxaborole) **2.1** and its complex are stable toward 5 wt% of water.

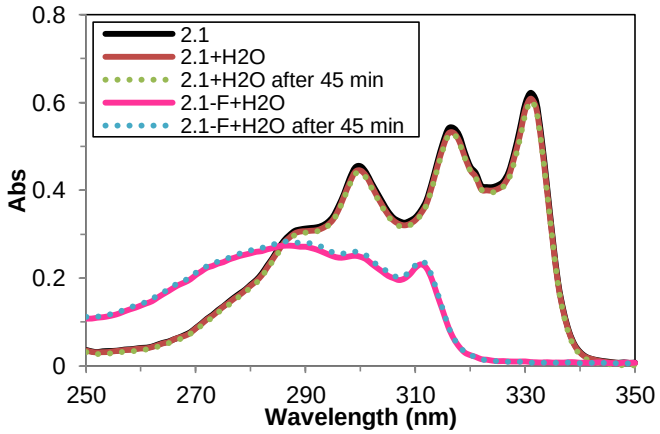

Figure 2.12 Absorption spectra of 1×10^{-5} M bis(dioxaborle) **2.1** and complex **2.1-F** (**2.1**: 1×10^{-5} M, TBAF: 2×10^{-5}) in CH_2Cl_2 in the absence and presence of 2.5×10^{-5} M H_2O in THF.

The binding stability of bis(dioxaborole) **2.1** at a higher concentration to fluoride was investigated by ^{1}H NMR spectroscopy. The peaks with chemical shift from 7.0 to 8.2 ppm are assigned to the aromatic protons on **2.1** (**Figure 2.13a**). The addition of 5 wt% water generates new peaks appearing in the range of 6.5 to 7.0 ppm (**Figure 2.13c**), resulting from the protons on catechol hydrolyzed from **2.1** (**Figure 2.13d**). Upon two equivalents of fluoride binding, a significant upfield shift was observed, indicating the fluoride binding to **2.1** forming the complex **2.1-F** shielding the aromatic protons. However, the presence of 5 wt% water does not hydrolyze the complex **2.1-F** (**Figure 2.13b**), verifying the binding stability of bis(dioxaborole) **2.1** to fluoride.

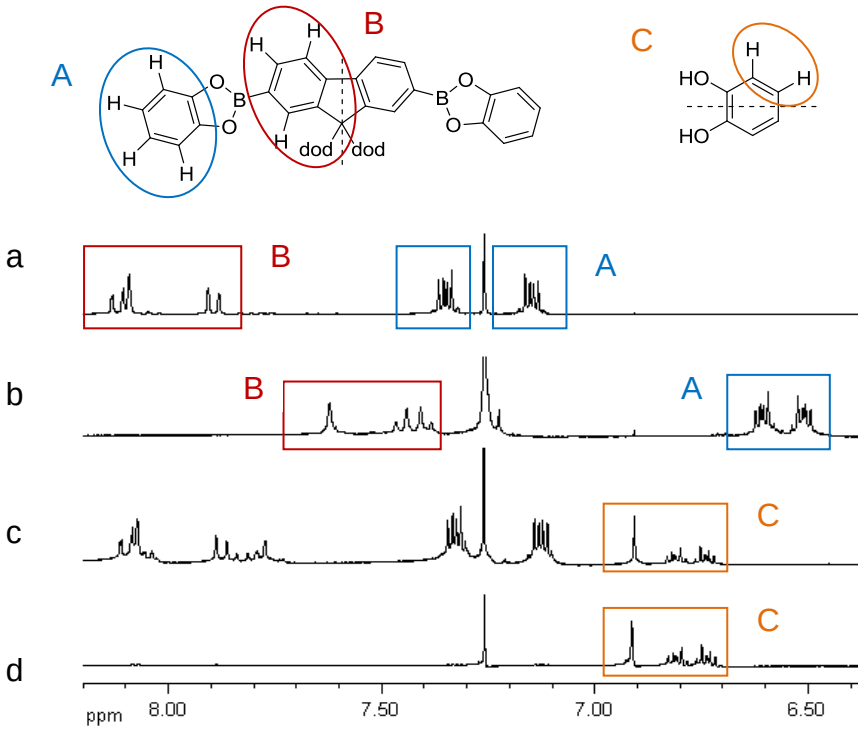

Figure 2.13 ^{1}H NMR spectra (300 MHz, $CDCl_3$) of (a) 15 mM bis(dioxaborole) **2.1**, (b) 15 mM **2.1** and 30 mM fluoride with 5 wt% H_2O added, (c) 15 mM **2.1** with 5 wt% H_2O added, and (d) starting materials of 15 mM 9,9-didodecylfluorene-2,7-diboronic acid and 30 mM catechol with 5 wt% H_2O added.

2.1.7 BINDING REVERSIBILITY

To demonstrate the reversibility of bis(dioxaborole)s binding fluoride, excess trimethylsilyl chloride (TMSCl) was added to the fluoride complexes to scavenge fluoride. Meanwhile, bis(dioxaborole)s and chloride were released (**Figure 2.14a**). However, choloride did not have any optical response to bis(dioxaborole)s (**Figure 2.15**). The process was monitored by absorption spectroscopy. Upon the addition of TMSCl to fluoride complexes, the absorption maxima of **2.1(-H)**, **2.4(-OCH_3)** and **2.5(-NO_2)** red-shifts back and absorbance restores (**Figure 2.14b-d**). These results indicate the reversible interaction between borole moieties on bis(dioxaborole)s and fluoride and further demonstrate the borole stability.

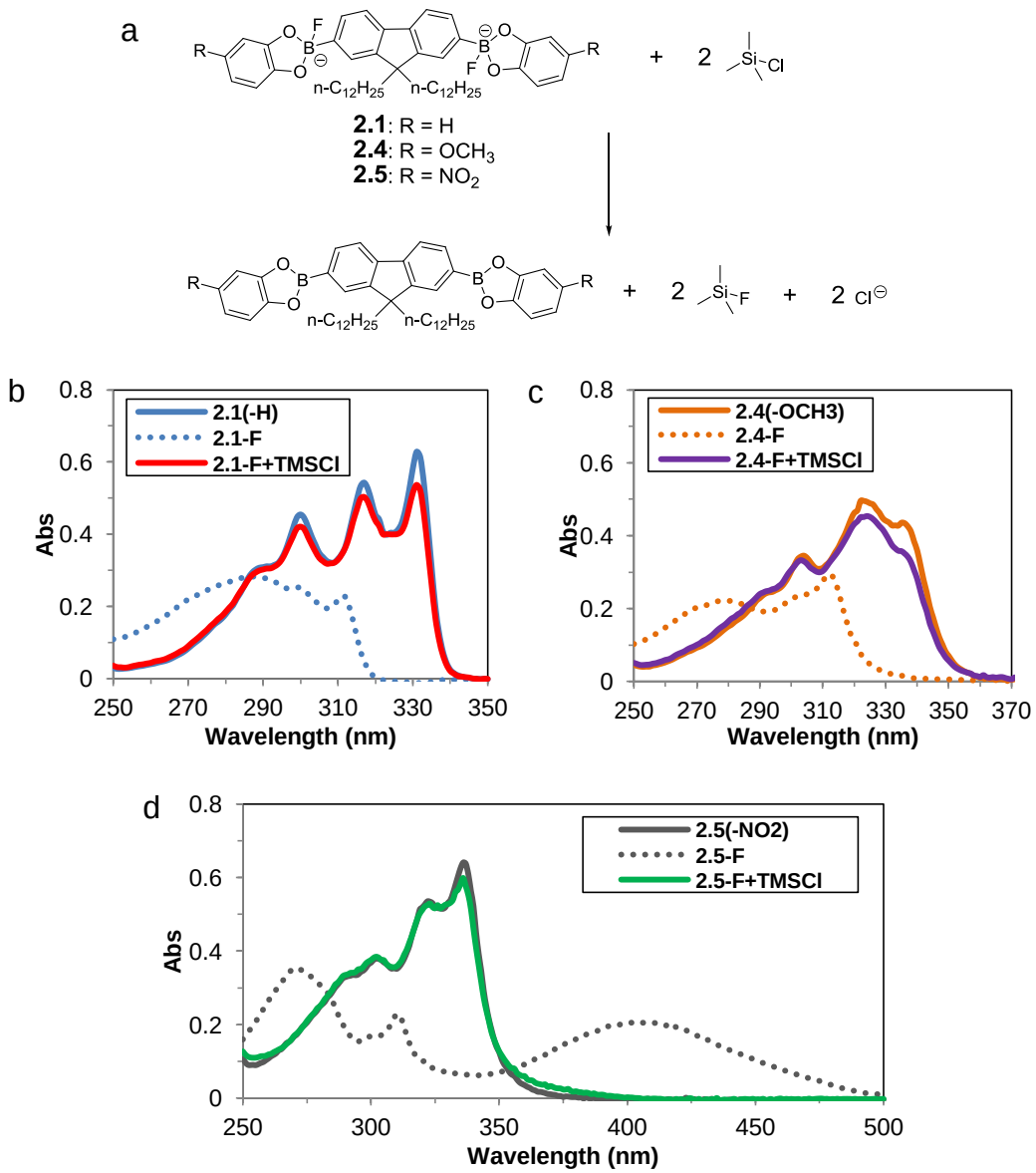

Figure 2.14 (a) Representation of fluoride-bis(dioxaborole) complexes reacting with TMSCl. Absorption spectra of 1×10^{-5} M bis(dioxaborole)s (b) **2.1(-H)**, (c) **2.4(-OCH_3)** and (d) **2.5(-NO_2)** in the presence of 2×10^{-5} M TBAF upon the addition of excess TMSCl in CH_2Cl_2.

2.1.8 Binding cross-reactivity

Fluoride was used to elucidate binding and transduction mechanisms, while the recognition ability of bis(dioxaborole)s towards different Lewis bases was of interest to

estimate their potential utility. Thus, selected anions as the tetrabutylammonium salts and amines were evaluated as Lewis bases for binding.

As shown in **Figure 2.15**, Bis(dioxaborole)s **2.1(-H)**, **2.4(-OCH_3)** and **2.5(-NO_2)** bind hard Lewis bases including F^- and CN^-, but they show no response to soft anions, such as Cl^-, Br^- and I^-. They also show some response to $H_2PO_4^-$, due to the hardness of binding oxygen atoms. It is noted that the weakest Lewis acid, **2.4(-OCH_3)**, binds to the hard Lewis bases in a broad response range, indicating that binding is more dependent on the Lewis basicity of anions. However, the strongest Lewis acid, **2.5(-NO_2)**, binds all the hard Lewis bases to the same degree. It suggests that that binding is determined by the Lewis acidity of borole moiety.

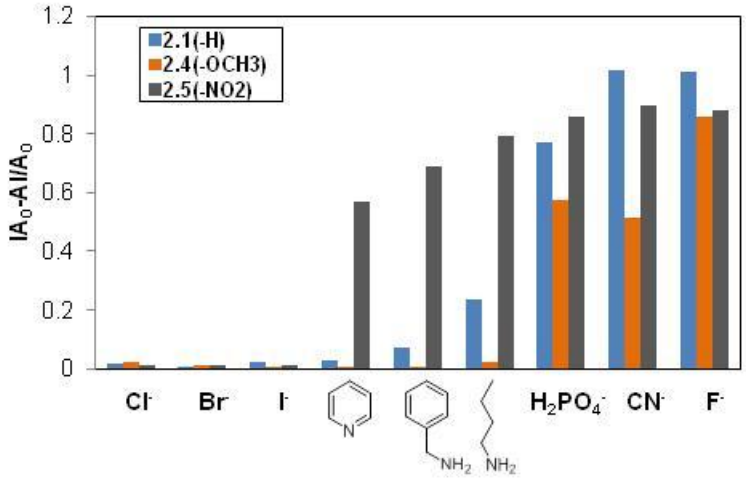

Figure 2.15 Relative change in absorbance for 1×10^{-5} M bis(dioxaborole)s responding to 5×10^{-5} M Lewis bases in CH_2Cl_2.

The binding of neutral amines to bis(dioxaborole)s followed the same trend as binding fluoride. Interestingly, the extent of binding is dependent not only on the Lewis acidity of borole but also on the Lewis basicity of amines. In general, the binding

response increases as the amine basicity increases from pyridine (pK_b = 8.75) to benzylamine (pK_b = 4.66), to n-butylamine (pK_b = 3.41).[19] As a weakest Lewis acid, **2.4(-OCH_3)** only binds the strongest Lewis base n-butylamine. On contrast, as a strongest Lewis acid, **2.5(-NO_2)** binds all the amines with a notable response. The intermediate **2.1(-H)** show the response to amines, similar to **2.5(-NO_2)** with less response. The cross-reactivity of bis(dioxaborole)s to different anions and amines may be useful to design a sensor array to differentiate Lewis bases.

2.1.9 BINDING AMPLIFICATION

Before studying binding amplification, the optical properties of poly(dioxaborole) **2.6** was investigated by absorption spectroscopy. As shown in **Figure 2.16**, poly(dioxaborole) **2.6** in CH_2Cl_2 or in THF shows a longer absorption maximum than that of bis(dioxaborole) **2.1** and monomers, indicating the extended π-conjugation on the main-chain of **2.6**. As the concentration of 2.6 in THF increasing, the absorbance at 332 nm increases. The increasing absorbance is linearly proportional to the concentration of **2.6** in the range of 1.1- 12.1×10^{-5} M, which is accorded with Beer's law indicating no aggregation occurs. The concentration of **2.6** is selected as 5×10^{-5} M for the following studies.

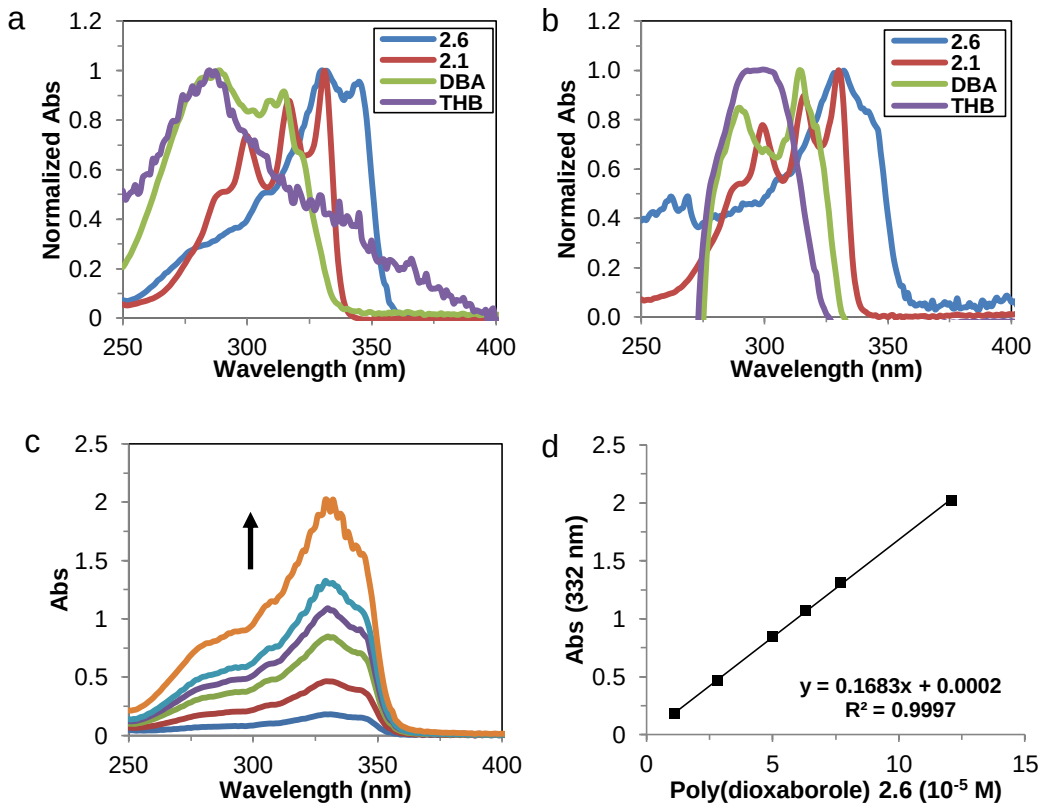

Figure 2.16 Absorption spectra of (a) saturated solution of poly(dioxaborole) **2.6**, 1×10^{-5} M bis(dioxaborole) **2.1** and monomers of 9,9-didodecylfluorene-2,7-diboronic acid (DBA) and 1,2,4,5-tetrahydroxybenzene (THB) in CH_2Cl_2, (b) 1×10^{-5} M poly(dioxaborole) **2.6**, bis(dioxaborle) **2.1** and monomers in THF, and (c) poly(dioxaborole) **2.6** at different concentrations in THF. (d) Plot of absorbance at 332 nm vesus the concentration of poly(dioxaborole) **2.6** in THF.

The quantitative response of poly(dioxaborole) **2.6** and bis(dioxaborole) **2.1** against TBAF in THF was recorded by absorption spectroscopy (**Figure 2.17a,b**). Similar to bis(dioxaborole) **2.1**, upon binding fluoride, poly(dioxaborole) **2.6** shows a blue shift of absorption maxima from 332 nm to 314 nm and a decrease in the absorbance at 332 nm, indicating the binding interrupts the π-conjugation of the poly(dioxaborole) backbone. The absorbance at 332 nm is linearly proportional to the concentration of TBAF in the range of $0\text{-}1.75\times10^{-6}$ M.

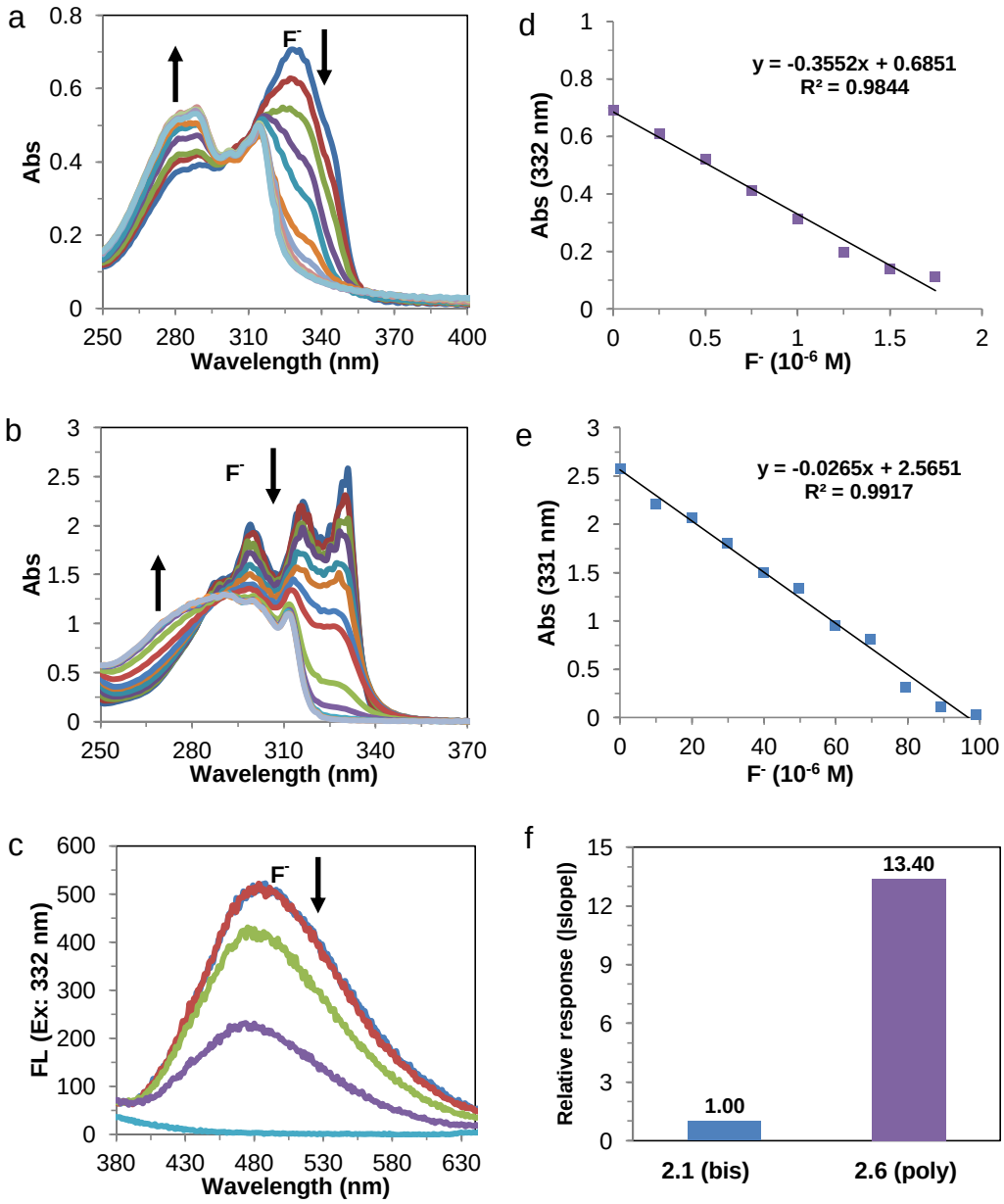

Figure 2.17 Absorption titration of (a) poly(dioxaborole) **2.6** (repeat unit: 5×10^{-5} M) and (b) bis(dioxaborole) **2.1** (5×10^{-5} M) upon TBAF addition in THF. (c) Fluorescence titration of poly(dioxaborole) **2.6** (repeat unit: 5×10^{-6} M) upon TBAF addition in THF. Plots of the change in absorbance at the specific absorption maxima vesus the concentration of fluoride (linear regression analysis data presented) for (d) poly(dioxaborole) **2.6** and (e) bis(dioxaborole) **2.1**. (f) Relative response of poly(dioxaborole) **2.6** to fluoride.

However, the sensitivity of poly(dioxaborole) **2.6** and bis(dioxaborole) **2.1** to TBAF are greatly different (**Figure 2.17d-f**). In the dynamic range, the absolute slope of

2.6 is 0.3552, larger than that of **2.1** (0.0265), suggesting that **2.6** exhibits a 13-fold enhancement in relative response compared to **2.1**. The highly sensitive response of poly(dioxaborole) **2.6** to TBAF shows an amplification effect[1] of conjugated polymers.

The response of poly(dioxaborole) **2.6** against TBAF at a lower concentration in THF was recorded by fluorescence spectroscopy (**Figure 2.17c**). Poly(dioxaborole) **2.6** shows an emission wavelength at 488 nm, with a huge Stock's shift of 156 nm. Upon the addition of TBAF, fluoride coordinates with the Lewis acidic boron to quench fluorescence. The required concentration of fluoride is lower than the theoretical 2×10^{-6} M, showing an amplification effect[2] of typical conjugated polymers.

2.2 CONCLUSION

In summary, a series of conjugated bis- and poly- dioxaboroles were developed as optical sensors for Lewis bases. Bis- and poly- dioxaboroles were synthesized by a facile dehydration reaction and characterized by ^{1}H NMR, ^{13}C NMR, FT-IR and mass spectroscopy. The optical and computational studies showed that fluoride binding with Lewis acidic borole moieties results in deplanarization of the conjugated borole and the entire π-conjugation structure of bis(dioxaborole)s is important for sensing. Compared to the optical response of bis(dioxaborole) to fluoride, poly(dioxaborole) shows an amplification effect of conjugated polymers, allowing a sensitive detection.

Incorporation of electron-withdrawing or electron-donating groups altered sensing parameters, including optical wavelength, absorbance, fluorescence intensity, and boron Lewis acidity, thereby impacting binding sensitivity and selectivity. It is also shown that water has little impact on fluoride binding and the binding between bis(dioxaborole)s and

fluoride is reversible. The cross-reactivity of bis(dioxaborole)s to different Lewis bases validate the compounds as adaptable sensors, providing insights into the design of bis(dioxaborole)-based sensor arrays to detect Lewis bases, which is detailed in Chapter 3.

2.3 EXPERIMENTAL

2.3.1 MATERIALS

9,9-didodecylfluorene-2,7-diboronic acid, 9,9-dihexylfluorene-2,7-diboronic acid, 4-nitrocatechol, and sodium percarbonate, were purchased from Sigma-Aldrich. Catechol, 2-hydroxy-4-methoxybenzaldehyde, tin and 2,5-dihydroxy-1,4-benzoquinone were purchased from Acros. Pinacol was purchased from Alfa Aesar. Acetic acid, ethyl ether, hydrochloric acid, sodium bicarbonate, sodium chloride, and magnisium sulfate, were purchased from Fisher Scientific. All chemicals were used without further purification. Toluene, tetrahydrofuran, dichloromethane and acetonitrile were obtained by using purification systems from Innovative Technologies.

2.3.2 INSTRUMENTATION

FT-IR spectra were performed on a PerkinElmer Spectrum 100 FT-IR Spectrometer. Sample (~0.5 mg) was put on a diamond/ZnSe crystal. The spectrometer scanned for 4 times with a resolution of 4.00 cm^{-1} from 4000 cm^{-1} to 650 cm^{-1}. ^{1}H NMR and ^{13}C NMR spectra were collected on a Varian Mercury/VX 300 MHz Spectrometer. Mass spectra were obtained on a VG 70S Mass Spectrometer and the sample was introduced by direct exposure probe. Absorbance data were recorded on a Beckman

Coulter 640 DU Spectrophotometer. Fluorescence data were recorded on a Cary Eclipse Fluorescence Spectrophotometer.

2.3.3 SYNTHESIS

2.3.3.1 SYNTHESIS OF BIS(DIOXABOROLE) ***2.1***

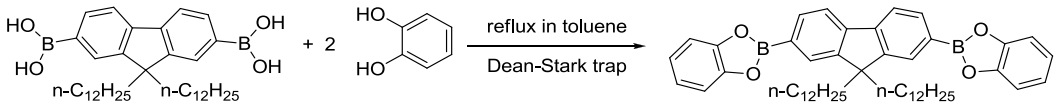

Glassware was first oven dried overnight. The starting materials were a mixture of 9,9-didodecylfluorene-2,7-diboronic acid (0.2960 g, 0.5 mmol) and catechol (0.1238 g, 1.1 mmol). In a round-bottom flask with a Dean-Stark trap, starting materials as well as 50 mL of distilled toluene were added. The solution was refluxed overnight under a nitrogen atmosphere. The resultant clear solution was cooled to room temperature. Then toluene was removed by rotavap and the crude product was further purified by Kugelrohr distillation. The product was a white solid (0.3784 g, quantitative). FT-IR: 2917, 2850, 1609, 1577, 1469, 1424, 1367, 1327, 1288, 1270, 1232, 1149, 1131, 1112, 1066, 1004, 911, 867, 827, 812, 738, 718, 695. ^{1}H NMR (300 MHz, $CDCl_3$, δ): 8.09 (m, 4H), 7.90 (d, J = 6.6 Hz, 2H), 7.34 (m, 4H), 7.16 (m, 4H), 2.15-2.05 (m, 4H), 1.14-1.02 (br m, 36H), 0.83 (t, J = 6.9 Hz, 6H), 0.66-0.54 (br m, 4H). ^{13}C NMR (75 MHz, $CDCl_3$, δ): 151.29, 148.79, 144.87, 134.18, 129.48, 123.03, 120.49, 112.74, 55.57, 40.48, 32.09, 30.19, 29.81, 29.77, 29.51, 29.46, 24.00, 22.88, 14.32. MS calcd for $C_{49}H_{64}B_2O_4$: 738.63; found (Direct Exposure Probe): 738.6.

2.3.3.2 SYNTHESIS OF BIS(DIOXABOROLE) ***2.2***

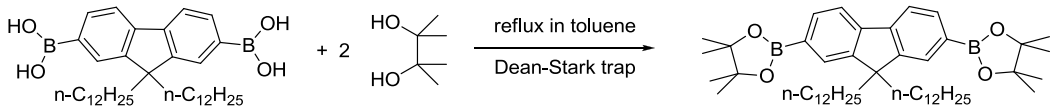

The starting materials were the mixture of 9,9-didodecylfluorene-2,7-diboronic acid (0.2949 g, 0.5 mmol) and pinacol (0.1313 g, 1.1 mmol). In a round-bottom flask fitted with a Dean-Stark trap, starting materials as well as 40 mL of distilled toluene were added. The solution was refluxed overnight under a nitrogen atmosphere. The resultant clear solution was cooled to room temperature and toluene was removed by rotavap. The crude product was further purified by using Kugelrohr distillation to remove unreacted pinacol. The product was dried under vaccum to give a white solid (0.3769 g, quantitative). FT-IR: 2922, 2851, 1609, 1576, 1469, 1424, 1346, 1308, 1269, 1142, 1117, 1079, 1004, 964, 908, 855, 825, 760, 740, 722, 708, 697, 672. ^{1}H NMR (300 MHz, $CDCl_3$, δ): 7.81-7.70 (m, 6H), 2.02-1.96 (m, 4H), 1.39 (s, 24H), 1.27-1.00 (br m, 36H), 0.86 (t, J = 6.9 Hz, 6H), 0.54 (br, 4H). ^{13}C NMR (75 MHz, $CDCl_3$, δ): 150.70, 144.13, 133.86, 129.14, 119.59, 83.93, 55.39, 40.34, 32.11, 30.22, 29.82, 29.54, 29.47, 29.15, 23.89, 22.90, 14.33. MS calcd for $C_{49}H_{80}B_2O_4$: 754.75; found (Direct Exposure Probe): 754.5.

2.3.3.3 SYNTHESIS OF BIS(DIOXABOROLE) ***2.3***

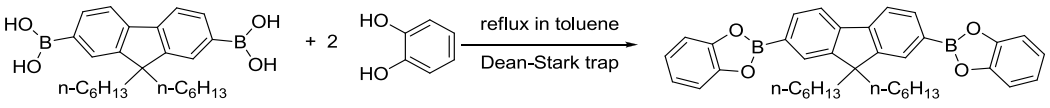

The starting materials, a mixture of 9,9-dihexylfluorene-2,7-diboronic acid (0.2109 g, 0.4996 mmol), catechol (0.1198 g, 1.1 mmol) as well as 40 mL of distilled toluene were placed in a round-bottom flask with a Dean-Stark trap. The solution was

refluxed overnight under a nitrogen atmosphere. The resultant clear solution was cooled to room temperature. Then toluene was removed by rotary evaporation and the crude product was further purified by Kugelrohr distillation. The product was a white solid (0.2098 g, yield 73.64%). FT-IR: 2954, 2928, 2854, 1609, 1577, 1468, 1425, 1366, 1327, 1285, 1235, 1129, 1114, 1065, 1004, 911, 867, 854, 830, 812, 798, 734, 690. ^{1}H NMR (300 MHz, $CDCl_3$, δ): 8.13-8.09 (m, 4H), 7.90 (d, J = 7.5 Hz, 2H), 7.35 (m, 4H), 7.15 (m, 4H), 2.14-2.09 (m, 4H), 1.09-1.03 (br m, 12H), 0.73 (t, J = 6.6 Hz, 6H), 0.61 (br, 4H). ^{13}C NMR (75 MHz, $CDCl_3$, δ): 151.29, 148.79, 144.86, 134.18, 129.47, 123.03, 120.50, 112.75, 55.57, 40.56, 31.73, 29.92, 24.03, 22.78, 14.19. MS calcd for $C_{37}H_{40}B_2O_4$: 570.31; found (Direct Exposure Probe): 570.0.

2.3.3.4 SYNTHESIS OF 4-METHOXYCATECHOL

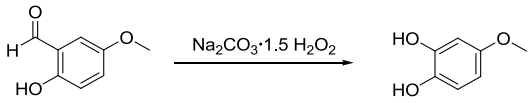

The diol, 4-methoxycatechol, was synthesized by using a literature procedure with some modifications.[12] A mixture of 0.4567 g of 2-hydroxy-4-methoxybenzaldehyde and 0.9443 g of sodium percarbonate were dissolved in a mixture of 8 mL of tetrahydrofuran and 4 mL of water. The resultant solution was sonicated under an argon atmosphere for 1 hour. The reaction was quenched with 2 mL of acetic acid and was extracted by 70 mL of diethyl ether under nitrogen. The organic layer was sequentially washed twice with 15 mL of 1 M hydrogen chloride, 25 mL of water, 25 mL of saturated sodium bicarbonate, 25 mL of saturated sodium chloride. Then the solution was dried by magnesium sulfate and the solvent was removed by rotary evaporation. The product was dried under vaccum to give a white solid (0.2856 g, yield 67.89 %). ^{1}H NMR (300 MHz, CD_3OD, δ):

6.66 (d, J = 8.7 Hz, 1H), 6.39 (d, J = 3.0 Hz, 1H), 6.24 (dd, J = 8.4, 3.0 Hz, 1H), 3.67 (s, 3H).

2.3.3.5 SYNTHESIS OF BIS(DIOXABOROLE) ***2.4***

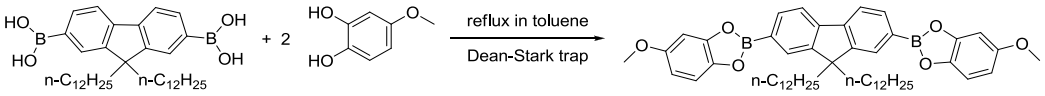

4-Methoxycatechol was used as synthesized above without further purification. The starting materials, a mixture of 9,9-didodecylfluorene-2,7-diboronic acid (0.2948 g, 0.4992 mmol) and 4-methoxycatechol (0.1551 g, 1.1 mmol), as well as 40 mL of distilled toluene were placed in a round-bottom flask with a Dean-Stark trap. The solution was refluxed overnight under a nitrogen atmosphere. The resultant clear solution was cooled to room temperature. Then toluene was removed by rotavap and the crude product was further purified by Kugelrohr distillation. The product was a yellow solid (0.4153 g, quantitative). FT-IR: 2923, 2852, 1609, 1577, 1490, 1422, 1353, 1335, 1319, 1269, 1253, 1230, 1191, 1157, 1133, 1086, 1064, 1027, 938, 824, 791, 741, 693. ^{1}H NMR (300 MHz, $CDCl_3$, δ): 8.11-8.06 (m, 4H), 7.89 (d, J = 7.5 Hz, 2H), 7.20 (d, J = 8.7 Hz, 2H), 6.96 (d, J = 2.4 Hz, 2H), 6.68 (dd, J = 8.4, 2.7 Hz, 2H), 3.84 (s, 6H), 2.12-2.07 (m, 4H), 1.25-1.02 (br m, 36H), 0.83 (t, J = 6.9 Hz, 6H), 0.70-0.50 (br m, 4H). ^{13}C NMR (75 MHz, $CDCl_3$, δ): 156.18, 151.25, 149.44, 144.79, 142.88, 134.07, 129.37, 120.46, 112.15, 107.94, 99.91, 56.26, 55.54, 40.47, 32.09, 30.18, 29.80, 29.76, 29.51, 29.45, 23.98, 22.87, 14.31. MS calcd for $C_{51}H_{68}B_2O_6$: 798.70; found (Direct Exposure Probe): 799.0.

2.3.3.6 SYNTHESIS OF BIS(DIOXABOROLE) ***2.5***

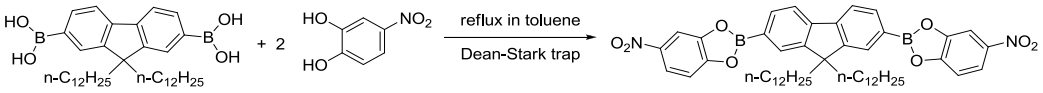

The starting materials were the mixture of 9,9-didodecylfluorene-2,7-diboronic acid (0.2959 g, 0.5011 mmol) and 4-nitrocatechol (0.1680 g, 1.08 mmol). In a round-bottom flask with a Dean-Stark trap, starting materials as well as 40 mL of distilled toluene were added. The solution was refluxed overnight under a nitrogen atmosphere. The resultant clear solution was cooled to room temperature. Then toluene was removed by rotavap and the crude product was further purified by Kugelrohr distillation. The product was a yellow solid (0.4152 g, yield 93.69%). FT-IR: 2922, 2852, 1609, 1576, 1524, 1470, 1422, 1378, 1330, 1256, 1231, 1131, 1117, 1066, 1053, 1004, 934, 876, 818, 747, 730, 686. ^{1}H NMR (300 MHz, $CDCl_3$, δ): 8.24-8.11 (m, 8H), 7.95 (d, J = 7.8 Hz, 2H), 7.46 (d, J = 8.7 Hz, 2H), 2.16-2.10 (m, 4H), 1.25-1.03 (br m, 36H), 0.83 (t, J = 6.9 Hz, 6H), 0.66-0.54 (br m, 4H). ^{13}C NMR (75 MHz, $CDCl_3$, δ): 153.92, 151.55, 148.80, 145.39, 144.03, 134.56, 129.75, 120.88, 120.29, 112.32, 108.98, 55.68, 40.41, 32.07, 30.13, 29.80, 29.76, 29.71, 29.51, 29.44, 24.01, 22.86, 14.30. MS calcd for $C_{49}H_{62}B_2N_2O_8$: 828.65; found (Direct Exposure Probe): 828.0.

2.3.3.7 SYNTHESIS OF 1,2,4,5-TETRAHYDROXYBENZENE (THB)

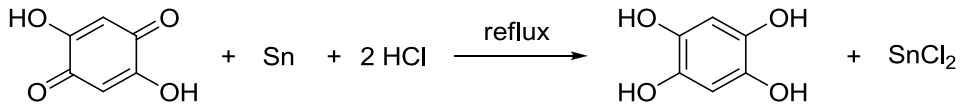

THB was synthesized by using a literature procedure with some modifications.[13] To a 500 mL of round-bottom flask, 150 mL of concentrated hydrochloric acid, 20.0100 g (0.1428 mol) of 2,5-dihydroxy-1,4-benzoquinone and 20.2814 g (0.1428 mol) of metal

tin were sequentially added. The mixture was heated to reflux for 2 hours and turned green. The solution was cooled to room temperature and put in the freezer at 0 ℃ for 17 hours. The resultant solid was collected by suction filtration to generate the crude product. After being recrystallized twice from THF, the white crystals were dried under vaccum to afford the pure product (9.6250 g, 47.46 %). FT-IR: 3182, 1552, 1535, 1473, 1369, 1346, 1297, 1219, 1160, 1056, 1033, 862, 845, 837, 714. ^{1}H NMR (300 MHz, CDOD, δ): 6.32 (s, 2H).

2.3.3.8 SYNTHESIS OF POLY(DIOXABOROLE) ***2.6***

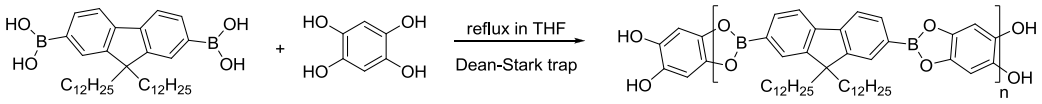

To a mixture of 177.1 mg (0.3 mmol) of 9,9-didodecylfluororene-2,7-diboronic acid and 47.4 mg (0.33 mmol) of recrystallized THB in a round bottom flask fitted with a Dean-Stark trap, 50 mL of distilled THF was added. Under a nitrogen atmosphere, this mixture was refluxed for 15 minutes and cooled to room temperature. Insoluble material was filtrated to yield a light yellowish solution. THF was then removed by rotary evaporator. The resulting solid was washed with distilled acetonitrile and collected by suction filtration to yield a brown yellow powder (71.6 mg, 36.1%). FT-IR: 2922, 2852, 1608, 1577, 1463, 1420, 1349, 1318, 1128, 1061, 1004, 844, 826, 741, 688. ^{1}H NMR (300 MHz, $CDCl_3$, δ): 8.11 (m, 4H), 7.93 (d, J = 6.6 Hz, 2H), 7.41 (s, 2H), 2.16 (m, 4H), 1.16-1.05 (br m, 36H), 0.83 (t, J = 6.0 Hz, 6H), 0.62 (m, 4H).

2.3.4 COMPUTATIONAL CALCULATIONS

Computational calculations were performed by using Spartan 08. The geometries were first optimized using semi-empirical AM1 calculations. The molecular orbitals and band gap energies were calculated using DFT B3LYP with a 6-31G* basis set. Band gaps were calculated as the difference in energies between HOMO and LUMO.

2.3.5 ABSORPTION TITRATIONS

Dichloromethane was used as a solvent and stock solutions were made in volumetric flasks. The solution of bis(dioxaborole) **2.1(-H)**, **2.4(-OCH_3)** or **2.5(-NO_2)** (10^{-5} M, 2 mL in a quartz cuvette) was titrated with the incremental amounts (3-5 μL) of a TBAF solution by a microinjector. Then absorbance data were recorded on an absorption spectrophotometer.

2.3.6 FLUORESCENCE TITRATIONS

The CH_2Cl_2 solution of bis(dioxaborole) **2.1(-H)** or **2.4(-OCH_3)** (10^{-6} M, 2 mL in a quartz cuvette) was titrated with the incremental amounts (3-5 μL) of a TBAF solution by a microinjector. Then fluorescence data were recorded on a fluorescence spectrophotometer.

2.4 REFERENCES

1 Cai, M.; Daniel, S. L.; Lavigne, J. J. Conjugated bis and poly(dioxaborole)s for optical sensing of Lewis bases based on main-chain perturbations. *Chem. Commun.*, **2013**, *49*, 6504-6506. Reproduced by permission of The Royal Society of Chemistry. http://pubs.rsc.org/en/content/articlelanding/2013/CC/c3cc41189c#!divAbstract

[2] Zhou, Q.; Swager, T. M. Fluorescent chemosensors based on energy migration in conjugated polymers: the molecular wire approach to increased sensitivity. *J. Am. Chem. Soc.*, **1995**, *117*(50), 12593-12602.

[3] (a) Liu, Y.; Ogawa, K.; Schanze K. S. Conjugated polyelectrolytes as fluorescent sensors. *J. Photochem. Photobiol. C: Photochem. Rev.*, **2009**, *10*, 173-190. (b) Thomas III, S. W.; Joly, G. D.; Swager, T. M. Chemical sensors based on amplifying fluorescent conjugated polymers. *Chem. Rev.*, **2007**, *107* (4), 1339-1386.

[4] Lee, K.; Povlich, L. K.; Kim, J. Recent advances in fluorescent and colorimetric conjugated polymer-based biosensors. *Analyst*, **2010**, *135*, 2179-2189.

[5] Wang, B.; Wasielewski, M. R. Design and synthesis of metal ion-recognition-induced conjugated polymers: an approach to metal ion sensory materials. *J. Am. Chem. Soc.*, **1997**, *119*(1), 12-21.

[6] Miyata, M.; Chujo, Y. π-Conjugated organoboron polymer as an anion sensor. *Polym. J.*, **2002**, *34*(12), 967-969.

[7] Bonifácio, V. D. B.; Morgado, J.; Scherf, U. Polyfluorenes with on-chain dibenzoborole units-synthesis and anion-induced photoluminescence quenching. *J. Polym. Sci., Part A: Polym. Chem.*, **2008**, *46*, 2878-2883.

[8] Li, H.; Jäkle, F. Universal scaffold for fluorescent conjugated organoborane polymers. *Angew. Chem., Int. Ed*., **2009**, *48*, 2313-2316.

[9] Sundararaman, A.; Victor, M.; Varughese, R.; Jäkle, F. A family of main-chain polymeric Lewis acids: synthesis and fluorescent sensing properties of boron-modified polythiophene. *J. Am. Chem. Soc.*, **2005**, *127*(40), 13748-13749.

[10] Jäkle, F. Advances in the synthesis of organoborane polymers for optical, electronic, and sensory applications. *Chem. Rev.*, **2010**, *110*(7), 3985-4022.

[11] (a) Niu, N.; Smith, M. D.; Lavigne, J. J. Self-assembling poly(dioxaborole)s as blue-emissive materials. *J. Am. Chem. Soc.*, **2006**, *128*(51), 16466-16467. (b) Niu, W. J.; Rambo, B.; Smith, M. D.; Lavigne, J. J., Substituent effects on the structure and supramolecular assembly of bis(dioxaborole)s. *Chem. Commun.* **2005**, (41), 5166-5168. (c) Niu, W.; Rambo, B. M.; Smith, M. D.; Lavigne, J. J., Self-assembling polymeric and oligomeric borole materials. *Polym. Mater. Sci. Eng.* **2005**, *91*, 147-148. (d) Niu, W. J.;

Smith, M. D.; Lavigne, J. J., Substituent effects on the structure and supramolecular assembly of bis(dioxaborole)s derived from 1,2,4,5-tetrahydroxybenzene. *Cryst. Growth & Des.* **2006**, *6*(6), 1274-1277. (e) Rambo, B. M.; Lavigne, J. J., Defining self-assembling linear oligo(dioxaborole)s. *Chem. Mater.* **2007**, *19*(15), 3732-3739.

[12] Lanni, L. M.; Tilford, R. W.; Bharathy, M.; Lavigne J. J. Enhanced hydrolytic stability of self-assembling alkylated 2-dimensional covalent organic frameworks. *J. Am. Chem. Soc*. **2011**, *133*(35), 13975-13983.

[13] Kabalka, G. W.; Reddy, N. K.; Narayana, C. Sodium percarbonate: a convenient reagent for the Dakin reaction. *Tetrahedron Lett.* **1992**, *33*, 865-866.

[14] Weider, P. R.; Hegedus, L. S.; Asada, H.; D'Andreq, S. V. Oxidative cyclization of unsaturated aminoquinones. Synthesis of quinolinoquinones. Palladium-catalyzed synthesis of pyrroloindoloquinones. *J. Org. Chem.* **1985**, *50*(22), 4276-4281.

[15] Mohammed, O. F.; Vauthey, E. Excited-state dynamics of nitroperylene in solution: solvent and excitation wavelength dependence. *J. Phy. Chem. A.* **2008,** *112*(17), 3823-3830.

[16] Lavigne, J. J. Molecular recognition and molecular sensing: single analyte analysis and multi-component sensor arrays for the simultaneous detection of a plethora of analytes. Ph.D. Thesis, The University of Texas at Austin, Austin, TX, August 2000.

[17] (a) Hargrove, A. E.; Zhong, Z.; Sessler, J. L.; Anslyn, E. V. Algorithms for the determination of binding constants and enantiomeric excess in complex host:guest equilibria using optical measurements. *New J. Chem.* 2010, **34**, 348-354. (b) Absorption titration worksheet (guest:host of 2:1) was used, with permission of Dr. Ken D. Shimizu in University of South Carolina, Columbia. The worksheet was found at http://www.chem.sc.edu/faculty/shimizu/Site/Group%20Stuff.html.

[18] (a) Arimori, S.; Davidson, M. G.; Fyles, T. M.; Hibbert, T. G.; James, T. D.; Kociok-Köhn, G. I. Synthesis and structural characterization of the first bis(bora)calixarene: a selective, bidentate, fluorescent fluoride sensor. *Chem. Commun.*, **2004**, 1640-1641. (b) Neumann, T.; Dienes, Y.; Baumgartner, T. Highly sensitive sensory materials for fluoride ions based on the dithieno[3,2-b:2',3'-d]phosphole system. *Org. Lett.*, **2006**, *8*(3), 495-497. (c) Liu, W.; Pink, M.; Lee, D. Conjugated polymer sensors built on π-extended borasiloxane cages. *J. Am. Chem. Soc.*, **2009**, *131*(24), 8703-8707.

[19] Hall, H. K., Jr. Correlation of the base strengths of amines. *J. Am. Chem. Soc.*, **1957**, *79*(20), 5441-5444.

CHAPTER 3

BIS(DIOXABOROLE)-BASED CROSS-REACTIVE SENSOR ARRAY FOR ANION DIFFERENTIATION

3.0 INTRODUCTION

The understanding of environment, industry, biology and medicine is in demand of multiple analyte sensing.[1] Recently, cross-reactive sensor arrays have been developed to differentiate multiple analytes. These arrays have interactions with structurally-similar analytes and produce different signals to generate the fingerprint patterns. These patterns can then be differentiated by statistical techniques.[2] By incorporation of optical detection methods, sensor arrays have been successfully applied to detect cations, small organic molecules and biologically relevant analytes.[2] However, sensors arrays that can distinguish anions are rare.

Anions play important roles in environment, industry, biology and our life.[3] However, anions are quite difficult to sense and discriminate based on the following reasons.[1] First, anions have low charge-to-radius ratios, allowing the ineffective binding to receptors. Second, anions have various geometries and charges, which make it hard to design anion receptors. Third, anions have high free energy of salvation, allowing receptors to compete with water when binding with anions. Thus, anions in aqueous

solutions are quite difficult to sense. Although a few sensor arrays have been reported to detect anions, they suffer from complicated synthetic[1] and detection procedures[3].

Boronate ester formation, with its covalent yet reversible nature, provides the attributes for sensory materials, including facile synthesis,[4a] hydrolytic[5] and oxidative stability, and planar geometries. In Chapter 2, a series of bis(dioxaborole)s were designed, synthesized, and characterized. The further evaluation of sensing mechanism showed that those Lewis acidic bis(dioxaborole)s were cross-reactive to Lewis bases, including anions and amines.

Herein, we reason that whether bis(dioxaborole)s can be used in a sensor array to discriminate anions. To establish a proof of concept, three bis(dioxaborole)-based sensors **3.1-3.3** (**Figure 3.1**) were used to form a sensor array. Nine anions (F^-, Cl^-, Br^-, $H_2PO_4^-$, HSO_4^-, BF_4^-, NO_3^-, PF_6^- and CN^-) with tetra-n-butylammonium as the cation were selected as the analyte pool. The sensing performance of bis(dioxaborole)-based sensor array for anions is studied below by absorption plate reader and statistical methods.

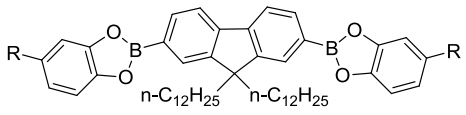

3.1, R = H
3.2, R = OCH_3
3.3, R = NO_2

Figure 3.1 Structures of bis(dioxaborole)s used in the sensor array.

3.1 Results and Discussion

3.1.1 Anion differentiation by sensor array

The absorption spectra of each sensor **3.1-3.3** in response to 9 anions in chloroform are shown in **Figure 3.2**. The sensors response differently to anions,

indicating these sensors are cross-reactive to anions. The sensors form unique patterns of sensor array by multiple wavelengths scanning across the entire spectra. The dimensionality of sensor array is increased by different sensors and multiple wavelengths.

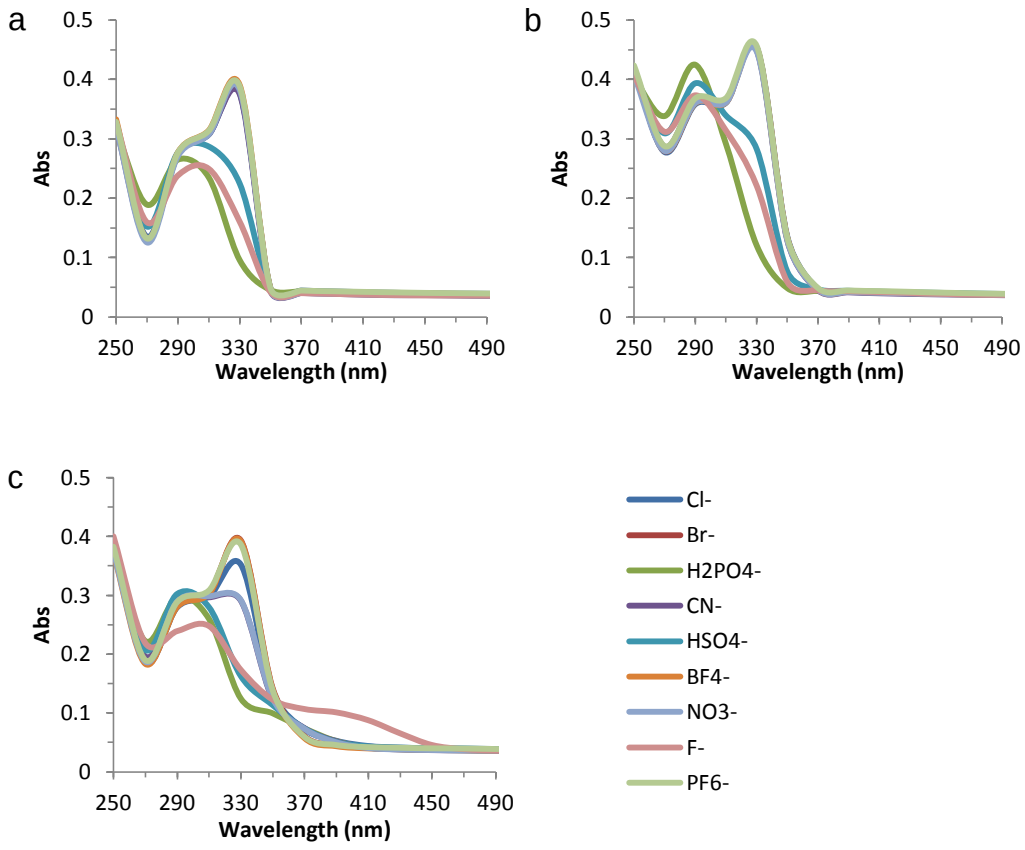

Figure 3.2 Absorption spectra of sensors (10^{-5} M) of (a) **3.1**, (b) **3.2** and (c) **3.3** sensing anions (2×10^{-5} M) in chloroform.

The sensor array to each anion is based on 21 dimensional responses (3 sensors × 7 wavelengths). Wavelengths are selected per 40 nm in the range of 250-490 nm. 594 absorption measurements (22 replicates × 9 analytes × 3 sensors) are carried out for data collection.

Multiple dimensional responses were analyzed by statistical technique of linear discriminate analysis (LDA) in the software of SYSTAT. LDA minimizes the variation within each anion, maximizing the differences between different anions. As shown in **Figure 3.3a**, the 2-D (two-dimensional) LDA plot successfully differentiates nine different anions. The plot reduces the original 21 dimensional data sets to two dimensions. In the plot, each symbol represents the response pattern for one anion replicate and each circle shows a 95% confidence limit, while the axis shows the weighted combination of 21 dimensions.

The 2-D LDA plot also indicates the relationship between analyte structures and sensing responses. For example, the sensor array is selective to F^-, which is a very hard Lewis base. It is also selective to $H_2PO_4^-$ and HSO_4^-, due to their hard binding atoms with hard Lewis acidic boron centers. However, $H_2PO_4^-$ and HSO_4^- are close to each other in the plot, because they have similar structures of multivalent bases. The sensor array is cross-reactive to other anions. But it shows differences between relatively hard bases (Cl^-, CN^- and NO_3^-) and soft bases (Br^-, BF_4^- and PF_6^-).

The Jackknifed classification matrix treats each anion as unknown and is put back to the new training set by the remaining measurements. It is shown that the anion discrimination is accurate with a classification accuracy of 99% (**Figure 3.3b**). The accuracy means that 188 anions out of 198 anion analytes can find the right group. However, the discrimination of CN^- and PF_6^- has a classification accuracy of 95%, because the similar structure or/and Lewis basicity between CN^- and NO_3^- as well as Br^- and PF_6^-.

a

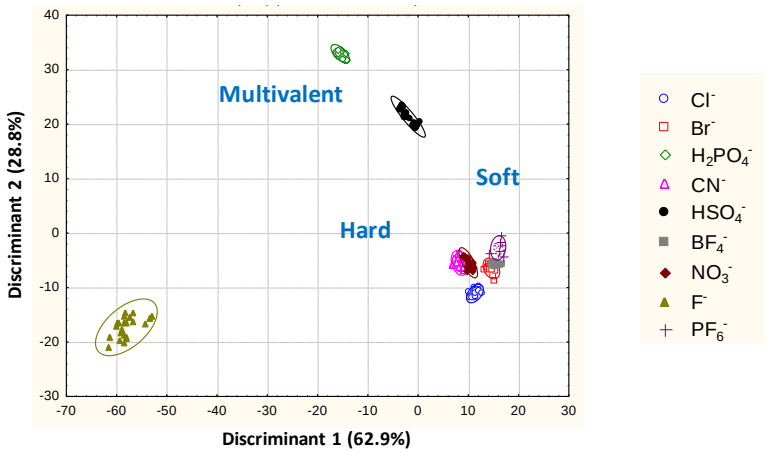

b

Group	BF_4^-	Br^-	CN^-	Cl^-	F^-	$H_2PO_4^-$	HSO_4^-	NO_3^-	PF_6^-	**%Correct**
BF_4^-	22	0	0	0	0	0	0	0	0	**100**
Br^-	0	22	0	0	0	0	0	0	0	**100**
CN^-	0	0	21	0	0	0	0	1	0	**95**
Cl^-	0	0	0	22	0	0	0	0	0	**100**
F^-	0	0	0	0	22	0	0	0	0	**100**
$H_2PO_4^-$	0	0	0	0	0	22	0	0	0	**100**
HSO_4^-	0	0	0	0	0	0	22	0	0	**100**
NO_3^-	0	0	0	0	0	0	0	22	0	**100**
PF_6^-	0	1	0	0	0	0	0	0	21	**95**
Total	**22**	**23**	**21**	**22**	**22**	**22**	**22**	**23**	**21**	**99**

Figure 3.3 (a) 2-D LDA plot of discrimination of nine anions by sensor array based on bis(dioxaborole) **3.1-3.3**. (b) Jackknifed classification matrix for sensor array.

3.1.2 Effect of Sensors

The performance of different sensors in the sensor array was investigated. One sensor was removed and the remaining two sensors form a new sensor array to differentiate nine anions. The sensor array without bis(dioxaborole) **3.3** differentiates $H_2PO_4^-$, HSO_4^- and F^- well (**Figure 3.4a**). However, it does not discriminate other anions, which cluster together in the 2-D LDA plot. The Jackknifed classification matrix shows a poor classification accuracy of 82%. The other two sensor arrays with **3.3** discriminates nine anions well (**Figure 3.4b,c**) with a classification accuracy of 99% and 98%, respectively. These results indicate the powerful ability of bis(dioxaborole) **3.3** to

discriminate anions, especially those cross-reactive anions, due to its strong Lewis acidity of boron centers increased by the electron-withdrawing nitro groups.

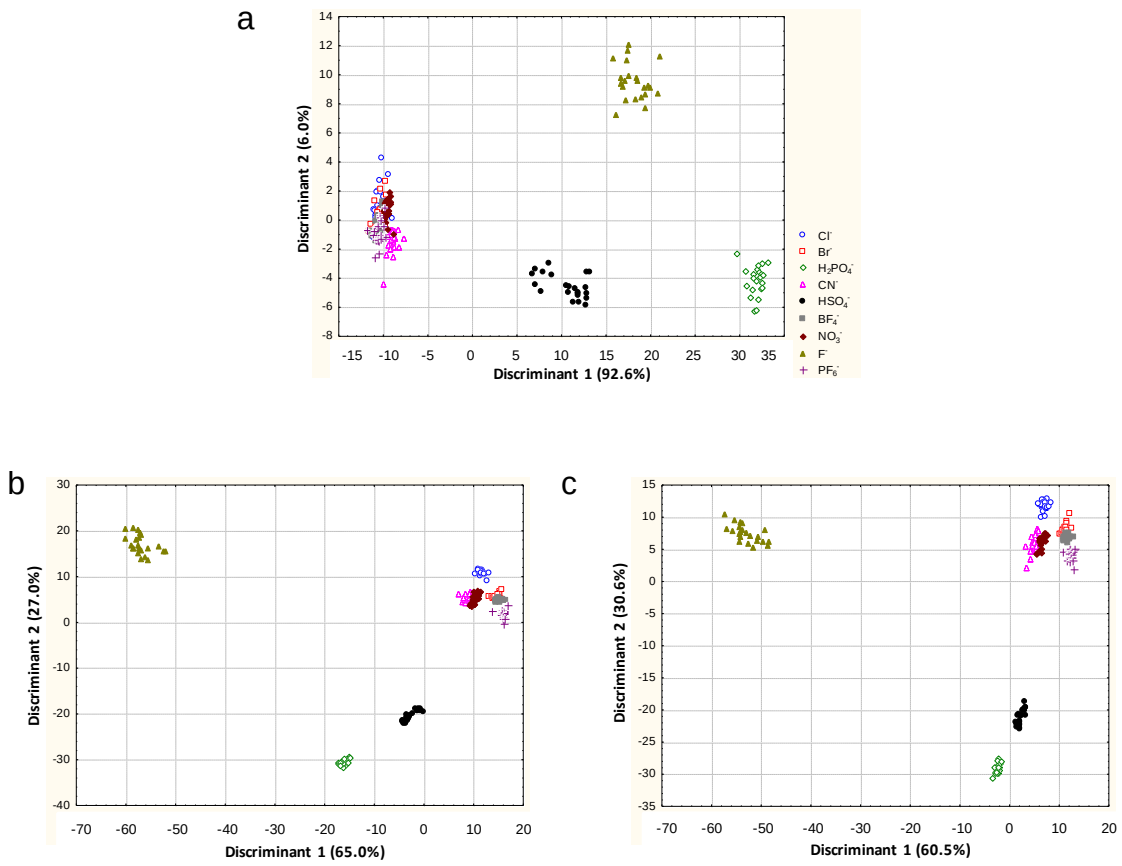

Figure 3.4 2-D LDA plot of anion discrimination by sensor array based on bis(dioxaborole) (a) **3.1** and **3.2**, (b) **3.2** and **3.3**, and (c) **3.1** and **3.3**.

The effect of each individual sensor on sensor array was also studied. All the three sensor arrays are able to differentiate $H_2PO_4^-$, HSO_4^- and F^-. However, the sensor array-based on bis(dioxaborole) **3.1** and **3.2** shows a poor discrimination of other cross-reactive anions clustering together in the plot (**Figure 3.5a,b**). The Jackknifed classification matrix shows a poor classification accuracy of 66% and 80% for sensor array based on **3.1** or **3.2**, respectively. However, the sensor array based on **3.3**

discriminates all the anions well with a classification accuracy of 96%. These results confirmed the strong discrimination ability of Lewis acidic bis(dioxaborole) **3.3**. It is also shown that the weak Lewis acidic bis(dioxaborole) **3.2** is important to discriminate strong multivalent Lewis bases $H_2PO_4^-$ and HSO_4^-, while the strong acidic bis(dioxaborole) **3.3** is good at differentiating the relatively weak soft anions.

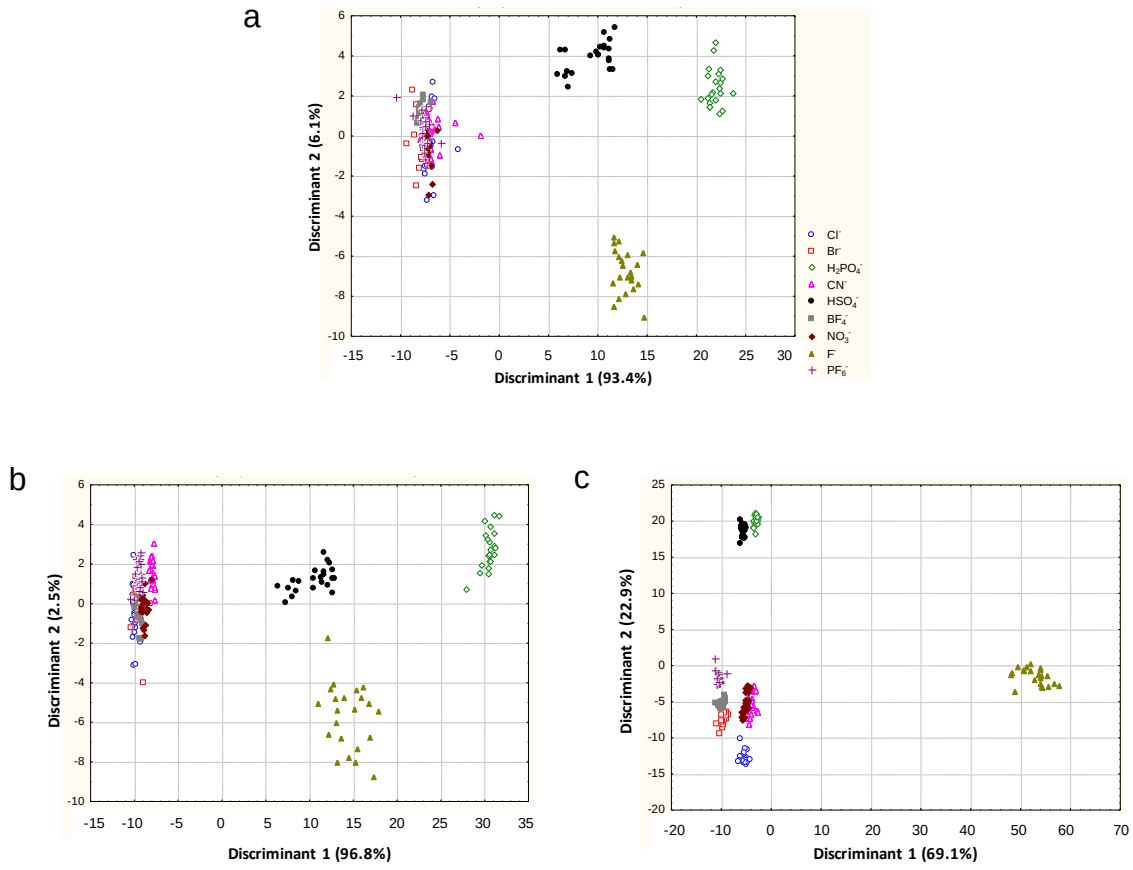

Figure 3.5 2-D LDA plot of discrimination of nine anions by sensor array based on bis(dioxaborole) (a) **3.1**, (b) **3.2**, and (c) **3.3**.

3.1.3 Effect of Wavelengths

The effect of changing the wavelength may influence the dimensions of sensor array and its differentiation ability. Thus, different wavelengths are selected to study

their effect on the discrimination ability of sensor arrays based on bis(dioxaborole) **3.1-3.3**. However, the sensor array shows an excellent classification accuracy of over 98% toward nine anions, at a range of different wavelengths (**Table 3.1**). These results indicate that the selection of wavelengths has little effect on anion differentiation.

Table 3.1 Classification accuracy for sensor array based on bis(dioxaborole) **3.1-3.3** toward anions

Wavelength	% Correct
250-490nm, 40 nm/scan, 7 wavelengths	99
250-510 nm, 20 nm/scan, 14 wavelengths	99
270-390 nm, 20 nm/scan, 7 wavelengths	99
Sensor **3.1**: 290 nm, sensor **3.2**: 290, 330 nm, sensor **3.3**: 250, 290, 330, 370, 410, 450 nm, 9 wavelengths	98

3.2 CONCLUSION

In summary, a cross-reactive sensor array based on bis(dioxaborole)s was developed to differentiate anions. The sensor array discriminated nine anions in chloroform by using absorption spectroscopy and LDA statistical analysis. The Jackknifed classification matrix showed that the anion discrimination is accurate with a classification accuracy of 99%. The investigation of sensor arrays based on one or two sensors indicated the powerful discrimination ability of nitro- bis(dioxaborole).

3.3 EXPERIMENTAL

3.3.1 MATERIALS

Bis(dioxabrole) **3.1-3.3** were synthesized according to the methods described in Chapter 2. Tetra-n-butyl ammonium fluoride (1M in THF), tetra-n-butyl ammonium bromide, tetra-n-butyl ammonium hydrogensulfate, and tetra-n-butyl ammonium cyanide

were purchased from Sigma-Aldrich. Tetra-n-butyl ammonium phosphate, tetra-n-butyl ammonium tetrafluoroborate, tetra-n-butyl ammonium nitrate, and tetra-n-butyl ammonium hexafluorophosphate were purchased from VWR. Chloroform (HPLC grade, 99.8%) was purchased from Acros. All chemicals were used without further purification.

3.3.2 INSTRUMENTATION

Absorption measurements were carried out in a quartz 96-well microplate from Hellma. Absorption data were recorded on a SpectraMax M_2^e from Molecular Devices. LDA statistical data were analyzed by using SYSTAT Software, Version 11.00.01. 2-D LDA plots were made by using Statistica Software, Version 6.1.

3.3.3 ABSORPTION MEASUREMENT

Solutions of each sensor (10^{-5} M) were made by chloroform in volumetric flasks. Solutions of each anion (1.2×10^{-3} M) were also made. To each well of 96-well microplate, 300 μL of sensor and 5 μL of anion solution were added. The concentration of sensor was kept at 10^{-5} M, while the concentration of anion was kept at 2×10^{-5} M. For each anion, 22 replicates were made. Each absorption measurement was scanned per 20 nm in the range of 250-510 nm by a plate reader. 594 absorption measurements (22 replicates $\times$ 9 analytes $\times$ 3 sensors) are carried out for data collection.

3.3.4 DATA ANALYSIS

The collected absorption data were processed by using the LDA statistical package provided by SYSTAT Software. 2-D LDA plots were processed by using

Statistica Software. The Jackknifed classfication matrixes for each sensor array are listed in **Table 3.2-3.10**.

Table 3.2 Jackknifed classification matrix for sensor array based on **3.1** and **3.2**

Group	BF_4^-	Br^-	CN^-	Cl^-	F^-	$H_2PO_4^-$	HSO_4^-	NO_3^-	PF_6^-	**%Correct**
BF_4^-	17	4	0	0	0	0	0	1	0	**77**
Br^-	6	9	1	2	0	0	0	4	0	**41**
CN^-	1	0	15	2	0	0	0	2	2	**68**
Cl^-	0	3	1	18	0	0	0	0	0	**82**
F^-	0	0	0	0	22	0	0	0	0	**100**
$H_2PO_4^-$	0	0	0	0	0	22	0	0	0	**100**
HSO_4^-	0	0	0	0	0	0	22	0	0	**100**
NO_3^-	2	0	2	1	0	0	0	17	0	**77**
PF_6^-	1	0	0	1	0	0	0	0	20	**91**
Total	**27**	**16**	**19**	**24**	**22**	**22**	**22**	**24**	**22**	**82**

Table 3.3 Jackknifed classification matrix for sensor array based on **3.2** and **3.3**

Group	BF_4^-	Br^-	CN^-	Cl^-	F^-	$H_2PO_4^-$	HSO_4^-	NO_3^-	PF_6^-	**%Correct**
BF_4^-	22	0	0	0	0	0	0	0	0	**100**
Br^-	1	21	0	0	0	0	0	0	0	**95**
CN^-	0	0	21	0	0	0	0	1	0	**95**
Cl^-	0	0	0	22	0	0	0	0	0	**100**
F^-	0	0	0	0	22	0	0	0	0	**100**
$H_2PO_4^-$	0	0	0	0	0	22	0	0	0	**100**
HSO_4^-	0	0	0	0	0	0	22	0	0	**100**
NO_3^-	0	0	0	0	0	0	0	22	0	**100**
PF_6^-	0	0	0	0	0	0	0	0	22	**100**
Total	**23**	**21**	**21**	**22**	**22**	**22**	**22**	**23**	**22**	**99**

Table 3.4 Jackknifed classification matrix for sensor array based on **3.1** and **3.3**

Group	BF_4^-	Br^-	CN^-	Cl^-	F^-	$H_2PO_4^-$	HSO_4^-	NO_3^-	PF_6^-	**%Correct**
BF_4^-	22	0	0	0	0	0	0	0	0	**100**
Br^-	0	22	0	0	0	0	0	0	0	**100**
CN^-	0	0	20	0	0	0	0	2	0	**91**
Cl^-	0	0	0	22	0	0	0	0	0	**100**
F^-	0	0	0	0	22	0	0	0	0	**100**
$H_2PO_4^-$	0	0	0	0	0	22	0	0	0	**100**
HSO_4^-	0	0	0	0	0	0	22	0	0	**100**
NO_3^-	0	0	1	0	0	0	0	21	0	**95**
PF_6^-	0	0	0	0	0	0	0	0	22	**100**
Total	**22**	**22**	**21**	**22**	**22**	**22**	**22**	**23**	**22**	**98**

Table 3.5 Jackknifed classification matrix for sensor array based on **3.1**

Group	BF_4^-	Br^-	CN^-	Cl^-	F^-	$H_2PO_4^-$	HSO_4^-	NO_3^-	PF_6^-	**%Correct**
BF_4^-	15	0	1	0	0	0	0	4	2	**68**
Br^-	4	5	1	7	0	0	0	2	3	**23**
CN^-	3	1	12	0	0	0	1	5	0	**55**
Cl^-	4	2	0	11	0	0	0	3	2	**50**
F^-	0	0	0	0	22	0	0	0	0	**100**
$H_2PO_4^-$	0	0	0	0	0	22	0	0	0	**100**
HSO_4^-	0	0	0	0	0	0	22	0	0	**100**
NO_3^-	5	0	1	0	0	0	0	16	0	**73**
PF_6^-	7	5	0	3	0	0	0	1	6	**27**
Total	**38**	**13**	**15**	**21**	**22**	**22**	**23**	**31**	**13**	**66**

Table 3.6 Jackknifed classification matrix for sensor array based on **3.2**

Group	BF_4^-	Br^-	CN^-	Cl^-	F^-	$H_2PO_4^-$	HSO_4^-	NO_3^-	PF_6^-	**%Correct**
BF_4^-	12	4	0	0	0	0	0	3	3	**55**
Br^-	3	11	1	4	0	0	0	3	0	**50**
CN^-	1	0	18	1	0	0	0	1	1	**82**
Cl^-	1	4	0	16	0	0	0	1	0	**73**
F^-	0	0	0	0	21	0	1	0	0	**95**
$H_2PO_4^-$	0	0	0	0	0	22	0	0	0	**100**
HSO_4^-	0	0	0	0	0	0	22	0	0	**100**
NO_3^-	1	3	1	1	0	0	0	16	0	**73**
PF_6^-	1	1	0	0	0	0	0	0	20	**91**
Total	**19**	**23**	**20**	**22**	**21**	**22**	**23**	**24**	**24**	**80**

Table 3.7 Jackknifed classification matrix for sensor array based on **3.3**

Group	BF_4^-	Br^-	CN^-	Cl^-	F^-	$H_2PO_4^-$	HSO_4^-	NO_3^-	PF_6^-	**%Correct**
BF_4^-	22	0	0	0	0	0	0	0	0	**100**
Br^-	0	22	0	0	0	0	0	0	0	**100**
CN^-	0	0	17	0	0	0	0	5	0	**77**
Cl^-	0	0	0	22	0	0	0	0	0	**100**
F^-	0	0	0	0	22	0	0	0	0	**100**
$H_2PO_4^-$	0	0	0	0	0	22	0	0	0	**100**
HSO_4^-	0	0	0	0	0	0	22	0	0	**100**
NO_3^-	0	0	2	0	0	0	0	20	0	**91**
PF_6^-	0	1	0	0	0	0	0	0	22	**100**
Total	**22**	**22**	**19**	**22**	**22**	**22**	**22**	**25**	**22**	**96**

Table 3.8 Jackknifed classification matrix for sensor array based on **3.1-3.3** (250-510 nm, 20 nm/scan, 14 wavelengths)

Group	BF_4^-	Br^-	CN^-	Cl^-	F^-	$H_2PO_4^-$	HSO_4^-	NO_3^-	PF_6^-	**%Correct**
BF_4^-	22	0	0	0	0	0	0	0	0	**100**
Br^-	1	21	0	0	0	0	0	0	0	**95**
CN^-	0	0	22	0	0	0	0	1	0	**100**
Cl^-	0	0	0	22	0	0	0	0	0	**100**
F^-	0	0	0	0	22	0	0	0	0	**100**
$H_2PO_4^-$	0	0	0	0	0	22	0	0	0	**100**
HSO_4^-	0	0	0	0	0	0	22	0	0	**100**
NO_3^-	0	0	0	0	0	0	0	22	0	**100**
PF_6^-	0	1	0	0	0	0	0	0	21	**95**
Total	**23**	**22**	**22**	**22**	**22**	**22**	**22**	**23**	**21**	**99**

Table 3.9 Jackknifed classification matrix for sensor array based on **3.1-3.3** (270-390 nm, 20 nm/scan, 7 wavelengths)

Group	BF_4^-	Br^-	CN^-	Cl^-	F^-	$H_2PO_4^-$	HSO_4^-	NO_3^-	PF_6^-	**%Correct**
BF_4^-	22	0	0	0	0	0	0	0	0	**100**
Br^-	1	21	0	0	0	0	0	0	0	**95**
CN^-	0	0	22	0	0	0	0	0	0	**100**
Cl^-	0	0	0	22	0	0	0	0	0	**100**
F^-	0	0	0	0	22	0	0	0	0	**100**
$H_2PO_4^-$	0	0	0	0	0	22	0	0	0	**100**
HSO_4^-	0	0	0	0	0	0	22	0	0	**100**
NO_3^-	0	0	0	0	0	0	0	22	0	**100**
PF_6^-	0	0	0	0	0	0	0	0	22	**100**
Total	**23**	**21**	**22**	**22**	**22**	**22**	**22**	**22**	**22**	**99**

Table 3.10 Jackknifed classification matrix for sensor array based on **3.1-3.3** (sensor **3.1**: 290 nm, sensor **3.2**: 290, 330 nm, sensor **3.3**: 250, 290, 330, 370, 410, 450 nm, 9 wavelengths)

Group	BF_4^-	Br^-	CN^-	Cl^-	F^-	$H_2PO_4^-$	HSO_4^-	NO_3^-	PF_6^-	**%Correct**
BF_4^-	22	0	0	0	0	0	0	0	0	**100**
Br^-	0	22	0	0	0	0	0	0	0	**100**
CN^-	0	0	19	0	0	0	0	3	0	**86**
Cl^-	0	0	0	22	0	0	0	0	0	**100**
F^-	0	0	0	0	22	0	0	0	0	**100**
$H_2PO_4^-$	0	0	0	0	0	22	0	0	0	**100**
HSO_4^-	0	0	0	0	0	0	22	0	0	**100**
NO_3^-	0	0	0	0	0	0	0	22	0	**100**
PF_6^-	0	0	0	0	0	0	0	0	22	**100**
Total	**22**	**22**	**19**	**22**	**22**	**22**	**22**	**25**	**22**	**98**

3.4 REFERENCES

[1] Nishiyabu, R.; Palacios, M. A.; Dehaen, W.; Anzenbacher, Jr. P. Synthesis, structure, anion binding, and sensing by calix[4]pyrrole isomers. *J. Am. Chem. Soc.*, **2006**, *128*, 11496-11504.

[2] Li, X. Development of conjugated boronate ester-linked materials for optical sensing applications targeting small molecules. Ph.D. Thesis, University of South Carolina, Columbia, SC, 2012.

[3] Feng, L.; Li, H.; Li, X.; Chen, L.; Shen, Z.; Guan, Y. Colorimetric sensing of anions in water using ratiometric indicator-displacement assay. *Anal. Chim. Acta*, **2012**, *743*, 1-8.

[4] (a) Niu, W.; Smith, M. D.; Lavigne, J. J. Self-assembling poly(dioxaborole)s as blue-emissive materials. *J. Am. Chem. Soc.*, **2006**, *128*(51), 16466-16467. (b) Niu, W. J.; Rambo, B.; Smith, M. D.; Lavigne, J. J., Substituent effects on the structure and supramolecular assembly of bis(dioxaborole)s. *Chem. Commun.* **2005**, (41), 5166-5168. (c) Niu, W.; Rambo, B. M.; Smith, M. D.; Lavigne, J. J., Self-assembling polymeric and oligomeric borole materials. *Polym. Mater. Sci. Eng.* **2005**, *91*, 147-148. (d) Niu, W. J.; Smith, M. D.; Lavigne, J. J., Substituent effects on the structure and supramolecular assembly of bis(dioxaborole)s derived from 1,2,4,5-tetrahydroxybenzene. *Cryst. Growth & Des.* **2006**, *6*(6), 1274-1277. (e) Rambo, B. M.; Lavigne, J. J., Defining self-assembling linear oligo(dioxaborole)s. *Chem. Mater.* **2007**, *19*(15), 3732-3739.

[5] Lanni, L. M.; Tilford, R. W.; Bharathy, M.; Lavigne J. J. Enhanced hydrolytic stability of self-assembling alkylated 2-dimensional covalent organic frameworks. *J. Am. Chem. Soc*. **2011**, *133*(35), 13975-13983.

CHAPTER 4

SYNTHESIS, CHARACTERIZATION, OPTOELECTRONIC PROPERTIES AND SENSING APPLICATIONS OF D-Π-A TRIPHENYLAMINOBOROLES

4.0 INTRODUCTION

Boranes have recently emerged as an important class of materials, due to their interesting optical and electronic properties. With an empty p orbital, the electron-deficient boron center acts as a Lewis acid or an electron acceptor. When connecting with an electron donor such as an amino group, a borane can form a donor-π-acceptor (D-π-A) system, resulting in an intramolecular charge transfer. Thus, boranes have wide applications in several areas, including chemical sensors for Lewis bases, blue emitters and charge transporters in organic light-emitting devices (OLEDs), non-linear optics and two-photon emitting materials.[1]

According to the relative positions of a donor and an acceptor, these D-π-A boranes have versatile structures. A donor and an acceptor can not only be located at the terminals of a π system to form a linear or through-space structure, but also be at the lateral positions to form a cruciform structure.[1] Due to their diverse structures, optical properties and sensing abilities, D-π-A boranes are easily tuned. However, boranes including D-π-A boranes suffer from the difficult and complicated synthesis using organometallic chemistry, and hydrolytic as well as oxidative instability. Furthermore,

the sensing targets are limited to small nucleophiles or Lewis bases due to the steric protection of the Lewis acidic boron center.[1b]

In the past decades, there has been an increase in the interest of boronate ester chemistry. Boronate esters, formed by covalent yet reversible bonds between boronic acids and 1,2- or 1,3- diols, create interesting materials, including covalent organic frameworks, linear polymers, and macrocycles with self-assembling abilities.[2] Except as a building block for materials, boronates provide the features for sensing. For example, boronate esters are relatively easy and facile to synthesize, using a dehydration reaction between boronic acid and diol.[2] Boronate esters are also stable towards hydrolysis.[3] In addition, their planar geometries with an extended π-conjugation allow a sensitive detection of Lewis bases.[4]

As of now, we doubt whether a D-π-A system can be introduced to boronate esters and used as novel alternative sensors for D-π-A boranes. Thus, nitrogen and boron are used as an electron donor-acceptor pair in a π-conjugation system and a series of D-π-A triphenylaminoboroles (**Figure 4.1**) were designed, synthesized and characterized. Boroles **4.1**-**4.4** were used as non-conjugated compound, monomer, dimer and trimer respectively to study how π-conjugation affects the optoelectronic properties. Electron-donating **4.5** and electron-withdrawing **4.6** were used to study the effect of electronics. Diazabrole **4.7** was designed to study the effect of linkage. Their optoelectronic properties are studied in detail studied by absorption, fluorescence and computational calculations. The sensing applications of the representative D-π-A boroles are also explored.

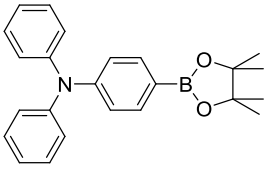

4.1

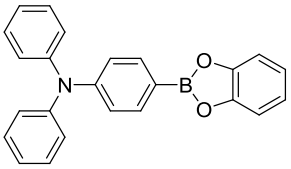

4.2

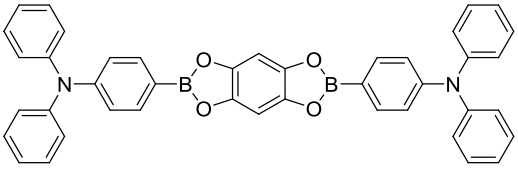

4.3

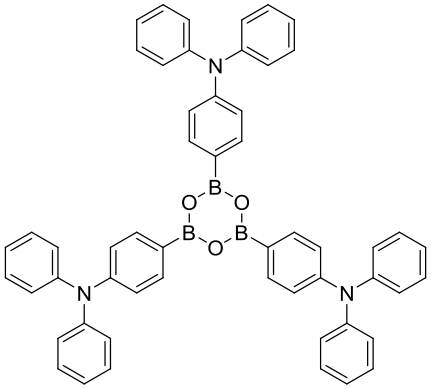

4.4

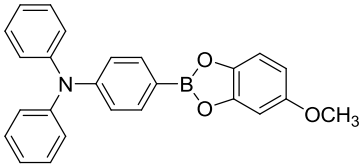

4.5

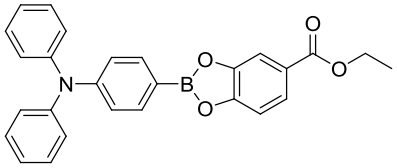

4.6

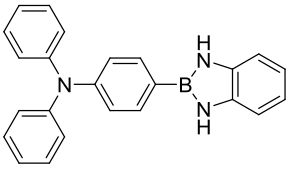

4.7

Figure 4.1 Structures of D-π-A triphenylaminoboroles **4.1**-**4.7**.

4.1 RESULTS AND DISCUSSION

4.1.1 SYNTHESIS AND CHARACTERIZATION

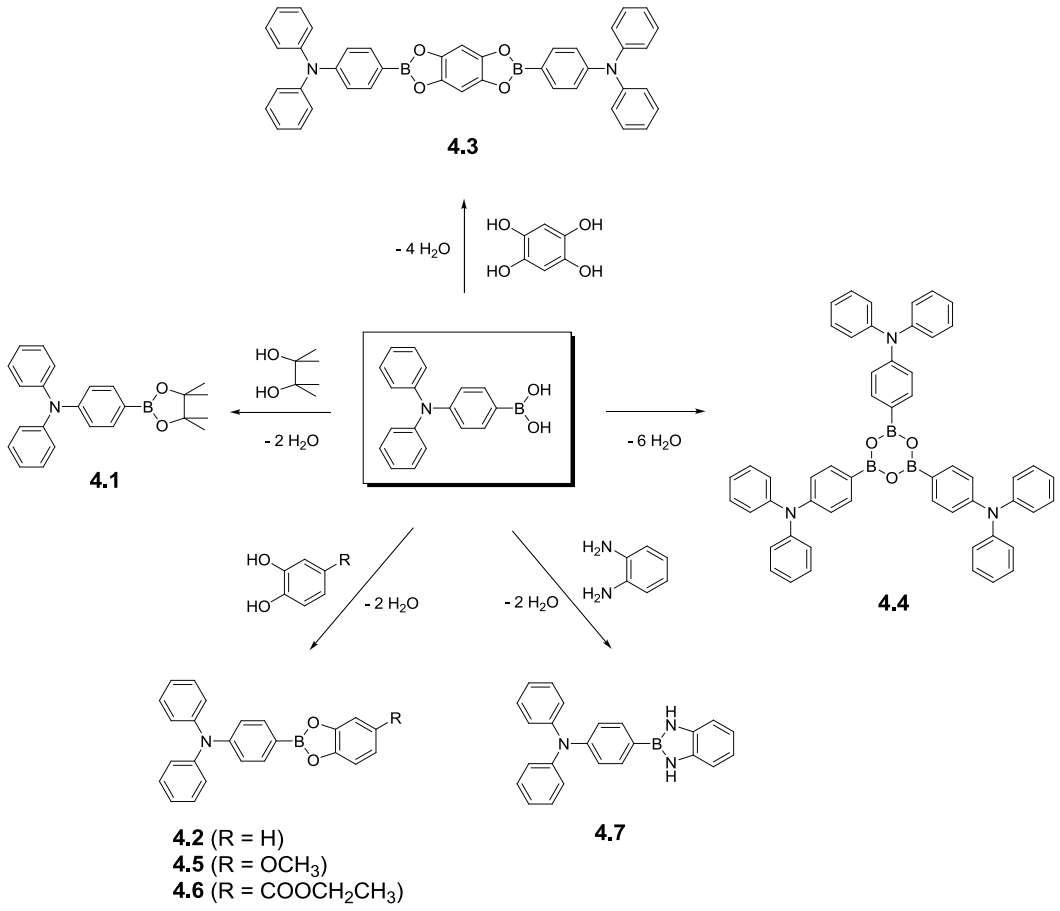

Figure 4.2 Synthesis of boroles **4.1**-**4.7** by condensation reactions.

All the starting materials were commercially available, except 4-methoxycatechol and THB were synthesized according to the literature.[4] Borole **4.4** was prepared by the self-condensation of 4-(diphenylamino)phenylboronic acid.[5] Other boroles were generated by the condensation between 4-(diphenylamino)phenylboronic acid and diol, THB or diamine (**Figure 4.2**). The mixture of starting materials was refluxed in toluene. To synthesize borole **4.3**, 10% methanol was added to increase the solubility of starting

materials. The resulting water was removed by Dean-Stark trap. After removing the excess toluene and the unreacting diol, THB or diamine, boroles were obtained in yields greater than 96.31 %. Boroles showed good solubility in organic solvents, such as toluene and dichloromethane.

The boronate ester linkages were characterized by FT-IR. **Figure 4.3** shows the FT-IR spectra of the representative boroles. For dioxaboroles **4.1-4.6**, the attenuation of a broad peak in the range of 3200-3400 cm^{-1} suggests the disappearance of the hydroxyl groups in diol or THB (**Figure 4.3c**). The diagnostic bands in 1300-1350 cm^{-1} demonstrate the B-O stretch. The bands during 1000-1050 cm^{-1} and 640-680 cm^{-1} indicate the formation of boronate esters or anhydride (**Figure 4.3a**). The band of 680-740 cm^{-1} indicates the THB-linked ester or anhydride.[5] For diazaborole **4.7**, a single band of N-H groups for secondary amine on diazaborole shows at 3400 cm^{-1} (**Figure 4.3b**). However, the starting material benzene 1,2-diamine displays two bands at 3400 and 3200 cm^{-1} (**Figure 4.3d**), referring to the asymmetrical and symmetrical N-H stretch.[6]

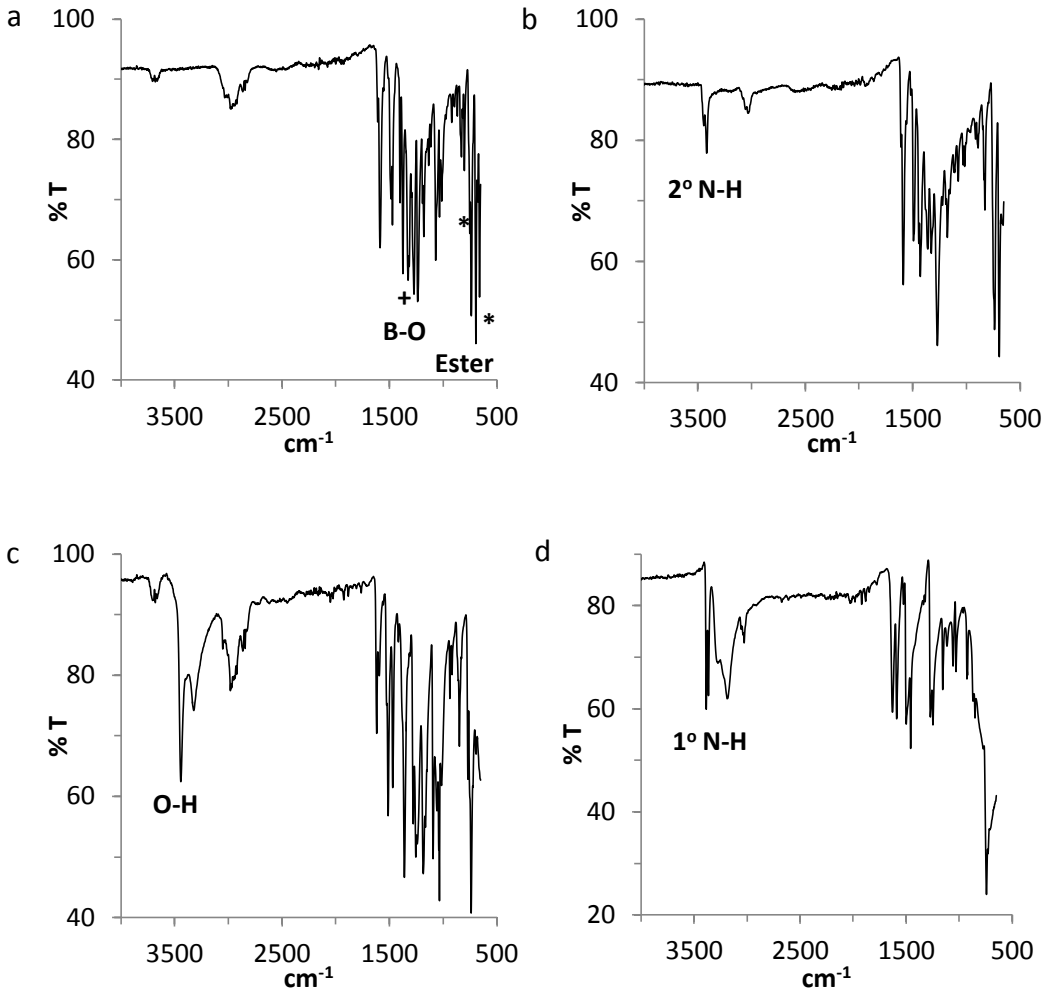

Figure 4.3 FT-IR spectra of (a) dioxaborole **4.2**, (b) diazaborole **4.7**, (c) catechol and (d) benzene 1,2-diamine.

^{1}H NMR spectroscopy is another easy way to confirm the boronate ester linkages.[5] Protons on the phenyl ring ortho to the boron centers are diagnostic. Those protons for free boronic acid have chemical shifts at 7.60 ppm and 8.03 ppm (**Figure 4.4a**). Free boronic acid may form an anhydride even in a small amount of water in CD_2Cl_2, thus water was added. As shown in **Figure 4.4b**, the intensity at 7.60 ppm increased, while the intensity at 8.03 ppm decreased, indicating that those protons for free boronic acid with a chemical shift at 7.60 ppm.

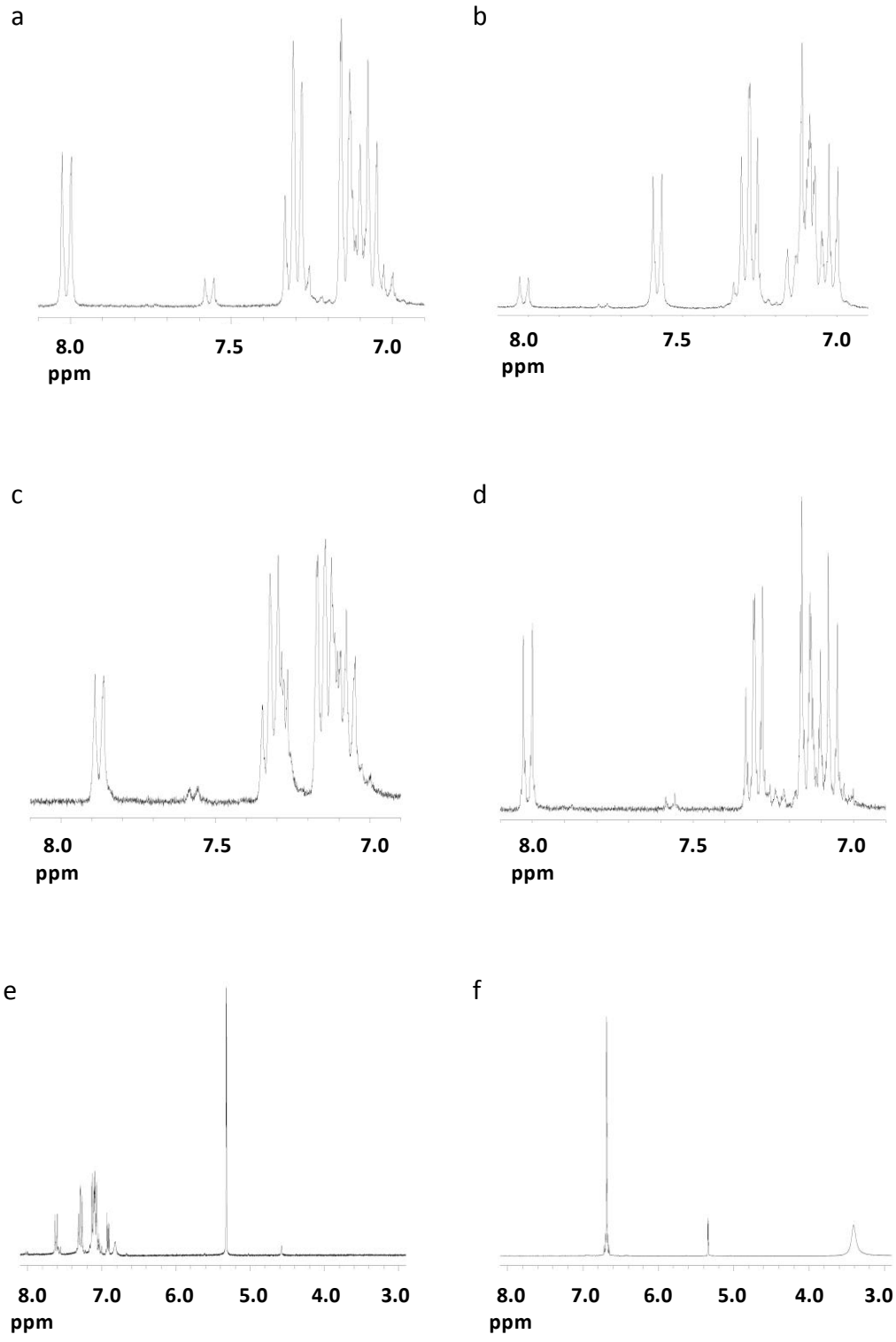

Figure 4.4 ^{1}H NMR spectra of (a) free boronic acid, (b) boronic acid with added water, (c) dioxaborole **4.2**, (d) dioxaborole **4.4**, (e) diazaborole **4.7** and (f) benzene 1,2-diamine.

The attenuation of the peak in 4.5-5.5 ppm range suggests the disappearance of the hydroxyl moieties in diols. The non-conjugated boronate ester **4.1** has the similar chemical shift as the free acid. The formation of conjugated boronate esters **4.2**, **4.3**, **4.5** and **4.6** allows chemical shift downfield to 7.90 ppm (**Figure 4.4c**), due to the extended π-conjugation through the vacant p-orbital of boron. The formation of anhydride **4.4** makes chemical shift downfield further to 8.03 ppm (**Figue 4.4d**), indicating a more extended π-conjugation. For diazaborole **4.7**, the attenuation of the peak in 3.92 ppm suggests the disappearance of NH_2 in diamine (**Figure 4.4f**). The formation of diazaborole gives protons on the secondary amine a peak at 4.58 ppm. The protons on the aromatic ring ortho to the boron have a peak at 7.60 ppm (**Figure 4.4e**). Compounds **4.1-4.7** were also characterized by ^{13}C NMR and mass spectroscopy. The synthetic routes and characterization data are summarized in Experimental section.

4.1.2 X-RAY STRUCTURE

X-ray structure can be used to probe the hybridization of boron, the planarity of the structure and intermolecular interactions.[7] Thus, boroles **4.1-4.7** were redissolved in CH_2Cl_2. Upon slow evaporation, the colorless block-shaped crystals of bis(dioxaborole) **4.3** were obtained. The solvent-free crystal structure was solved by Dr. Mark Smith in USC.

As shown in **Figure 4.5**, the molecule of **4.3** is centrosymmetric. It slightly deviates from planarity with a dihedral angle of 6.82° between the central phenyl ring and the neighboring phenyl ring. Three bond angles around the boron center B1 are 111.14 °,

124.34 ° and 124.49 °, respectively. The summarized 360 ° bond angles indicate the sp^2 hybridized trigonal planar boron.

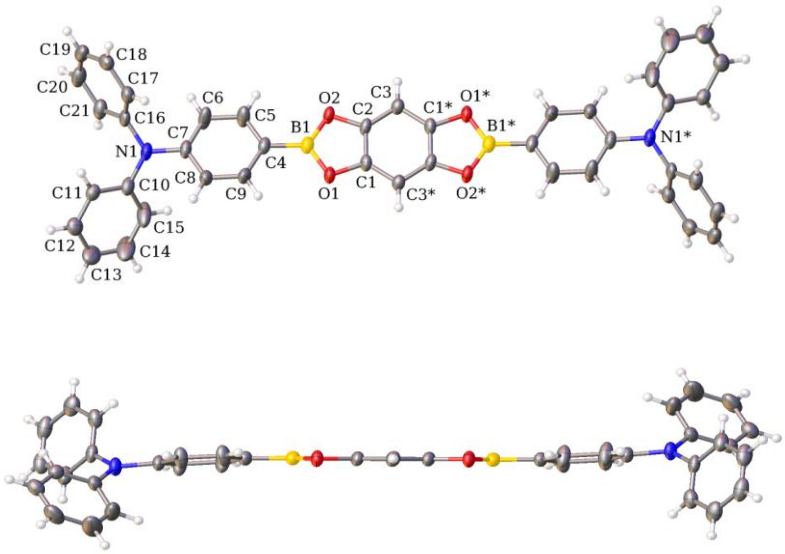

Figure 4.5 Molecular structure of bis(dioxaborole) **4.3**. All atoms are shown with 60% probability level of displacement ellipsoids. Atoms labeled with asterisk (*) are related to their unstarred counterparts by inversion.

The crystal shows the offset π-stacking interactions between parallel molecules. The interesting feature is the electron-deficient boron has the interactions with the π-clouds on the terminal phenyl rings of adjacent layers (**Figure 4.6a**). It also shows that the terminal phenyl rings and the central bis(dioxaborole) ring participate in the CH-O hydrogen bonding (**Figure 4.6b**). Two distances shown are 2.716 Å and 2.682 Å, respectively.

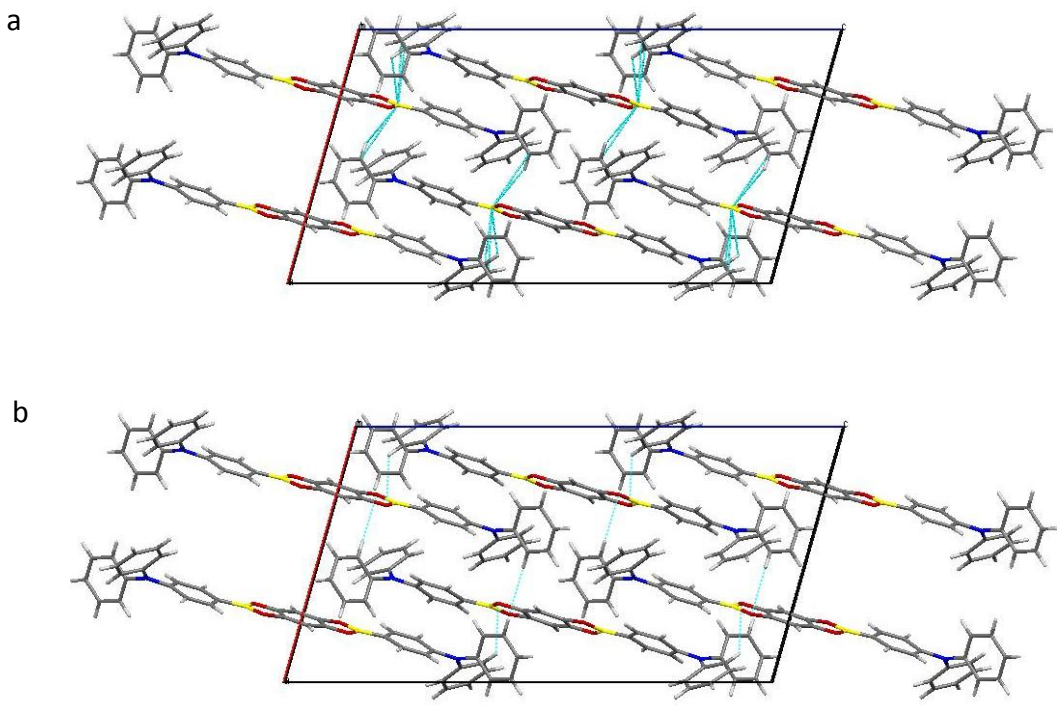

Figure 4.6 Packing view of bis(dioxaborole) **4.3** of (a) phenyl-boron-phenyl π-stacking and (b) CH-O hydrogen bonding.

4.1.3 OPTOELECTRONIC PROPERTIES

4.1.3.1 ABSORPTION STUDIES

In order to choose the proper concentration for absorption studies, the representative boroles **4.2-4.4** (monomer, dimer and trimer) were investigated. The spectra in **Figure 4.7** show that the absorption maxima of **4.2-4.4** is 332 nm, 343 nm and 340 nm, respectively. As the concentration increases, absorbance increases in response. The increasing absorbance is in a linear regression with the concentration in the dynamic range of 0-2.9×10^{-5} M, 0-1.5×10^{-5} M and 0-1.9×10^{-5} M, respectively. This regression follows Beer's law, suggesting no aggregation occurs. The molar absorptivity of **4.2-4.4** is calculated to be 2.7×10^{4} M^{-1} cm^{-1}, 9.7×10^{4} M^{-1} cm^{-1} and 8.5×10^{4} M^{-1} cm^{-1}, respectively. To keep the concentration of boron consistent, compound **4.1**, **4.2**, **4.5**, **4.6** and **4.7** of

1.8×10^{-5} M, **4.3** of 0.9×10^{-5} M and **4.4** of 0.6×10^{-5} M were used for the following absorption studies.

The extended π-conjugation is confirmed by absorption (**Figure 4.8a**). The non-conjugated **4.1** shows the absorption maxima at 308 nm, while conjugated monomer **4.2** shows the absorption maxima at 332 nm, 24 nm longer than **4.1**. As π-conjugation extends, dimer **4.3** with two linear bis(dioxaborole) units shows a larger absorption maxima at 343 nm, while trimer **4.4** has a similar wavelength at 340 nm, due to the three cyclic bis(dioxaborole) units.

Apart from π-conjugation, the effects of electronics and linkage are also studied (**Figure 4.8b**). Electron-donating **4.5** and electron-withdrawing **4.6** have a similar absorption maxima as **4.2** at 332 nm, indicating electron-donating methoxy group and electron-withdrawing ester group on diol moiety have little impact on absorption. Diazaborole **4.7** has the absorption maxima at 328 nm, which suggests that linkage also has impact on absorption.

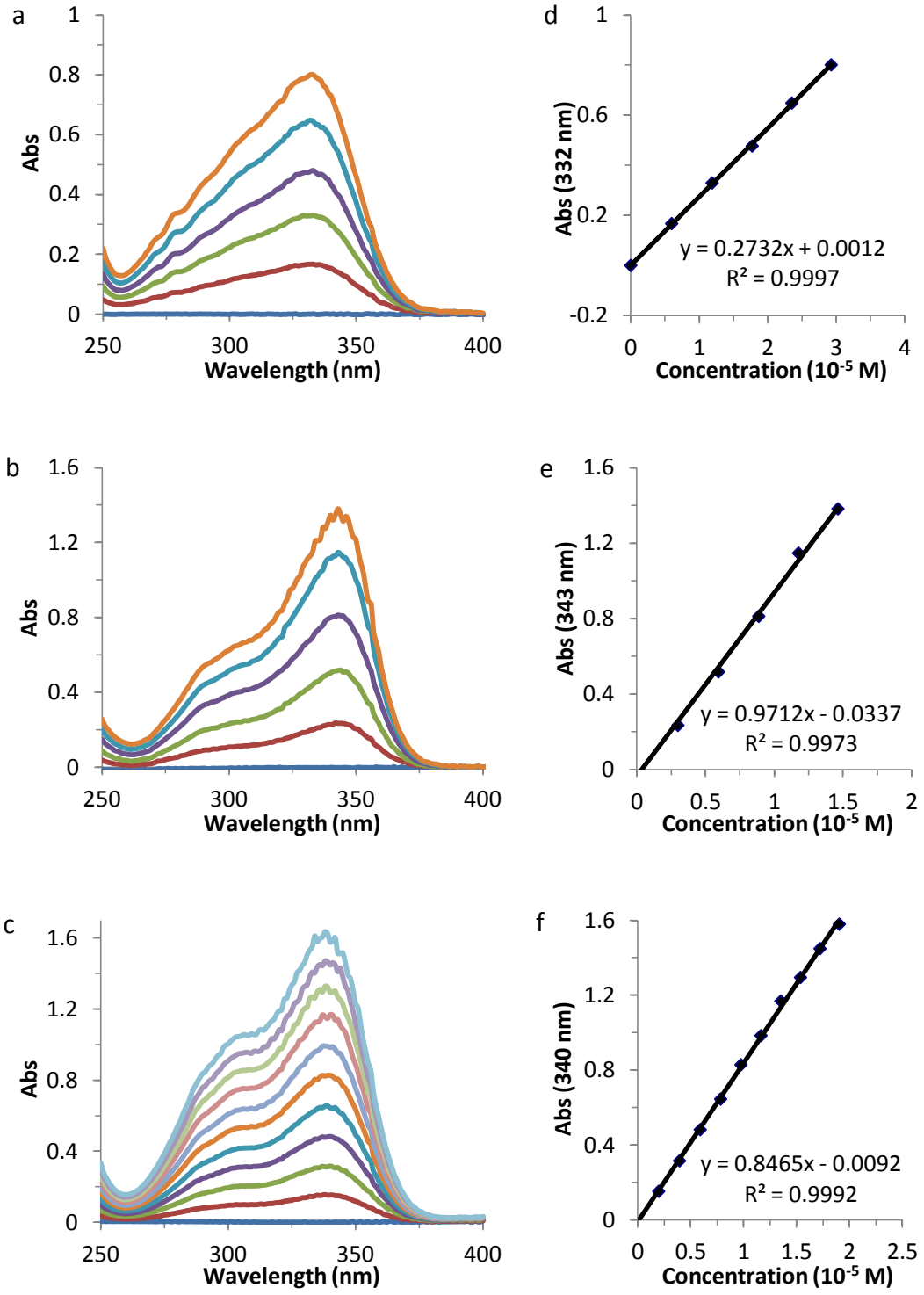

Figure 4.7 Absorption spectra of (a) monomer **4.2**, (b) dimer **4.3** and (c) timer **4.4** at different concentrations in CH_2Cl_2. Plots of absorbance at the absorption maxima vesus the concentration of (a) **4.2**, (b) **4.3** and (c) **4.4** in CH_2Cl_2.

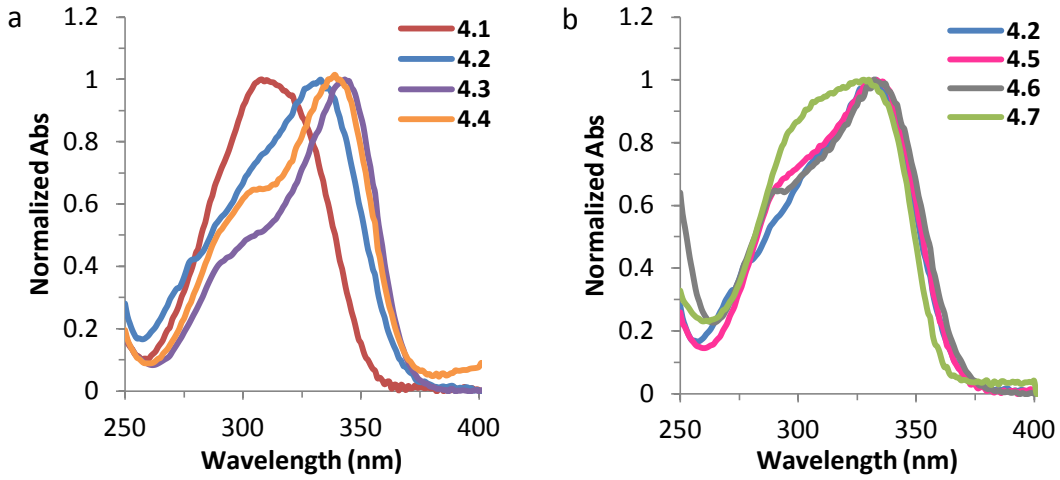

Figure 4.8 Absorption spectra of boroles of (a) **4.1-4.4** and (b) **4.2**, **4.5-4.7** with 1.8×10^{-5} M boron in CH_2Cl_2.

4.1.3.2 COMPUTATIONAL STUDIES

Computational calculations for boroles were performed on the basis of DFT (B3LYP-6-31G*) in software Spartan 08. The calculated geometries and energies for the HOMOs and LUMOs are listed in **Table 4.1**. Generally, the HOMO is primarily located on the terminal triphenylamino group. The energy of the HOMO is approximately -5.00 eV. And the LUMO is located on the central phenyl dioxa- or diaza- borole ring, where the p orbital of boron overlaps with the neighboring phenyl ring and two oxygen or nitrogen atoms. Thus, for borole **4.5** and **4.6**, electron-donating methoxy group and electron-withdrawing ester group on the diol moiety do not have an obvious impact on optical properties of boroles. Boron makes a significant contribution to the LUMO and increases LUMO energy to about -1.00 eV. It is anticipated that an intramolecular charge transfer happens from the HOMO to the LUMO, which will be discussed in detail below.

Table 4.1 Computed orbitals and energies for boroles **4.1-4.7**.

Compound	HOMO	LUMO
4.1	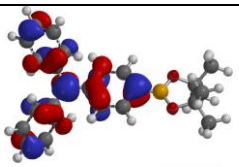 -4.93 eV	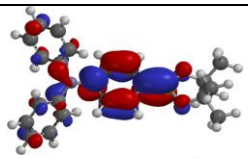 -0.60 eV
4.2	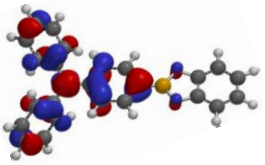 -5.09 eV	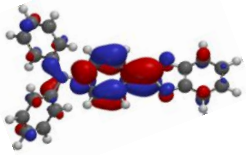 -0.94 eV
4.3	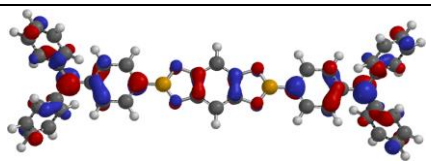 -5.02 eV	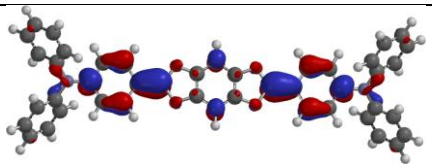 -1.03 eV
4.4	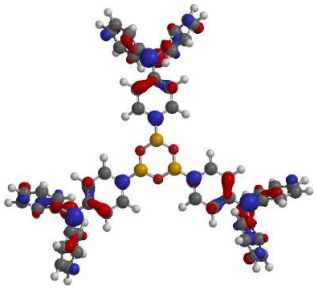 -4.99 eV	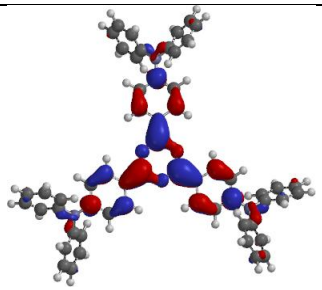 **LUMO & LUMO (+1)** -1.01 eV
4.5	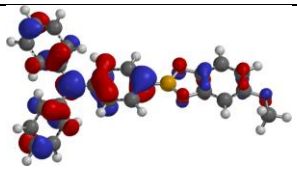 -5.04 eV	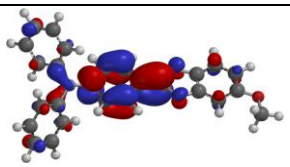 -0.90 eV
4.6	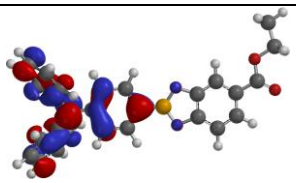 -4.89 eV	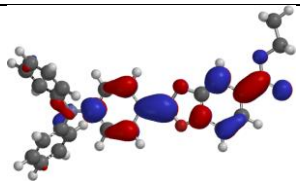 -0.71 eV
4.7	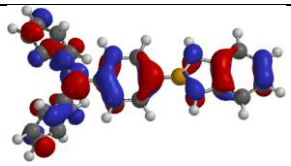 -5.17 eV	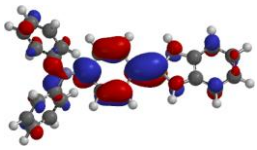 -1.18 eV

The calculated and experimental band gaps and optical wavelengths are summarized in **Table 4.2**. The conjugated **4.2** has a band gap of 4.15 eV, 0.18 eV smaller the non-conjugated **4.1**. Borole **4.3** and **4.4** have a smaller band gap of 4.00 eV, indicating a more extended π-conjugation. The decreasing band gap is consistent with the experimental bathochromic shift of the absorption maxima of boroles **4.1**-**4.4**.

Table 4.2 Computed and experimental band gaps and wavelengths for boroles

Compound	E_{cal} (eV)	E_{exp} (eV)	λ_{cal} (nm)	λ_{exp} (nm)
4.1	4.33	4.03	287	308
4.2	4.15	3.74	299	332
4.3	3.99	3.62	311	343
4.4	3.98	3.65	312	340
4.5	4.14	3.71	300	334
4.6	4.18	3.74	297	332
4.7	3.99	3.78	311	328

4.1.3.3 FLUORESCENCE STUDIES

The previous computational studies suggest that an intramolecular charge transfer may occur from the triphenylamino group to the phenyl boronate ester moiety. Charge transfer was demonstrated by studying the fluorescent behavior of boroles **4.1**-**4.7** in solvents with different polarities. When excited by light, boroles will have a dipole due to the charge transfer, which is stabilized by a polar solvent.[1a] Thus, as the solvent polarity increases, the emission wavelength of boroles increases (**Figure 4.9**). The emission wavelengths are listed in **Table 4.3**.

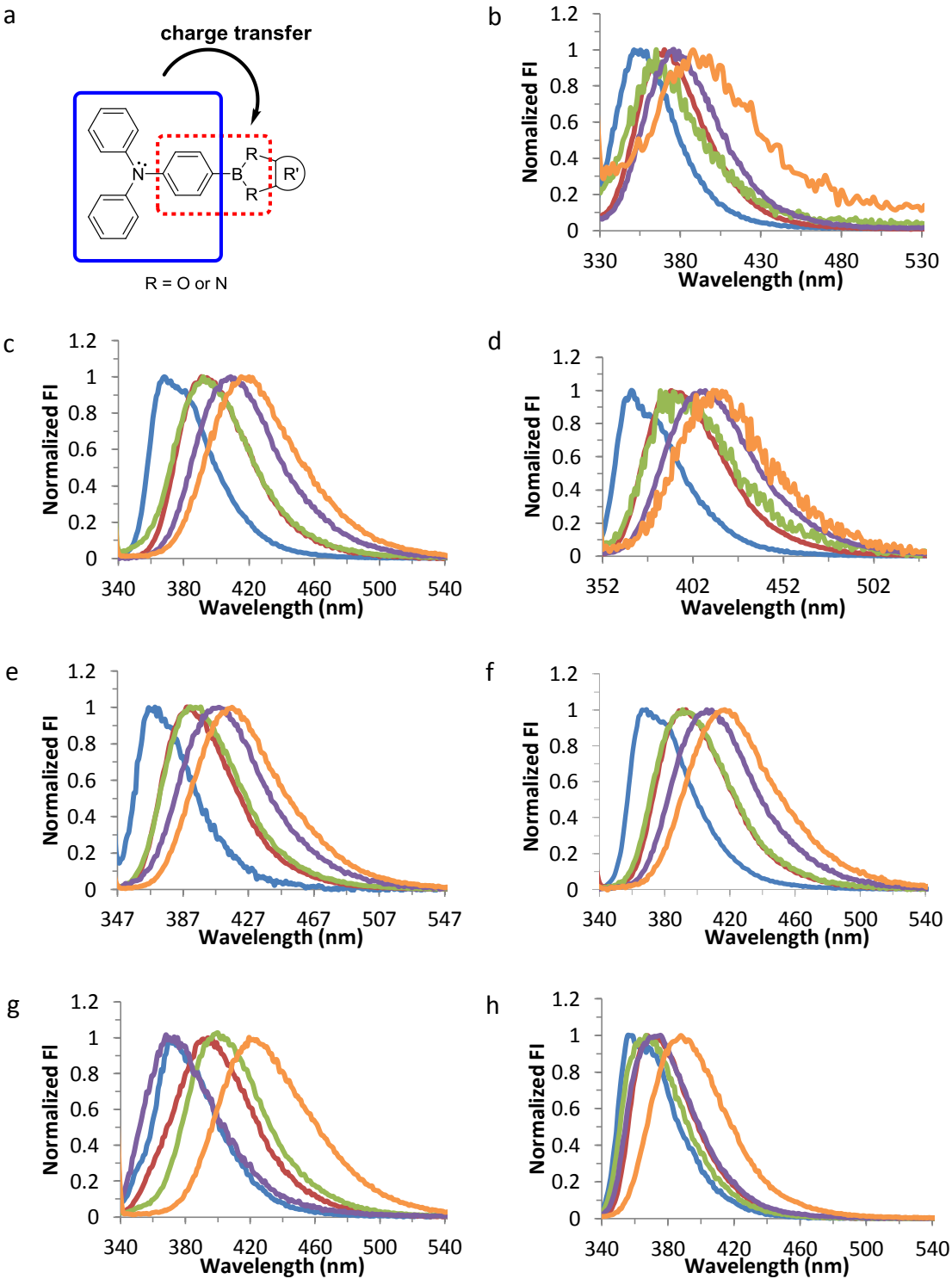

Figure 4.9 (a) Intramolecular charge transfer of boroles. Fluorescence spectra of boroles of (b)-(h) **4.1-4.7** with 1.8×10^{-6} M boron in solvents of increasing polarities from hexane (blue), toluene (red), ether (green), THF (purple) to CH_2Cl_2 (orange).

Table 4.3 Emission wavelengths of boroles in different solvents.

Compound	hexane (nm)	toluene (nm)	ether (nm)	THF (nm)	CH_2Cl_2 (nm)
4.1	368	370	365	376	388
4.2	368	391	392	409	420
4.3	367	390	389	408	413
4.4	370	390	398	409	417
4.5	369	393	391	406	417
4.6	373	396	400	415	419
4.7	356	368	367	376	388

The extension of charge transfer was quantitatively studied by $E_T(30)$[8], Py[9] and Pi*[8a,10] scales. The energy of boroles has a linear relationship with $E_T(30)$, Py and Pi* values. The parameters are listed in **Table 4.4**. Taken the $E_T(30)$ scale for example (**Figure 4.10a**), borole **4.2** has a large relative slope of 0.9313, indicating the effective intramolecular charge transfer. Since the subtituents on the diol moiety make no contribution to the HOMO and LUMO, boroles **4.3-4.6** have a similar response as **4.2**. However, borole **4.1** has a small relative slope of 0.4437, indicating the intramolecular charge transfer is 50% less effective than **4.2** (**Figure 4.10d**). And diazaborole **4.7** has a small relative slope of 0.6450, indicating a 31% less intermolecular charge transfer than **4.2** (**Figure 4.10d**). Py and Pi*scales have similar results as $E_T(30)$ sales (**Figure 4.10b-c**).

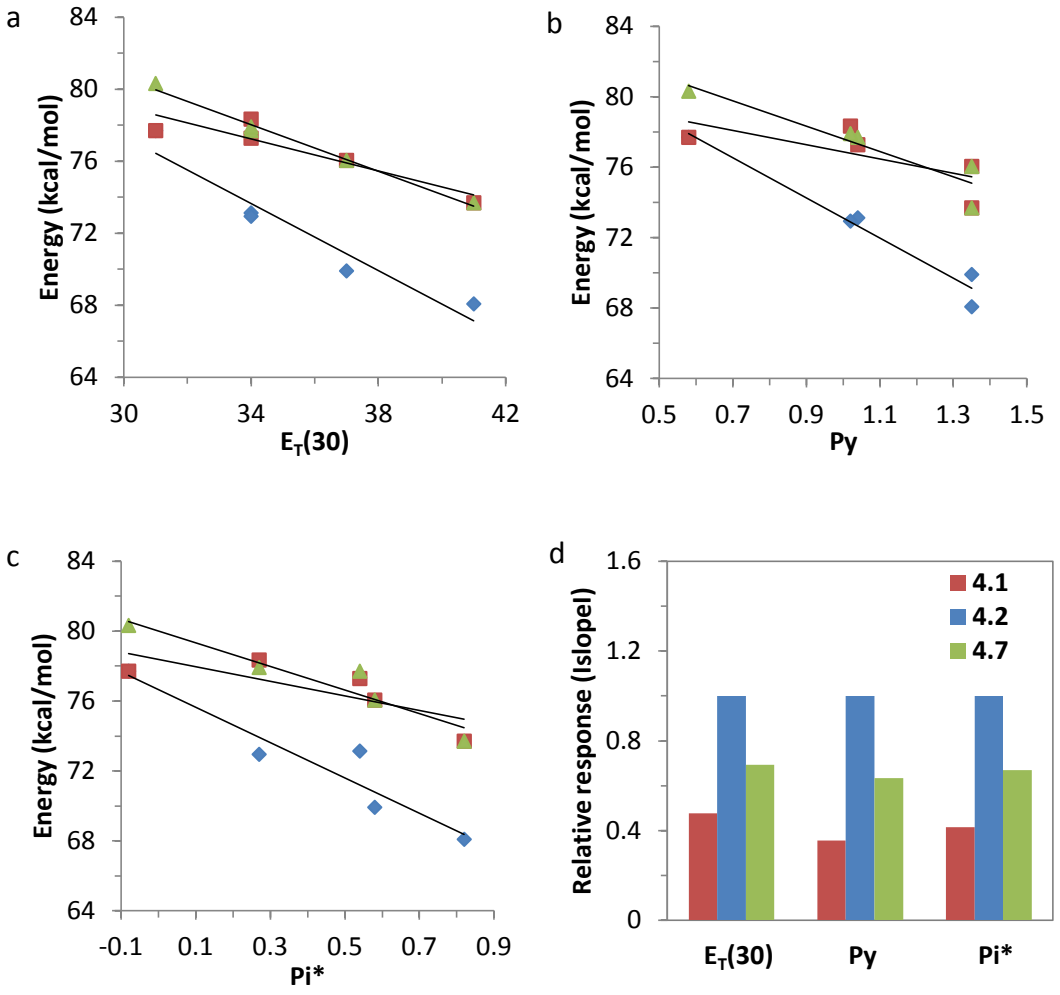

Figure 4.10 Plots of energy of 1.8×10^{-6} M borole **4.1** (red), **4.2** (blue) and **4.7** (green) versus (a) $E_T(30)$, (b) Py and (c) Pi* value. (d) Relative response of boroles to different values.

Table 4.4 Charge transfer properties studied by $E_T(30)$, Py and Pi* scales.

Compound	$E_T(30)$		Py		Pi*	
	Slope	R^2	Slope	R^2	Slope	R^2
4.1	-0.4437	0.8379	-4.0333	0.4845	-4.1921	0.6176
4.2	-0.9313	0.9229	-11.374	0.9633	-10.096	0.8955
4.3	-0.8482	0.8758	-10.779	0.9897	-9.4447	0.8966
4.4	-0.8288	0.8617	-10.398	0.9492	-8.8288	0.8075
4.5	-0.8482	0.9127	-10.405	0.9610	-9.4446	0.9344
4.6	-0.8053	0.8341	-10.462	0.9852	-8.9150	0.8441
4.7	-0.6450	0.9883	-7.2043	0.8629	-6.7554	0.8952

4.1.4 SENSING APPLICATIONS

4.1.4.1 EFFECT OF Π-CONJUGATION ON SENSING

To investigate how π-conjugation affects fluoride binding, the optical properties of the non-conjugated control **4.1**, conjugated **4.2** and their fluoride complexes were studied. As illustrated in **Figure 4.11a,c**, the addition of one equivalent of fluoride to the non-conjugated **4.1** afforded no significant change to either absorption or emission.

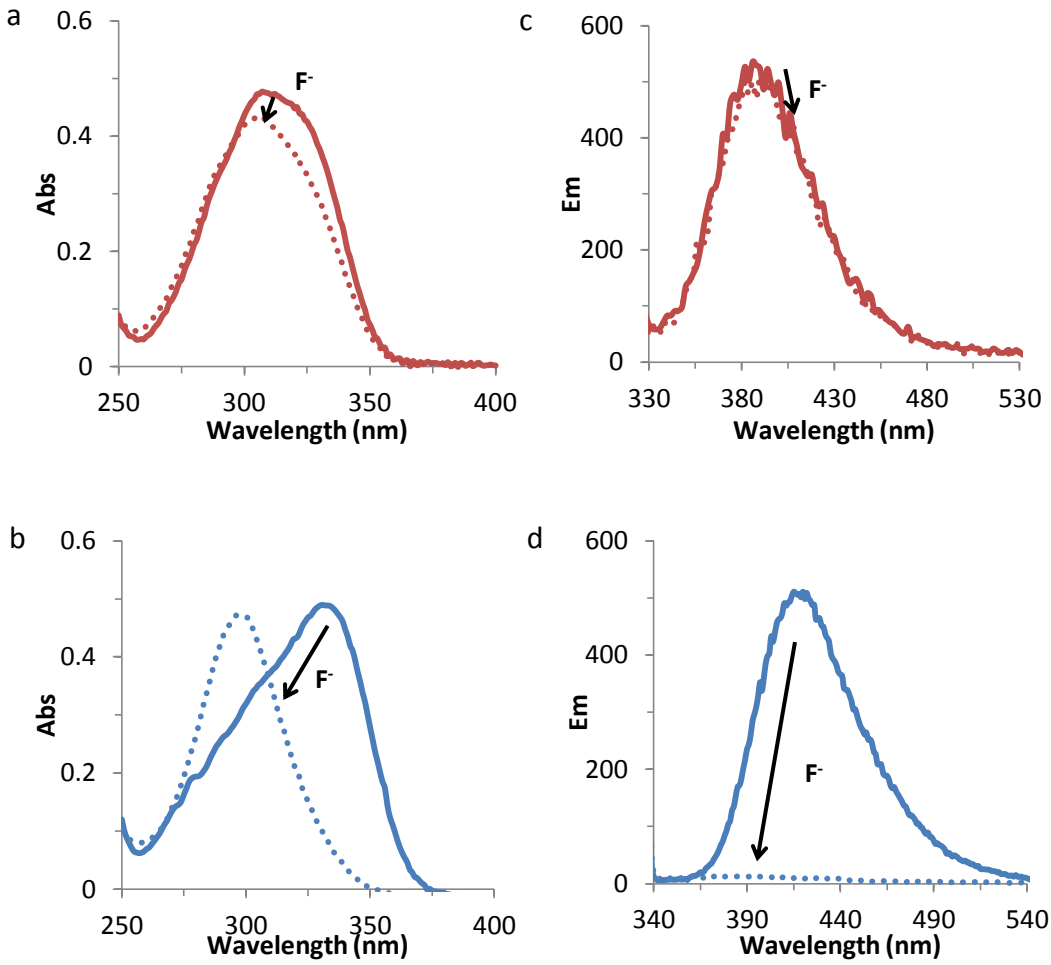

Figure 4.11 Absorption spectra of borole (a) **4.1** and (b) **4.2** (1.8×10^{-5} M) and fluorescence spectra of (c) **4.1** and (d) **4.2** (1.8×10^{-6} M) in the absence and presence of one equivalent of fluoride in CH_2Cl_2.

However, upon the addition of fluoride, the absorption maxima of conjugated **4.2** blue shifted from 332 nm to 297 nm (**Figure 4.11b**). The fluorescence intensity of **4.2** centered at 420 nm was quenched (**Figure 4.11d**). These results suggest that the fluoride coordination converts the trigonal planar boron to tetrahedral geometry, thereby interrupting the π-conjugation along the backbone of **4.2**. Different from the bis(dioxaborole)s studied in Chapter 2, the emission wavelength of **4.2** blue-shifted to 398 nm, due to the slightly fluorescent **4.2-F**. It can be explained that the intramolecular charge transfer is turned off by fluoride addition.

4.1.4.2 OPTICAL TITRATIONS

To investigate the binding interactions between boroles and fluoride, absorption and fluorescence titrations were conducted by the sequential addition of fluoride to the representative boroles **4.2-4.4**. As depicted in **Figure 4.12**, the addition of fluoride makes the absorption maxima blue shift, indicating the interruption of π-conjugation. Fluoride also quenches the fluorescence of boroles. The emission wavelength blue-shifts, due to the turned-off charge transfer.

Stoichiometric ratios of fluoride to boron on boroles were studied by mole ratio plot (**Figure 4.13**).[11] It is shown that boroles **4.2-4.4** afford a 1:1 ratio of fluoride to boron. Binding constants were calculated by fitting 1:1 or 2:1 (guest:host) binding isotherms (**Figure 4.13**).[12] The calculated binding constant of K_1 is as high as 10^7 M^{-1}, indicating a high affinity of boroles to fluoride.

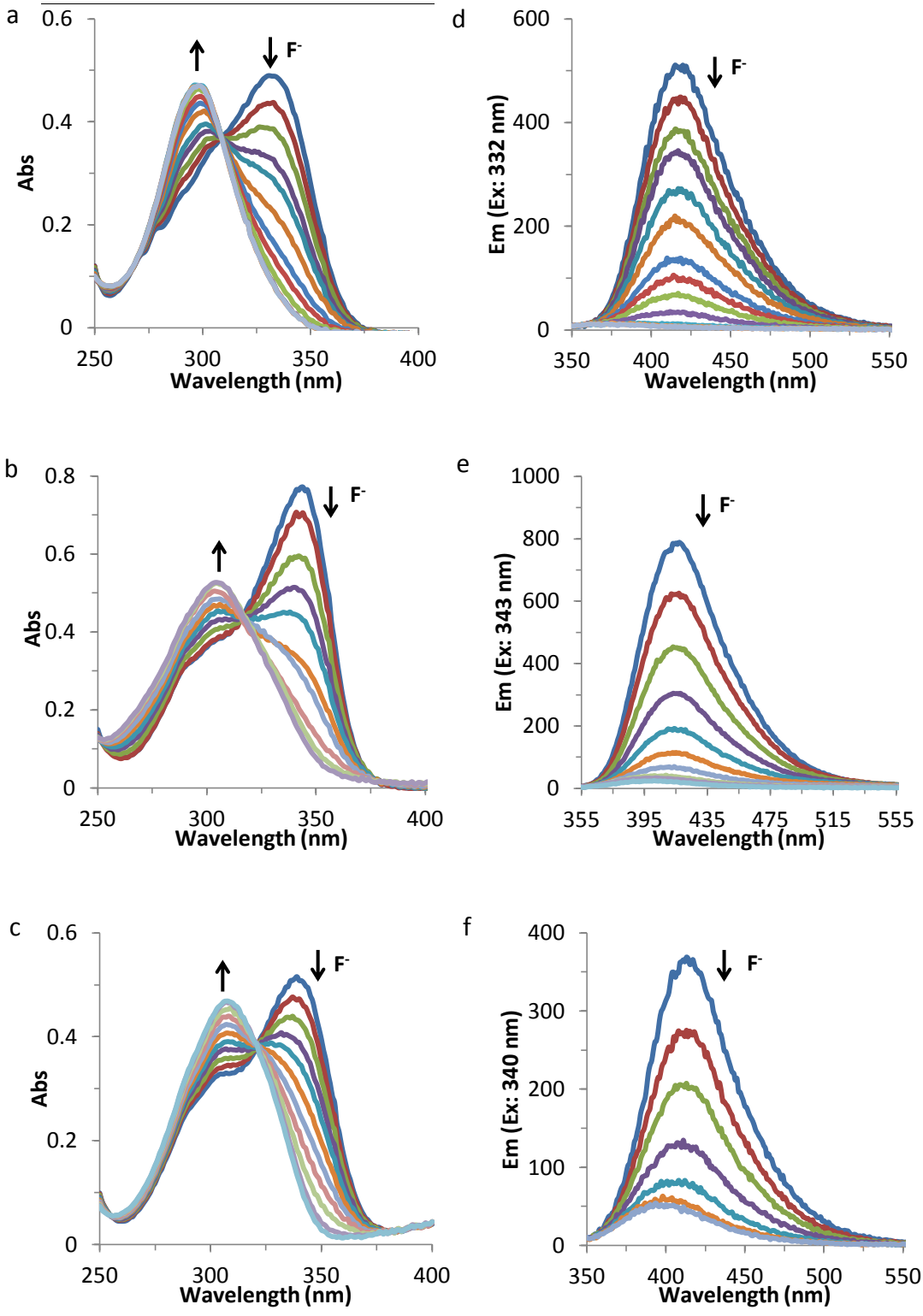

Figure 4.12 Absorption titrations of borole (a) **4.2**, (b) **4.3** and (c) **4.4** (boron: 1.8 × 10^{-5} M) and fluorescence titrations of (d) **4.2**, (e) **4.3** and (f) **4.4** (boron: 1.8 × 10^{-6} M) upon the addition of fluoride in CH_2Cl_2.

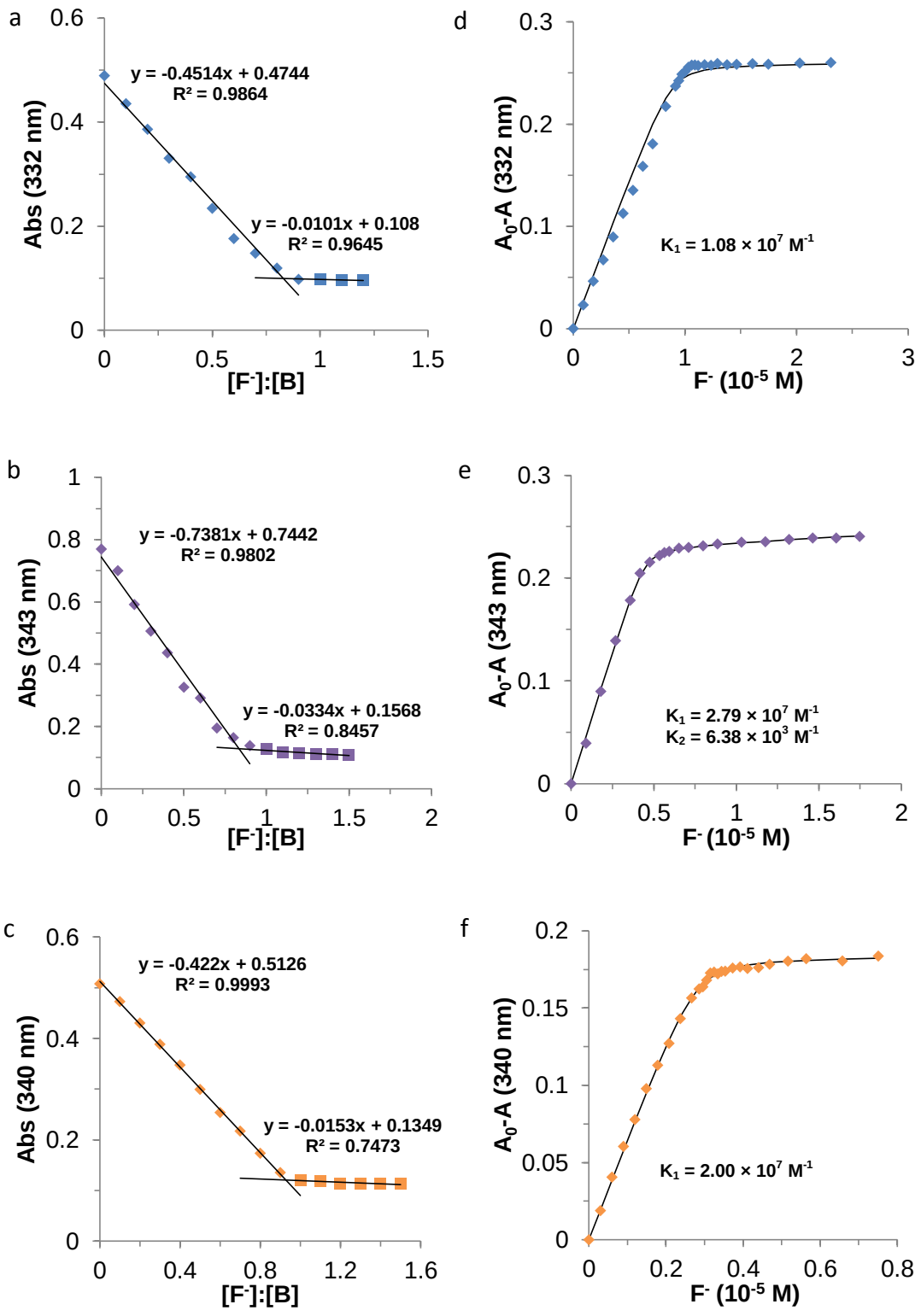

Figure 4.13 Mole ratio plots of borole (a) **4.2**, (b) **4.3** and (c) **4.4** and binding isotherms of (d) **4.2**, (e) **4.3** and (f) **4.4** (boron: 1.8 × 10^{-5} M) upon the addition of fluoride in CH_2Cl_2.

4.1.4.3 BINDING REVERSIBILITY

The reversibility of boroles binding fluoride was studied by absorption. Excess trimethylsilyl chloride (TMSCl) was added to the fluoride complex to scavenge fluoride. The released chloride did not have any optical responses to boroles. As shown in **Figure 4.14**, upon the addition of TMSCl to fluoride complexes, the absorption maxima red shifts back and absorbance at the maximum wavelength restores. These results indicate the reversible binding between borole **4.2** or **4.4** and fluoride, further demonstrating the borole stability.

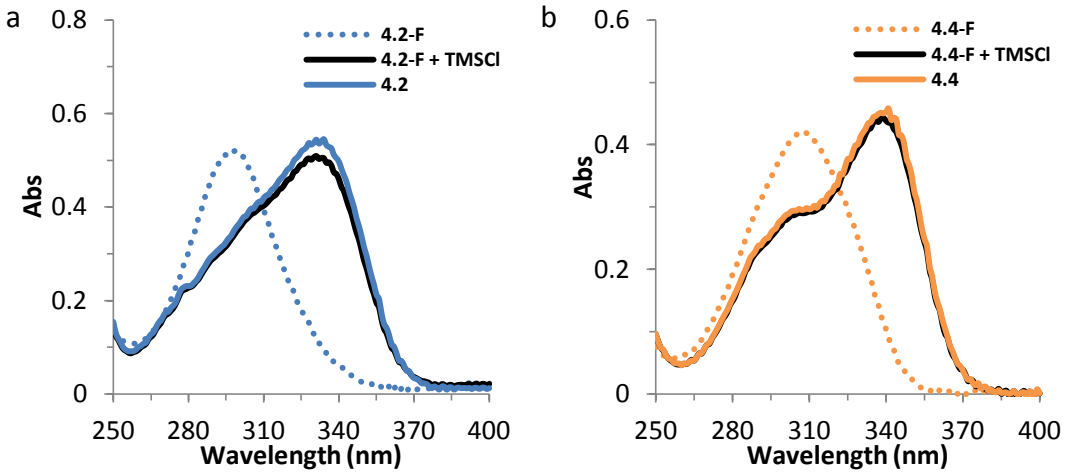

Figure 4.14 Absorption spectra of fluoride-borole (a) **4.2** and (b) **4.4** complexes upon the addition of excess TMSCl in CH_2Cl_2 (boron: 1.8×10^{-5} M, fluoride: 1.8×10^{-5} M).

4.1.4.4 BINDING CROSS-REACTIVITY

The recognition ability of boroles towards different Lewis bases was estimated by absorption spectroscopy. Thus, selected anions as the tetrabutylammonium salts and amines were evaluated as Lewis bases for binding. As shown in **Figure 4.15**, boroles selectively bind hard Lewis base F^- and CN^-, but they do not show any response to soft

anions, such as Cl^-, Br^- and I^-. They also show obvious response to $H_2PO_4^-$, due to the hardness of oxygen atoms. Apart from anions, the neutral amines can also bind to boroles. Interestingly, the binding response increases when the amine basicity increases from pyridine, to benzylamine, to n-butylamine.[13] The cross-reactivity of boroles to different anions and amines may be useful to design a sensor array to differentiate Lewis bases.

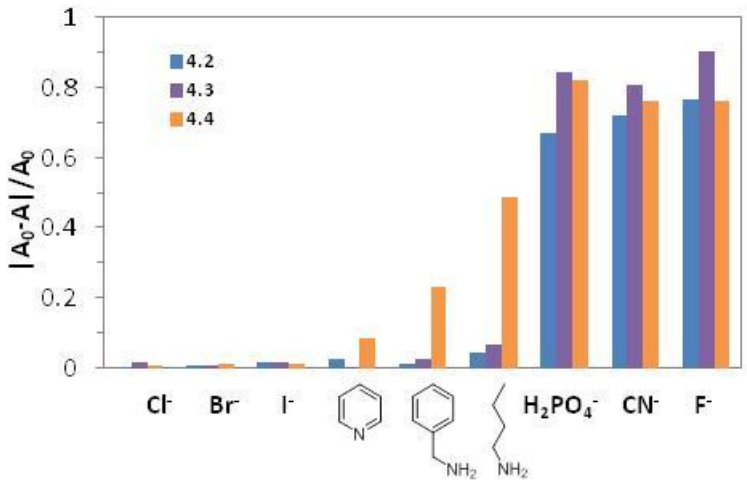

Figure 4.15 Degree of the absorbance response of boroles **4.2-4.4** (boron: 1.8×10^{-5} M) upon the addition of 9×10^{-5} M Lewis bases in CH_2Cl_2.

4.2 CONCLUSION

In summary, a new family of D-π-A triphenylaminoboroles was developed. Boroles were synthesized by dehydration reactions and characterized by FT-IR, ^{1}H NMR, ^{13}C NMR and mass spectroscopy. The single crystal of bis(dioxaborole) was solved, indicating the planar sp^2 hybridized boron centers. The absorption studies showed the extended π-conjugation of boroles, which was consistent with the computational results. The electronics and linkages had little impact on the absorption properties of boroles.

Boroles showed solvatochromism by fluorescence, due to the intramolecular charge transfer from the triphenyl amino group to borole moiety.

The sensing applications of the representative D-π-A boroles were also explored. Compared to the non-conjugated borole, the entire π-conjugation played an important role for fluoride binding. The fluoride addition made the absorption maxima blue shift and fluorescence quench. And the emission wavelength also blue shifted, due to the turned-off intramolecular charge transfer. The absorption titrations showed that the binding stoichiometry between fluoride and boron was 1:1 and the binding constant was over 10^7 M^{-1}. The binding was reversible and cross-reactive to different Lewis bases. These D-π-A triphenylaminoboroles may provide new sensory materials for Lewis base detection.

4.3 EXPERIMENTAL

4.3.1 MATERIALS

4-(diphenylamino)phenylboronic acid was purchased from Sigma-Aldrich. Catechol was purchased from Acros. Pinacol and ethtyl 3,4-dihydroxybenzoate were purchased from Alfa Aesar. 4-methoxycatechol and THB were synthesized according to the methods described in Chapter 2. All the chemicals were used without further purification. Toluene, methanol, hexane, ether, tetrahydrofuran and dichloromethane were obtained from Innovative Technologies by using purification systems.

4.3.2 INSTRUMENTATION

FT-IR spectra were performed on a PerkinElmer Spectrum 100 FT-IR Spectrometer. Sample (~0.5 mg) was put on a diamond/ZnSe crystal. The spectrometer scanned for 4 times with a resolution of 4.00 cm^{-1} from 4000 cm^{-1} to 650 cm^{-1}. ^{1}H NMR and ^{13}C NMR spectra were performed on a Varian Mercury/VX 300 MHz Spectrometer. Mass spectra were obtained on a VG 70S Mass Spectrometer and sample was introduced by direct exposure probe. Absorbance data were recorded on a Beckman Coulter 640 DU Spectrophotometer. Fluorescence data were recorded on a Cary Eclipse Fluorescence Spectrophotometer.

4.3.3 SYNTHESIS

*4.3.3.1 SYNTHESIS OF **4.1***

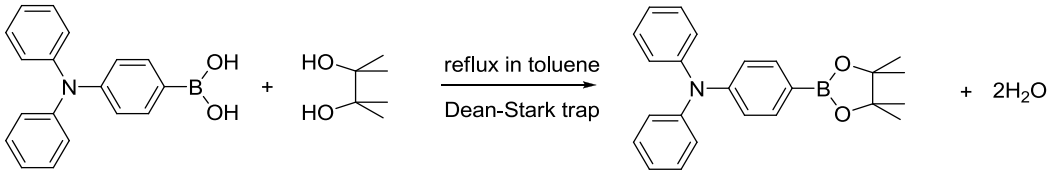

The starting materials were the mixture of 4-(diphenylamino) phenylboronic acid (116.0 mg, 0.4012 mmol) and pinacol (50.2 mg, 0.4248 mmol). In a round-bottom flask with a Dean-Stark trap, starting materials as well as 40 mL of distilled toluene were added. The solution was refluxed overnight under a nitrogen atmosphere. The resultant clear solution was cooled to room temperature. Toluene was removed by rotary evaporation and the crude product was further purified by Kugelrohr distillation. The product was an off-white solid (150.9 mg, quantitative). FT-IR: 2978, 1588, 1488, 1400, 1357, 1316, 1270, 1141, 1088, 1015, 962, 859, 826, 752, 694, 673, 656. ^{1}H NMR (300 MHz, CD_2Cl_2, δ): 7.61 (d, J = 8.7 Hz, 2H), 7.25-7.30 (m, 4H), 7.04-7.10 (m, 6H), 7.00

(m, J = 8.4 Hz, 2H), 1.31 (s, 12H). ^{13}C NMR (75 MHz, CD_2Cl_2, δ): 151.12, 147.90, 136.22, 129.86, 129.73, 125.64, 124.66, 124.03, 121.94, 84.08, 25.20. MS calcd for $C_{24}H_{26}BNO_2$: 370.2093; found (Direct Exposure Probe): 370.2088.

*4.3.3.2 SYNTHESIS OF **4.2***

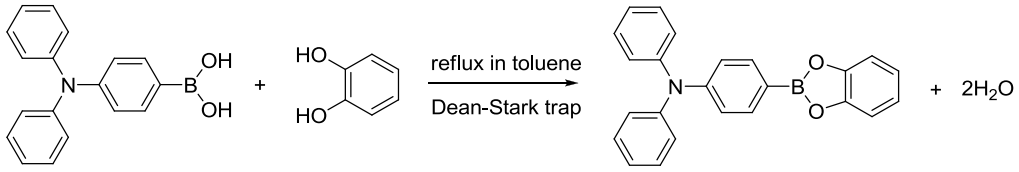

The starting materials were the mixture of 4-(diphenylamino) phenylboronic acid (114.4 mg, 0.3957 mmol) and catechol (46.6 mg, 0.4232 mmol). In a round-bottom flask with a Dean-Stark trap, starting materials as well as 40 mL of distilled toluene were added. The solution was refluxed overnight under a nitrogen atmosphere. The resultant clear solution was cooled to room temperature. Then toluene was removed by rotary evaporation and the crude product was further purified by Kugelrohr distillation. The product was an off-white solid (150.9 mg, quantitative). FT-IR: 2974, 1587, 1485, 1472, 1401, 1374, 1325, 1315, 1271, 1236, 1191, 1179, 1069, 1033, 1012, 829, 801, 751, 737, 694, 660. ^{1}H NMR (300 MHz, CD_2Cl_2, δ): 7.89 (d, J = 9.0 Hz, 2H), 7.27-7.35 (m, 6H), 7.05-7.17 (m, 10H). ^{13}C NMR (75 MHz, CD_2Cl_2, δ): 152.20, 149.21, 147.48, 136.52, 130.05, 126.29, 124.71, 123.15, 121.10, 112.83. MS calcd for $C_{24}H_{18}BNO_2$: 363.1431; found (Direct Exposure Probe): 363.1433.

*4.3.3.3 SYNTHESIS OF **4.3***

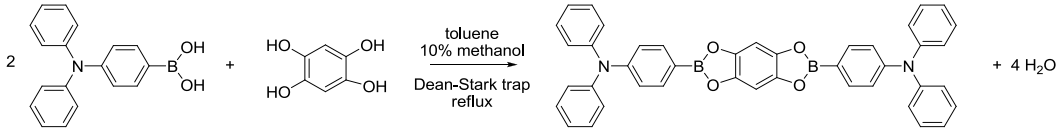

The starting materials were the mixture of 4-(diphenylamino) phenylboronic acid (116.0 mg, 0.4012 mmol) and THB (29.4 mg, 0.2069 mmol). In a round-bottom flask with a Dean-Stark trap, starting materials as well as 40 mL of distilled toluene and 4 mL of methanol were added. The solution was refluxed overnight under a nitrogen atmosphere. The resultant solution was cooled to room temperature and THB was removed by suction filtration. Then the excess toluene was removed by rotary evaporation and Kugelrohr distillation. The resulting product was an off-white solid (125.2 mg, 96.31%). FT-IR: 2973, 1587, 1489, 1468, 1360, 1322, 1277, 1180, 1131, 1060, 1033, 1010, 859, 839, 823, 754, 733, 695, 671, 653. ^{1}H NMR (300 MHz, CD_2Cl_2, δ): 7.88 (d, J = 8.4 Hz, 4H), 7.28-7.35 (m, 8H), 7.08-7.17 (m, 16H), 7.05 (s, 2H). ^{13}C NMR (75 MHz, CD_2Cl_2, δ): 152.14, 147.47, 144.36, 136.38, 130.0, 126.29, 124.71, 121.10, 98.46. MS calcd for $C_{42}H_{30}B_2N_2O_4$: 648.2406; found (Direct Exposure Probe): 648.2422.

*4.3.3.4 SYNTHESIS OF **4.4***

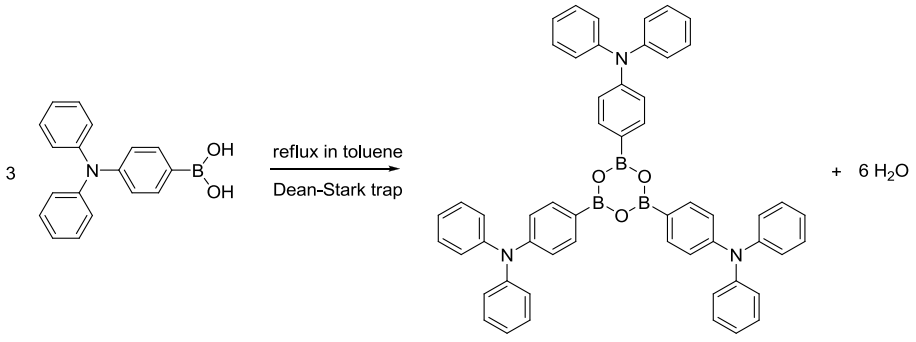

In a round-bottom flask with a Dean-Stark trap, 4-(diphenylamino) phenylboronic acid (106.1 mg, 0.3670 mmol) and 40 mL of distilled toluene were added. The solution was refluxed overnight under a nitrogen atmosphere. The resultant solution was cooled to room temperature and the excess toluene was removed by rotary evaporation. The product was an off-white solid (131.0 mg, quantitative). FT-IR: 3033, 1586, 1492, 1417, 1362, 1325, 1307, 1273, 1190, 1176, 1115, 1074, 1027, 1013, 893, 827, 752, 738, 692, 668. ^{1}H NMR (300 MHz, CD_2Cl_2, δ): 8.03 (d, J = 8.4 Hz, 6H, Ar H *o*-B), 7.28-7.34 (m, 12H, Ar H), 7.05-7.17 (m, 24H, Ar H). ^{13}C NMR (75 MHz, CD_2Cl_2, δ): 152.30, 147.69, 137.18, 130.0, 126.11, 124.48, 121.19. MS calcd for $C_{54}H_{42}B_3N_3O_3$: 813.3530; found (Direct Exposure Probe): 813.3536.

*4.3.3.5 SYNTHESIS OF **4.5***

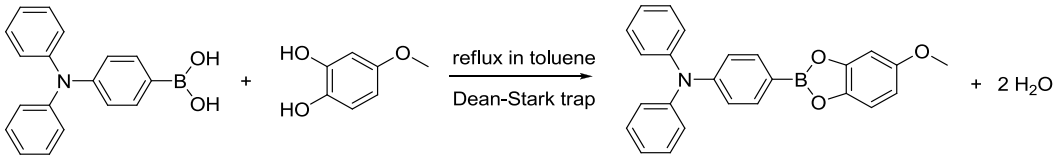

4-Methoxycatechol did not undergo any extra purifications for the following use. 46.6 mg (0.3325 mmol) of 4-methoxycatechol was combined with 93.5 mg (0.3323 mmol) of 4-(diphenylamino)phenylboronic acid in a 100 mL of round bottom flask. 40 mL of toluene was added and the solution went through an overnight reflux under a nitrogen atmosphere. A Dean-Strak trap packed with 4 Å molecular sieves was used to remove water. The resultant solution was cooled to room temperature and placed under rotary evaporation to remove toluene. The crude product was purified by Kugelrohr distillation for 5 hours. The final product was an amber solid (135.2 mg, quantitative). ^{1}H NMR (300 MHz,CD_2Cl_2, δ): 7.87 (d, J = 8.4 Hz, 2H, o-B), 7.32 (t, J = 7.5 Hz, 8.1 Hz, 4H, o-N),

7.17 (m, 9H, Ar), 6.90 (d, J = 2.7 Hz, 1H, between O and OCH_3) 6.66 (dd, J = 8.7, 2.7 Hz, 1H, o-OCH_3) 3.80 (s, 3H, -OCH_3). ^{13}C NMR (75 Hz, CD_2Cl_2, δ): 152.1, 147.5, 136.4, 130.0, 126.3, 124.7, 121.1, 112.2, 108.0, 100.0, 56.5. IR: 3203, 3035, 2939, 2832, 1609, 1587, 1487, 1393, 1363, 1318, 1270, 1225, 1190, 1154, 1066, 1025, 937, 824, 752, 735, 694, 679, 658. MS calcd for $C_{25}H_{20}BNO_3$: 393.1536, found (Direct Exposure Probe): 393.1535.

*4.3.3.6 SYNTHESIS OF **4.6***

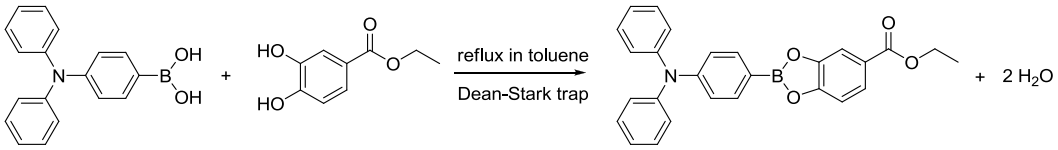

The starting materials were the mixture of 4-(diphenylamino) phenylboronic acid (115.7 mg, 0.4002 mmol) and ethtyl 3,4-dihydroxybenzoate (74.4 mg, 0.4084 mmol). In a round-bottom flask with a Dean-Stark trap, starting materials as well as 40 mL of distilled toluene were added. The solution was refluxed overnight under a nitrogen atmosphere. The resultant clear solution was cooled to room temperature. Then toluene was removed by rotary evaporation and Kugelrohr distillation. The product was an off-white solid (253.4 mg, quantitative). FT-IR: 3038, 1712, 1586, 1484, 1446, 1394, 1368, 1333, 1275, 1260, 1210, 1175, 1145, 1102, 1074, 1065, 1025, 1011, 935, 891, 829, 803, 753, 734, 695, 671, 654. ^{1}H NMR (300 MHz, CD_2Cl_2, δ): 7.87-7.94 (m, 4H, Ar H *o*-B and *o*-ester), 7.31-7.36 (m, 4H, Ar H), 7.14-7.18 (m, 6H, Ar H), 7.05-7.08 (m, 3H, Ar H), 4.35 (q, 2H, OCH_2), 1.39 (t, 3H, CH_3). ^{13}C NMR (75 MHz, CD_2Cl_2, δ): 166.48, 152.99, 152.51, 149.15, 147.37, 136.69, 130.08, 129.74, 126.41, 126.19, 125.79, 124.88, 124.67,

120.87, 113.94, 112.39, 61.63, 14.68. MS calcd for $C_{27}H_{22}BNO_4$: 435.1647; found (Direct Exposure Probe): 435.1645.

*4.3.3.7 SYNTHESIS OF **4.7***

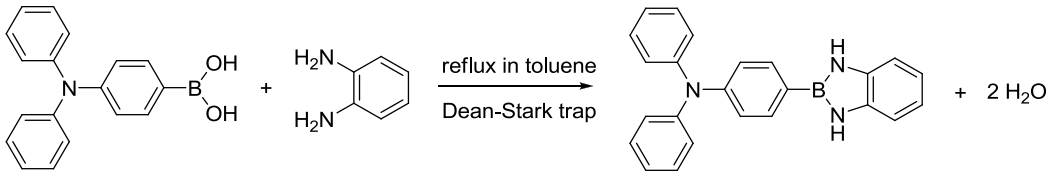

The starting materials were the mixture of 4-(diphenylamino) phenylboronic acid (57.5 mg, 0.1989 mmol) and benzene 1,2-diamine (22.6 mg, 0.2090 mmol). In a round-bottom flask with a Dean-Stark trap, starting materials as well as 40 mL of distilled toluene were added. The solution was refluxed overnight under a nitrogen atmosphere. The resultant clear solution was cooled to room temperature. Then toluene was removed by rotary vaporation. The crude product was further purified by Kugelrohr distillation. The product was an orange solid (253.4 mg, quantitative). FT-IR: 3446, 3419, 3035, 1587, 1491, 1442, 1428, 1358, 1326, 1269, 1176, 1107, 1075, 1028, 1015, 913, 889, 826, 736, 692, 656. ^{1}H NMR (300 MHz, CD_2Cl_2, δ): 7.60 (d, 2H, J = 8.4 Hz, Ar H *o*-B), 7.26-7.32 (m, 4H, Ar H), 7.07-7.17 (m, 8H, Ar H), 6.90-6.93 (m, 2H, Ar H), 6.82 (br, 2H, Ar H), 4.58 (s, NH). ^{13}C NMR (75 MHz, CD_2Cl_2, δ): 148.02, 137.04, 134.55, 129.88, 125.75, 125.45, 123.89, 122.86, 119.73, 111.43. MS calcd for $C_{24}H_{20}BN_3$: 361.1755; found (Direct Exposure Probe): 361.1761.

4.3.4 X-RAY STRUCTURE

X-ray intensity data from a colorless blocklike crystal of bis(dioxaborole) **4.3**

were measured at 100(2) K using a Bruker SMART APEX diffractometer (Mo Kα radiation, λ = 0.71073 Å).[14a] The raw area detector data frames were reduced with the SAINT+ program.[15a] Final unit cell parameters were determined by least-squares refinement of 6319 reflections from the data set. Direct methods structure solution, difference Fourier calculations and full-matrix least-squares refinement against F^2 were performed with SHELXTL.[15b]

The compound crystallizes in the space group C2/c (No. 15) as determined by the pattern of systematic absences in the intensity data, and by the successful solution and refinement of the structure. The asymmetric unit consists of half of one molecule, which is located on a crystallographic inversion center. Non-hydrogen atoms were refined with anisotropic displacement parameters. Hydrogen atoms were placed in geometrically idealized positions and included as riding atoms. The structure data of bis(dioxabrole) **4.3** are listed in **Table 4.5-4.10**.

Table 4.5 Crystal data and structure refinement for **4.3**.

Empirical formula	$C_{42}H_{30}B_2N_2O_4$	
Formula weight	648.30	
Temperature	100(2) K	
Wavelength	0.71073 Å	
Crystal system	Monoclinic	
Space group	C 2/c	
Unit cell dimensions	a = 14.2445(7) Å	α = 90 °.
	b = 9.1170(5) Å	β = 105.7580(10) °.
	c = 26.2041(13) Å	γ = 90 °.
Volume	3275.2(3) $Å^3$	
Z	4	
Density (calculated)	1.315 Mg/m^3	
Absorption coefficient	0.084 mm^{-1}	
F(000)	1352	
Crystal size	0.34 x 0.24 x 0.20 mm^3	
Theta range for data collection	1.61 to 26.39 °.	
Index ranges	-17<=h<=17, -11<=k<=11, -32<=l<=32	
Reflections collected	22761	
Independent reflections	3365 [R(int) = 0.0413]	
Completeness to theta = 26.39 °	100.0 %	
Absorption correction	None	
Refinement method	Full-matrix least-squares on F^2	
Data / restraints / parameters	3365 / 0 / 226	
Goodness-of-fit on F^2	1.033	
Final R indices [I>2sigma(I)]	R1 = 0.0420, wR2 = 0.1085	
R indices (all data)	R1 = 0.0458, wR2 = 0.1117	
Largest diff. peak and hole	0.253 and -0.227 $e.Å^{-3}$	

Table 4.6 Atomic coordinates (x 10^4) and equivalent isotropic displacement parameters ($Å^2$ x 10^3) for **4.3**. U(eq) is defined as one third of the trace of the orthogonalized U^{ij} tensor.

	x	y	z	U(eq)
B(1)	2022(1)	3551(2)	3770(1)	26(1)
C(1)	2458(1)	3587(1)	4645(1)	25(1)
C(2)	2198(1)	2162(1)	4479(1)	25(1)
C(3)	2228(1)	1004(1)	4827(1)	26(1)
C(4)	1783(1)	4057(1)	3188(1)	26(1)
C(5)	1361(1)	3116(2)	2770(1)	39(1)
C(6)	1092(1)	3598(2)	2249(1)	43(1)
C(7)	1236(1)	5050(2)	2129(1)	28(1)
C(8)	1699(1)	5986(2)	2539(1)	35(1)
C(9)	1957(1)	5487(2)	3058(1)	36(1)
C(10)	586(1)	7005(2)	1475(1)	30(1)
C(11)	764(1)	7729(1)	1045(1)	27(1)
C(12)	450(1)	9159(2)	925(1)	34(1)
C(13)	-37(1)	9898(2)	1233(1)	50(1)
C(14)	-240(2)	9167(2)	1654(1)	69(1)
C(15)	55(1)	7730(2)	1773(1)	57(1)
C(16)	952(1)	4579(1)	1179(1)	29(1)
C(17)	1814(1)	3885(1)	1173(1)	33(1)
C(18)	1836(1)	2939(2)	760(1)	38(1)
C(19)	995(1)	2700(2)	351(1)	41(1)
C(20)	142(1)	3393(2)	359(1)	42(1)
C(21)	113(1)	4333(2)	771(1)	35(1)
N(1)	927(1)	5556(1)	1600(1)	32(1)
O(1)	2341(1)	4478(1)	4205(1)	26(1)
O(2)	1917(1)	2118(1)	3930(1)	27(1)

Table 4.7 Bond lengths [Å] and angles [°] for **4.3**.

B(1)-O(1)	1.3916(16)
B(1)-O(2)	1.3926(17)
B(1)-C(4)	1.5395(17)
C(1)-O(1)	1.3841(14)
C(1)-C(3)#1	1.3848(16)
C(1)-C(2)	1.3879(17)
C(2)-O(2)	1.3845(14)
C(2)-C(3)	1.3872(17)
C(3)-C(1)#1	1.3847(16)
C(3)-H(3)	0.9500
C(4)-C(9)	1.3880(19)
C(4)-C(5)	1.3927(18)
C(5)-C(6)	1.3865(18)
C(5)-H(5)	0.9500
C(6)-C(7)	1.3890(19)
C(6)-H(6)	0.9500
C(7)-C(8)	1.3904(18)
C(7)-N(1)	1.4125(15)
C(8)-C(9)	1.3834(17)
C(8)-H(8)	0.9500
C(9)-H(9)	0.9500
C(10)-C(11)	1.3878(18)
C(10)-C(15)	1.392(2)
C(10)-N(1)	1.4143(18)
C(11)-C(12)	1.3867(19)
C(11)-H(11)	0.9500
C(12)-C(13)	1.375(2)
C(12)-H(12)	0.9500
C(13)-C(14)	1.384(3)
C(13)-H(13)	0.9500
C(14)-C(15)	1.384(3)
C(14)-H(14)	0.9500
C(15)-H(15)	0.9500
C(16)-C(17)	1.384(2)
C(16)-C(21)	1.3883(18)
C(16)-N(1)	1.4269(16)
C(17)-C(18)	1.3913(19)
C(17)-H(17)	0.9500
C(18)-C(19)	1.391(2)
C(18)-H(18)	0.9500
C(19)-C(20)	1.375(2)
C(19)-H(19)	0.9500
C(20)-C(21)	1.389(2)
C(20)-H(20)	0.9500

C(21)-H(21)	0.9500
O(1)-B(1)-O(2)	111.14(10)
O(1)-B(1)-C(4)	124.34(12)
O(2)-B(1)-C(4)	124.49(11)
O(1)-C(1)-C(3)#1	127.47(11)
O(1)-C(1)-C(2)	109.03(10)
C(3)#1-C(1)-C(2)	123.50(11)
O(2)-C(2)-C(3)	127.48(11)
O(2)-C(2)-C(1)	109.28(10)
C(3)-C(2)-C(1)	123.24(11)
C(1)#1-C(3)-C(2)	113.27(11)
C(1)#1-C(3)-H(3)	123.4
C(2)-C(3)-H(3)	123.4
C(9)-C(4)-C(5)	116.87(11)
C(9)-C(4)-B(1)	121.30(11)
C(5)-C(4)-B(1)	121.81(12)
C(6)-C(5)-C(4)	121.69(13)
C(6)-C(5)-H(5)	119.2
C(4)-C(5)-H(5)	119.2
C(5)-C(6)-C(7)	120.41(13)
C(5)-C(6)-H(6)	119.8
C(7)-C(6)-H(6)	119.8
C(6)-C(7)-C(8)	118.57(11)
C(6)-C(7)-N(1)	120.46(12)
C(8)-C(7)-N(1)	120.97(12)
C(9)-C(8)-C(7)	120.10(13)
C(9)-C(8)-H(8)	119.9
C(7)-C(8)-H(8)	119.9
C(8)-C(9)-C(4)	122.23(12)
C(8)-C(9)-H(9)	118.9
C(4)-C(9)-H(9)	118.9
C(11)-C(10)-C(15)	118.36(13)
C(11)-C(10)-N(1)	120.38(12)
C(15)-C(10)-N(1)	121.25(13)
C(12)-C(11)-C(10)	120.87(12)
C(12)-C(11)-H(11)	119.6
C(10)-C(11)-H(11)	119.6
C(13)-C(12)-C(11)	120.70(14)
C(13)-C(12)-H(12)	119.6
C(11)-C(12)-H(12)	119.6
C(12)-C(13)-C(14)	118.64(15)
C(12)-C(13)-H(13)	120.7
C(14)-C(13)-H(13)	120.7
C(15)-C(14)-C(13)	121.24(15)
C(15)-C(14)-H(14)	119.4

C(13)-C(14)-H(14)	119.4
C(14)-C(15)-C(10)	120.09(16)
C(14)-C(15)-H(15)	120.0
C(10)-C(15)-H(15)	120.0
C(17)-C(16)-C(21)	119.97(13)
C(17)-C(16)-N(1)	120.15(12)
C(21)-C(16)-N(1)	119.88(13)
C(16)-C(17)-C(18)	119.94(13)
C(16)-C(17)-H(17)	120.0
C(18)-C(17)-H(17)	120.0
C(19)-C(18)-C(17)	119.99(14)
C(19)-C(18)-H(18)	120.0
C(17)-C(18)-H(18)	120.0
C(20)-C(19)-C(18)	119.76(13)
C(20)-C(19)-H(19)	120.1
C(18)-C(19)-H(19)	120.1
C(19)-C(20)-C(21)	120.61(13)
C(19)-C(20)-H(20)	119.7
C(21)-C(20)-H(20)	119.7
C(16)-C(21)-C(20)	119.74(14)
C(16)-C(21)-H(21)	120.1
C(20)-C(21)-H(21)	120.1
C(7)-N(1)-C(10)	121.85(11)
C(7)-N(1)-C(16)	119.26(11)
C(10)-N(1)-C(16)	118.89(10)
C(1)-O(1)-B(1)	105.36(10)
C(2)-O(2)-B(1)	105.16(9)

Symmetry transformations used to generate equivalent atoms:
#1 -x+1/2,-y+1/2,-z+1

Table 4.8 Anisotropic displacement parameters ($Å^2$ x 10^3) for **4.3**. The anisotropic displacement factor exponent takes the form: $-2\pi^2[h^2 a^{*2}U^{11} + ... + 2 h k a^* b^* U^{12}]$.

	U^{11}	U^{22}	U^{33}	U^{23}	U^{13}	U^{12}
B(1)	25(1)	33(1)	19(1)	1(1)	6(1)	0(1)
C(1)	26(1)	30(1)	17(1)	4(1)	7(1)	0(1)
C(2)	26(1)	34(1)	14(1)	0(1)	5(1)	-2(1)
C(3)	30(1)	28(1)	19(1)	0(1)	7(1)	-3(1)
C(4)	26(1)	34(1)	17(1)	2(1)	5(1)	2(1)
C(5)	52(1)	41(1)	21(1)	4(1)	6(1)	-20(1)
C(6)	58(1)	48(1)	17(1)	0(1)	3(1)	-26(1)
C(7)	30(1)	38(1)	16(1)	4(1)	5(1)	1(1)
C(8)	57(1)	27(1)	19(1)	2(1)	6(1)	5(1)
C(9)	56(1)	30(1)	18(1)	-2(1)	2(1)	4(1)
C(10)	29(1)	42(1)	18(1)	3(1)	3(1)	7(1)
C(11)	26(1)	33(1)	22(1)	-2(1)	5(1)	-1(1)
C(12)	32(1)	37(1)	29(1)	2(1)	1(1)	3(1)
C(13)	53(1)	52(1)	37(1)	2(1)	1(1)	29(1)
C(14)	80(1)	91(2)	41(1)	10(1)	24(1)	59(1)
C(15)	62(1)	85(1)	30(1)	19(1)	23(1)	39(1)
C(16)	42(1)	29(1)	16(1)	5(1)	8(1)	-5(1)
C(17)	45(1)	31(1)	22(1)	5(1)	5(1)	-1(1)
C(18)	59(1)	28(1)	31(1)	7(1)	17(1)	4(1)
C(19)	72(1)	29(1)	23(1)	-1(1)	15(1)	-10(1)
C(20)	56(1)	44(1)	23(1)	-1(1)	5(1)	-17(1)
C(21)	40(1)	42(1)	22(1)	3(1)	7(1)	-10(1)
N(1)	41(1)	37(1)	15(1)	3(1)	5(1)	2(1)
O(1)	33(1)	30(1)	15(1)	3(1)	6(1)	-1(1)
O(2)	32(1)	34(1)	13(1)	1(1)	4(1)	-3(1)

Table 4.9 Hydrogen coordinates (x 10^4) and isotropic displacement parameters ($Å^2$ x 10^3) for **4.3**.

	x	y	z	U(eq)
H(3)	2051	28	4714	31
H(5)	1255	2119	2844	47
H(6)	807	2930	1972	51
H(8)	1837	6969	2464	42
H(9)	2265	6146	3333	43
H(11)	1106	7239	830	33
H(12)	573	9634	627	41
H(13)	-232	10889	1158	60
H(14)	-587	9660	1865	83
H(15)	-106	7240	2058	68
H(17)	2389	4055	1451	40
H(18)	2426	2455	758	46
H(19)	1011	2061	67	49
H(20)	-432	3227	80	50
H(21)	-480	4806	775	42

Table 4.10 Torsion angles [°] for **4.3**.

O(1)-C(1)-C(2)-O(2)	0.39(13)
C(3)#1-C(1)-C(2)-O(2)	179.81(11)
O(1)-C(1)-C(2)-C(3)	-179.48(11)
C(3)#1-C(1)-C(2)-C(3)	0.0(2)
O(2)-C(2)-C(3)-C(1)#1	-179.79(11)
C(1)-C(2)-C(3)-C(1)#1	0.04(19)
O(1)-B(1)-C(4)-C(9)	5.9(2)
O(2)-B(1)-C(4)-C(9)	-176.35(12)
O(1)-B(1)-C(4)-C(5)	-172.49(13)
O(2)-B(1)-C(4)-C(5)	5.3(2)
C(9)-C(4)-C(5)-C(6)	-2.5(2)
B(1)-C(4)-C(5)-C(6)	176.00(14)
C(4)-C(5)-C(6)-C(7)	-0.2(2)
C(5)-C(6)-C(7)-C(8)	3.2(2)
C(5)-C(6)-C(7)-N(1)	-177.49(14)
C(6)-C(7)-C(8)-C(9)	-3.5(2)
N(1)-C(7)-C(8)-C(9)	177.15(13)
C(7)-C(8)-C(9)-C(4)	0.9(2)
C(5)-C(4)-C(9)-C(8)	2.1(2)
B(1)-C(4)-C(9)-C(8)	-176.36(13)
C(15)-C(10)-C(11)-C(12)	2.2(2)
N(1)-C(10)-C(11)-C(12)	-178.77(11)
C(10)-C(11)-C(12)-C(13)	0.6(2)
C(11)-C(12)-C(13)-C(14)	-2.3(2)
C(12)-C(13)-C(14)-C(15)	1.2(3)
C(13)-C(14)-C(15)-C(10)	1.7(3)
C(11)-C(10)-C(15)-C(14)	-3.3(3)
N(1)-C(10)-C(15)-C(14)	177.68(16)
C(21)-C(16)-C(17)-C(18)	-0.21(19)
N(1)-C(16)-C(17)-C(18)	-179.69(12)
C(16)-C(17)-C(18)-C(19)	0.6(2)
C(17)-C(18)-C(19)-C(20)	-0.6(2)
C(18)-C(19)-C(20)-C(21)	0.2(2)
C(17)-C(16)-C(21)-C(20)	-0.13(19)
N(1)-C(16)-C(21)-C(20)	179.36(12)
C(19)-C(20)-C(21)-C(16)	0.1(2)
C(6)-C(7)-N(1)-C(10)	146.80(14)
C(8)-C(7)-N(1)-C(10)	-33.88(19)
C(6)-C(7)-N(1)-C(16)	-32.84(19)
C(8)-C(7)-N(1)-C(16)	146.48(13)
C(11)-C(10)-N(1)-C(7)	146.10(12)
C(15)-C(10)-N(1)-C(7)	-34.9(2)
C(11)-C(10)-N(1)-C(16)	-34.26(18)
C(15)-C(10)-N(1)-C(16)	144.75(15)

C(17)-C(16)-N(1)-C(7)	-55.66(17)
C(21)-C(16)-N(1)-C(7)	124.85(13)
C(17)-C(16)-N(1)-C(10)	124.68(13)
C(21)-C(16)-N(1)-C(10)	-54.80(17)
C(3)#1-C(1)-O(1)-B(1)	179.49(12)
C(2)-C(1)-O(1)-B(1)	-1.11(13)
O(2)-B(1)-O(1)-C(1)	1.47(13)
C(4)-B(1)-O(1)-C(1)	179.47(12)
C(3)-C(2)-O(2)-B(1)	-179.64(12)
C(1)-C(2)-O(2)-B(1)	0.51(13)
O(1)-B(1)-O(2)-C(2)	-1.23(13)
C(4)-B(1)-O(2)-C(2)	-179.23(11)

Symmetry transformations used to generate equivalent atoms:
#1 -x+1/2,-y+1/2,-z+1

4.3.5 COMPUTATIONAL CALCULATIONS

Computational study was performed using the software Spartan 08. The geometries of boroles **4.1-4.7** were first optimized by using semi-empirical AM1 calculations. Then molecular orbitals and band gap energies were calculated by using DFT B3LYP with a 6-31G* basis set.

4.3.6 OPTICAL TITRATIONS

Dichloromethane was used as a solvent and stock solutions were made in volumetric flasks. The solution of boroles (2 mL in a quartz cuvette) was titrated with incremental amounts (3-5 μL) of a TBAF solution by a microinjector. The absorbance data were recorded on an absorption spectrophotometer and the fluorescence intensity was recorded on a fluorescence spectrophotometer.

[1] (a) Hudson, Z. M.; Wang, S. Impact of donor-acceptor geometry and metal chelation on photophysical properties and applications of triarylboranes. *Acc. Chem. Res.*, **2009**, *42*(10): 1584-1596. (b) Jäkle, F. Advances in the synthesis of organoborane polymers for optical, electronic, and sensory applications. *Chem. Rev.*, **2010**, *110*(7), 3985-4022. (c) Mou, X.; Liu, S. J.; Dai, C. L.; Ma, T. C.; Zhao, Q.; Ling, Q. D.; Huang, W. A class of fascinating optoelectronic materials: triarylboron compounds. *Sci. China Chem.*, **2010**, *53*(6): 1235-1245. (d) Hudnall, T. W.; Chiu, C.-W.; Gabbai, F. P. Fluoride ion recognition by chelating and cationic boranes. *Acc. Chem. Res.*, **2009**, *42*(2): 388-397. (e) Wade, C. R.; Broomsgrove, A. E. J.; Aldridge, S.; Gabbai, F. P. Fluoride ion complexation and sensing using organoboron compounds. *Chem. Rev.*, **2010**, *110*(7), 3958-3984. (f) Galbraith, E.; James, T. D. Boron based anion receptors as sensor. *Chem. Soc. Rev.*, **2010**, *39*, 3831-3842. (g) Hudson, Z. M.; Wang, S. Metal-containing triarylboron compounds for optoelectronic applications. *Dalton Trans.*, **2011**, *40*: 7805-7816.

[2] Niu, W.; Smith, M. D.; Lavigne, J. J. Self-assembling poly(dioxaborole)s as blue-emissive materials. *J. Am. Chem. Soc.*, **2006**, *128*(51), 16466-16467.

[3] Lanni, L. M.; Tilford, R. W.; Bharathy, M.; Lavigne J. J. Enhanced hydrolytic stability of self-assembling alkylated 2-dimensional covalent organic frameworks. *J. Am. Chem. Soc.*, **2011**, *133*(35), 13975-13983.

[4] See Chapter 2 for details.

[5] Rambo, B. M.; Lavigne, J. J. Defining self-assembling linear oligo(dioxaborole)s. *Chem. Mater.*, **2007**, *19*(15), 3732-3739.

[6] (a) Silverstein, R. M.; Webster, F. X.; Kiemle D. J. Infrared spectrometry. *Spectrometric identification of organic compounds*, 7th ed.; Wiley & Sons: Hoboken, NJ, 2005; p 101. (b) Yamaguchi, I.; Choi, B.-J.; Koizumi, T.; Kubota, K.; Yamamoto, T. π-Conjugated polyphenylenes with diazaborole side chains synthesized via 1,2-phenylenediamine polymer. *Macromolecules*, **2007**, *40*, 438-443.

[7] Niu, W. J.; Smith, M. D.; Lavigne, J. J. Substituent effects on the structure and supramolecular assembly of bis(dioxaborole)s derived from 1,2,4,5-tetrahydroxybenzene. *Cryst. Growth & Des.*, **2006**, *6*(6), 1274-1277.

[8] (a) Anslyn, E. V.; Dougherty, D. A. Solutions and non-covalent binding forces. *Modern physical organic chemistry*; University Science Books, 2004; p 147. (b) Reichardt, C. Solvatochromic dyes as solvent polarity indicators. *Chem. Rev.*, **1994**, *94*, 2319-2358.

[9] Dong, D. C.; Winnik, M. A. The Py scale of solvent polarities. *Can. J. Chem.*, **1984**, *62*, 2560-2565.

[10] Kamlet, M. J.; Abboud, J. L.; Taft, R. W. The solvatochromic comparison method. 6. The π* scale of solvent polarities. *J. Am. Chem. Soc*., **1977**, *99*(18): 6027-6038.

[11] Lavigne, J. J. Molecular recognition and molecular sensing: single analyte analysis and multi-component sensor arrays for the simultaneous detection of a plethora of analytes. Ph.D. Thesis, The University of Texas at Austin, Austin, TX, August 2000.

[12] (a) Hargrove, A. E.; Zhong, Z.; Sessler, J. L.; Anslyn, E. V. Algorithms for the determination of binding constants and enantiomeric excess in complex host:guest equilibria using optical measurements. *New J. Chem.*, **2010**, *34*, 348-354. (b) Absorption titration worksheet (guest:host of 2:1) was used, with permission of Dr. Ken D. Shimizu in University of South Carolina, Columbia. The worksheet was found at http://www.chem.sc.edu/faculty/shimizu/Site/Group%20Stuff.html.

[13] Hall, H. K., Jr. Correlation of the base strengths of amines. *J. Am. Chem. Soc*., **1957**, *79*(20), 5441-5444.

[14] (a) SMART Version 5.630, SAINT+ Version 6.45. Bruker Analytical X-ray Systems, Inc., Madison, Wisconsin, USA, 2003. (b) Sheldrick, G. M. A short history of SHELX. *Acta Cryst.*, **2008**, *A64*, 112-122.

CHAPTER 5

SYNTHESIS, CHARACTERIZATION, AND OPTOELECTRONIC PROPERTIES OF D-π-A TRIPHENYLAMINO DI- AND POLY- BOROLES

5.0 INTRODUCTION

Due to the interesting optical properties, donor-π-acceptor (D-π-A) boranes have wide applications as chemical sensors, organic light-emitting devices, non-linear optics and two-photon emitters.[1] However, D-π-A boranes suffer from several drawbacks, including difficult synthesis, hydrolytic and oxidative instability, and limited sensing targets, that hinder their real world applications. As an alternative to D-π-A boranes, a series of novel D-π-A boroles were developed in Chapter 4. Their synthesis, characterization, optoelectronic properties and sensing performance were studied. D-π-A boroles were proved to be promising sensory materials for Lewis bases.

Inspired by the previous results, another series of D-π-A boroles were designed and studied using triphenylamino- tetra-ol and boronic acid building blocks. Herein, diborole **5.1** was used as a model compound for polyborole **5.2** (**Figure 5.1**). Their optoelectronic properties and sensing applications are explored by absorption, fluorescence and computational calculations.

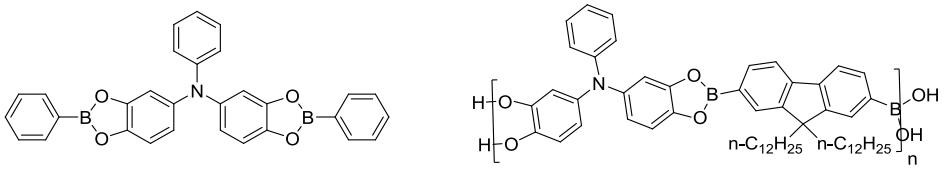

Figure 5.1 Structures of D-π-A triphenylamino di- and poly- boroles.

5.1 Results and Discussion

5.1.1 Synthesis and characterization

The main chain boronate linked dimer and polymer were prepared as shown in **Figure 5.2**. The monomer di(3,4-dihydroxyphenyl)phenylamine was synthesized according to a modified literature procedure.[2] Aniline reacted with 4-iodo-1,2-dimethoxybenzene by the Ullmann reaction to give the protected triphenylamino- tetra-ol, which was demethylated by pyridine hydrochloride. The resultant tetral-ol reacted with mono- or di- boronic acid by a dehydration reaction and produced diborole **5.1** and polyborole **5.2** in modest yields (>73.4%). The products exhibit good solubility in organic solvents: such as chloroform, toluene, tetrahydrofuran, and 1,4-dioxane.

Boroles **5.1**-**5.2** were characterized by FT-IR and ^{1}H NMR spectroscopy. In FT-IR spectra, a broad peak centered at 3348 cm^{-1} disappeared, indicating the disappearance of hydroxyl groups in the monomer tetra-ol. The peaks approaching 1350, 1050, and 660 cm^{-1} confirmed the formation of boronate ester.[3] In ^{1}H NMR spectra, the peak appeared at 8.05 ppm was assigned to the protons on the aromatic ring *ortho*- to borons, which further confirmed the formation of boronate ester.[3] The synthetic routes and characterization are detailed summarized in Experimental section.

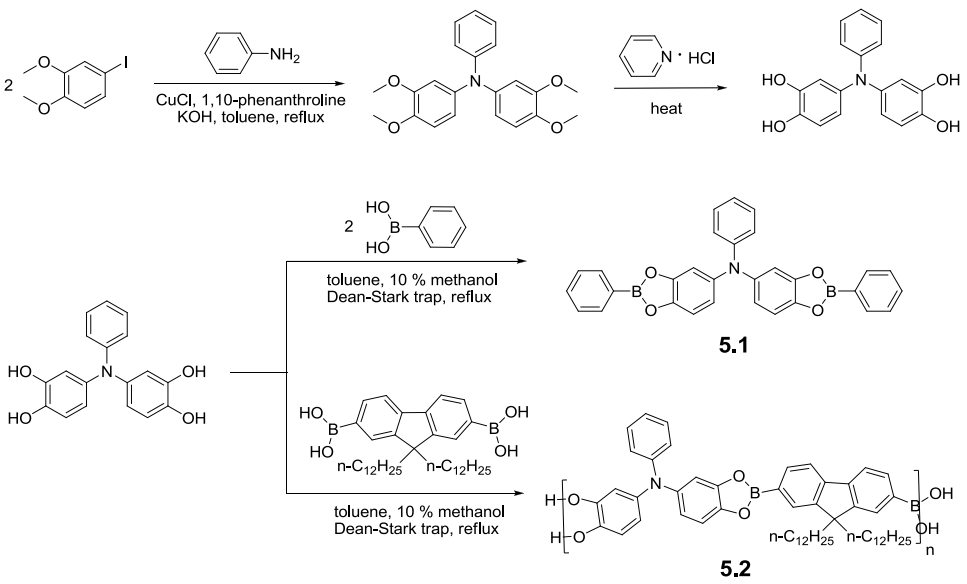

Figure 5.2 Synthesis of boroles **5.1-5.2**.

5.1.2 OPTICAL AND ELECTRONIC PROPERTIES

5.1.2.1 ABSORPTION STUDIES

The absorption properties of boroles **5.1-5.2** were studied. As shown in **Figure 5.3a**, the absorption maxima of diborole **5.1** is at 310 nm, while the absorption maxima of polyborole **5.2** is at 322 nm. The red-shift absorption maxima going from compound **5.1** to **5.2** results from the extended π-conjugation through the borole backbone.

In order to select the proper concentration for optical titrations, the absorption properties of control **5.1** are further studied. As the concentration of **5.1** increases, the absorbance increases accordingly (**Figure 5.3b**). The absorbance at 310 nm is in a linear relationship with the concentration in the range of 0-5.2×10^{-5} M (**Figure 5.3b, insert**). The linear regression follows Beer's law, indicating no aggregation occurs. The molar absorptivity is calculated to be 2.7×10^{4} M^{-1} cm^{-1}. For the following absorption studies, boroles **5.1-5.2** of 2×10^{-5} M are selected.

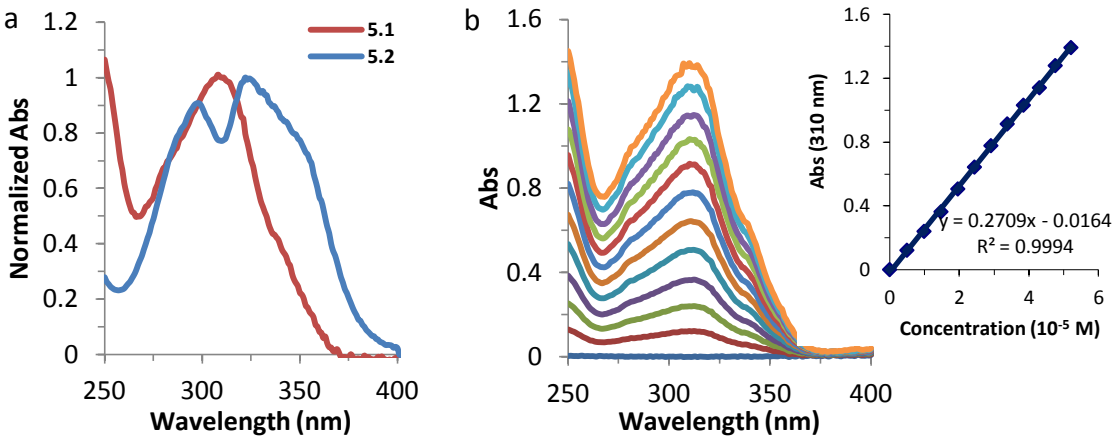

Figure 5.3 (a) Absorption spectra of 2×10^{-5} M boroles **5.1-5.2** in CH_2Cl_2. (b) Absorption spectra of diborole **5.1** at different concentrations in CH_2Cl_2, insert: plot of absorbance at the absorption maxima vesus the concentration of **5.1** in CH_2Cl_2.

5.1.2.2 COMPUTATIONAL STUDIES

To obtain theoretical information about the electronic/optical properties, computational calculations were performed by DFT (B3LYP-6-31G*) package in the Spartan 08 software for diborole **5.1** and its fluoride complex. The calculated orbital geometries and energies are listed in **Table 5.1**. The HOMO of diborole **5.1** is located on the central triphenylamino- tetra-ol moiety with an energy of -4.95 eV. the LUMO is mainly found on the terminal phenyl borole parts, where boron atoms make a large contribution and increase the energy to -1.03 eV. It is anticipated that an intramolecular charge transfer may occur from the HOMO to the LUMO, studied detailed by fluorescence below.

Upon fluoride binding, the fluoride complex **5.1-F** changes the boron atoms from trigonal planar geometry to tetrahedral. The resulting interruption of the extended π-conjugation prevents borons involved in the LUMO, increasing the band gap energy to

3.99 eV. The calculated increasing band gap is consistent with the hypsochromic shift of absorption maxima upon the addition of fluoride.

Table 5.1 Computed orbitals and energies for diborole and its fluoride complex.

Compound	**5.1**	**5.1-F**
HOMO	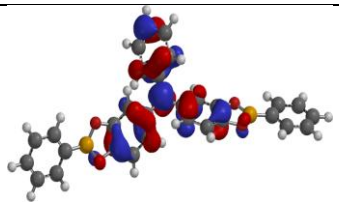 -4.95 eV	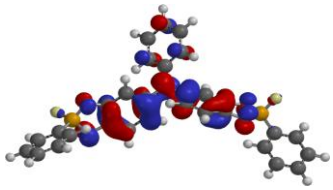 0.66 eV
LUMO	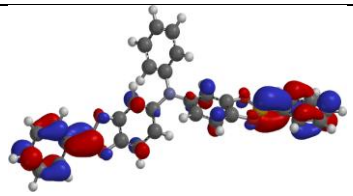 -1.03 eV	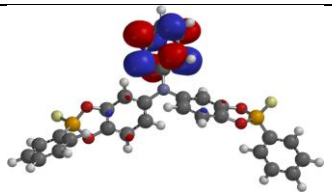 4.65 eV
Band gap	3.92 eV	3.99 eV
λcal	316 nm	311 nm
λexp	308 nm	305 nm

5.1.2.3 FLUORESCENCE STUDIES

The computational study of diborole **5.1** indicated that an intramolecular charge transfer may happen from the central triphenylamino- tetra-ol to the terminal phenyl boronate ester moiety. However, the charge transfer property of polyborole **5.2** is more interesting, which will be conducted by studying the fluorescent behavior in different solvents.

Due to charge transfer, polyborole **5.2** has a dipole when excited by light and is stabilized by a polar solvent.[1a] Thus, the emission wavelength of polyborole **5.2** becomes longer as the solvent polarity increases (**Figure 5.4**). It is noteworthy to mention that

polyborole **5.2** has an emissive wavelength of 506 nm in CH_2Cl_2, indicating a green emissive material.

Charge transfer of polyborole **5.2** was further studied by $E_T(30)$[4], Py[5] and Pi*[4a,6] scales (**Figure 5.4c-e**). The energy has a linear regression with $E_T(30)$ value, with a large relative slope of 1.6839, indicating an effective intramolecular charge transfer. Py and Pi*scales have similar trends as $E_T(30)$.

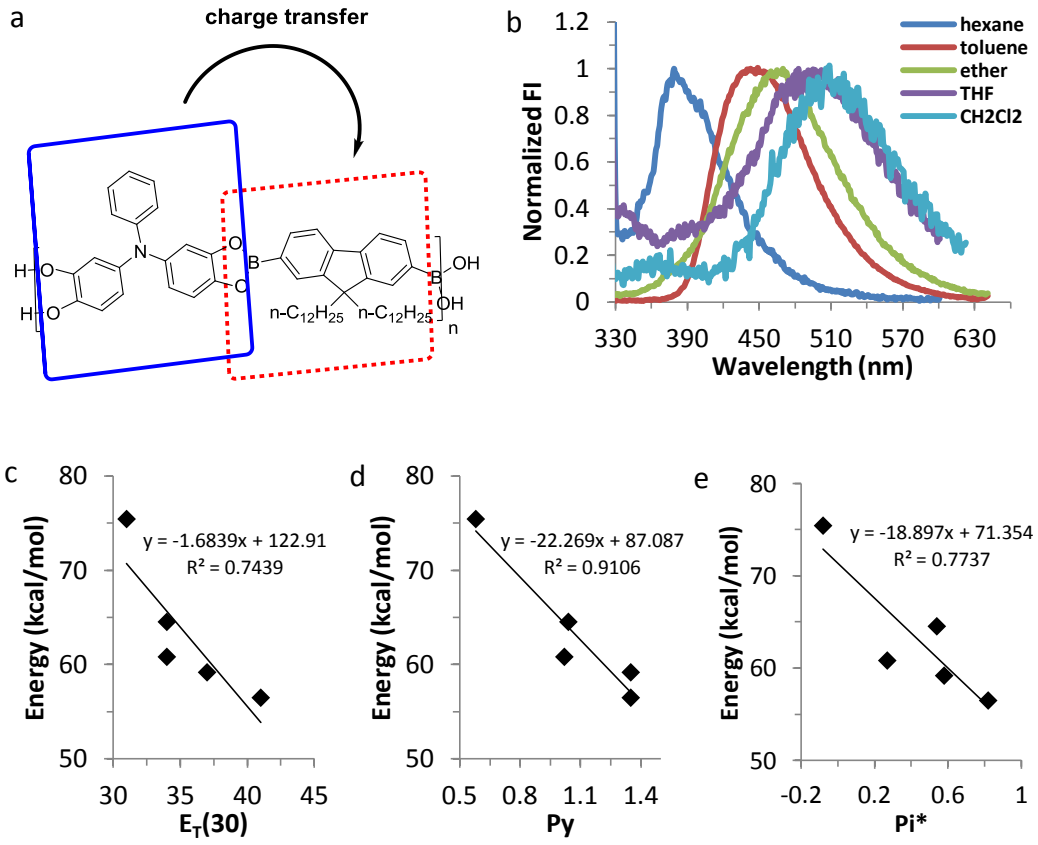

Figure 5.4 (a) Representation of intramolecular charge transfer of polyboroe **5.2**. (b) Fluorescence spectra of **5.2** (saturated solutions in hexane and ether, 5×10^{-6} M in toluene and THF, and 2×10^{-6} M in CH_2Cl_2). Plots of energy of **5.2** versus (a) $E_T(30)$, (b) Py, and (c) Pi* values.

5.1.3 SENSING APPLICATIONS

5.1.3.1 OPTICAL TITRATIONS

The binding interactions between boroles **5.1**-**5.2** and fluoride were investigated by absorption and fluorescence titrations. As shown in **Figure 5.5**, the sequential addition of fluoride allows the absorption maxima of **5.1** blue-shifted, indicating the interruption of π-conjugation. Fluoride also quenches the fluorescence of diborole **5.1**. Polyborole **5.2** has the similar response to fluoride as **5.1**. It is noteworthy to mention that the emission wavelength also blue-shifted, due to turned-off charge transfer. The mole ratio plot[7] shows that diborole **5.1** afford a 0.89:1 ratio of fluoride to boron, approaching 1:1. The binding constant of K_1 is calculated as 1.48×10^5 M^{-1}, by fitting the 2:1 (guest:host) binding isotherm[8].

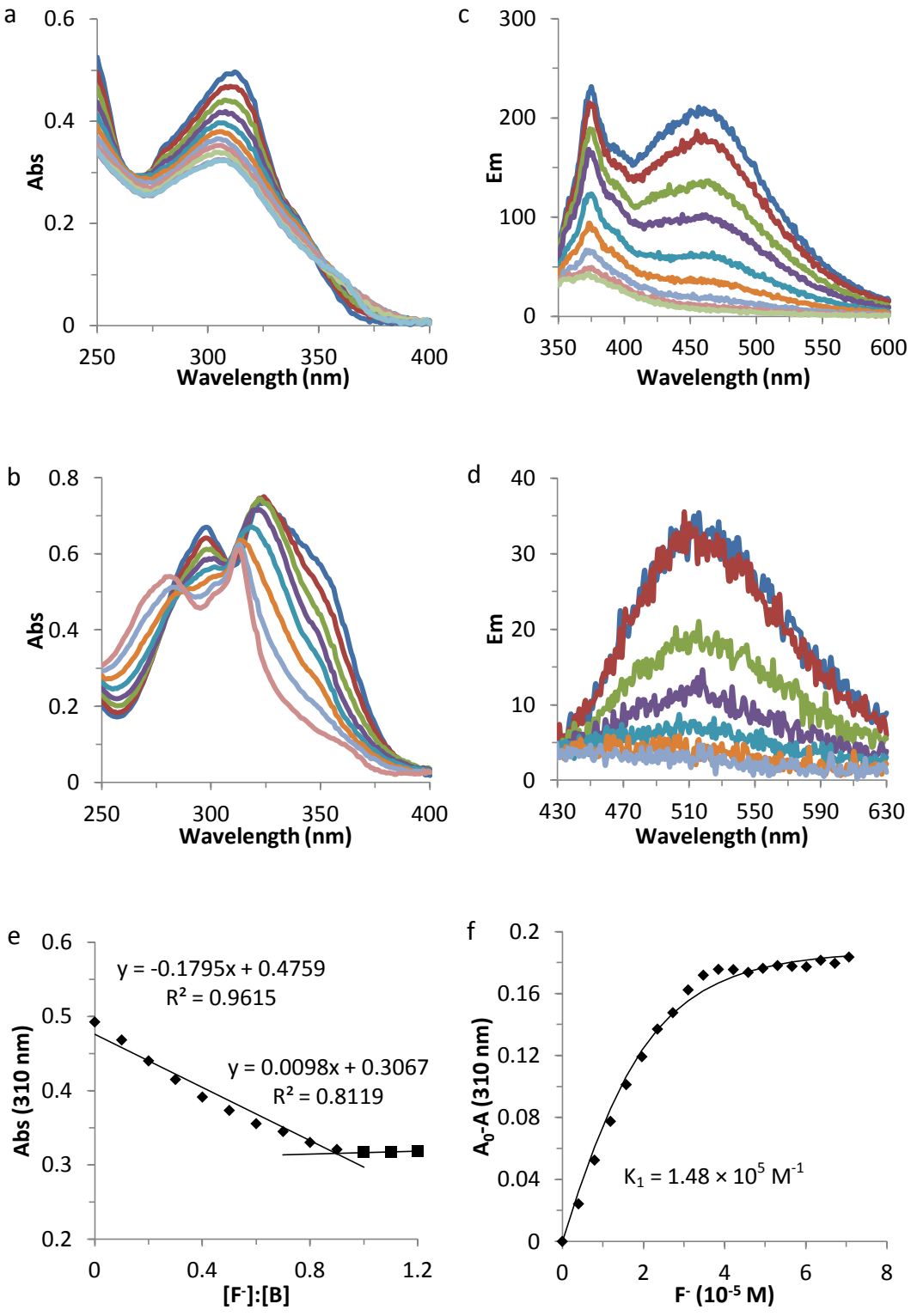

Figure 5.5 Absorption titrations of 2×10^{-5} M borole (a) **5.1** and (b) **5.2**, and fluorescence titrations of 2×10^{-6} M borole (c) **5.1** and (d) **5.2** upon the addition of fluoride in CH_2Cl_2. (e) Mole ratio plot and (f) binding isotherm of 2×10^{-5} M diborole **5.1** upon the addition of fluoride in CH_2Cl_2.

5.1.3.2 BINDING REVERSIBILITY

The binding reversibility between boroles and fluoride was studied by absorption spectroscopy. As shown in **Figure 5.6**, upon the addition of excess trimetylsilyl chloride (TMSCl) to fluoride-borole complexes, the absorption maxima of borole **5.1** or **5.2** red shifts back and absorbance at the maximum wavelength restores. These results indicate that TMSCl scavenges fluoride and releases the original borole **5.1** or **5.2**, which further demonstrates the reversible binding between borole and fluoride and borole stability.

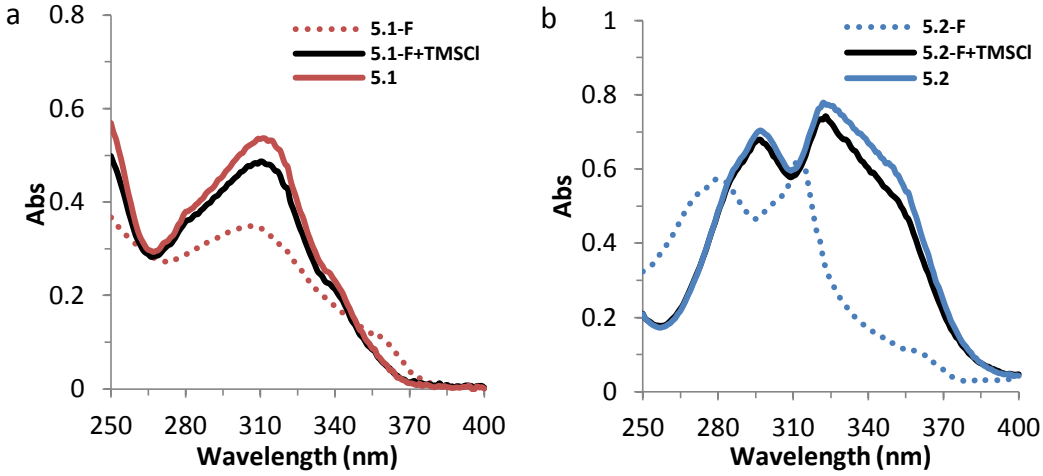

Figure 5.6 Absorption spectra of fluoride-borole (a) **5.1** and (b) **5.2** complexes upon the addition of excess TMSCl in CH_2Cl_2 (borole: 2×10^{-5} M, fluoride: 4×10^{-5} M).

5.1.3.3 BINDING CROSS-REACTIVITY

In addition to fluoride, other anions and amines are also selected as Lewis bases to study the recognition ability of boroles. As shown in **Figure 5.7**, borole **5.1** and **5.2** selectively bind hard Lewis bases F^- and $H_2PO_4^-$, but they do not show any response to soft anions Cl^- and Br^-. The neutral amines can also bind to boroles. It was found that the binding ability increases as the amine basicity increases from pyridine, to

benzylamine, to n-butylamine.[9] The cross-reactivity of boroles **5.1**-**5.2** may provide insights to differentiate Lewis bases by using a sensor array.

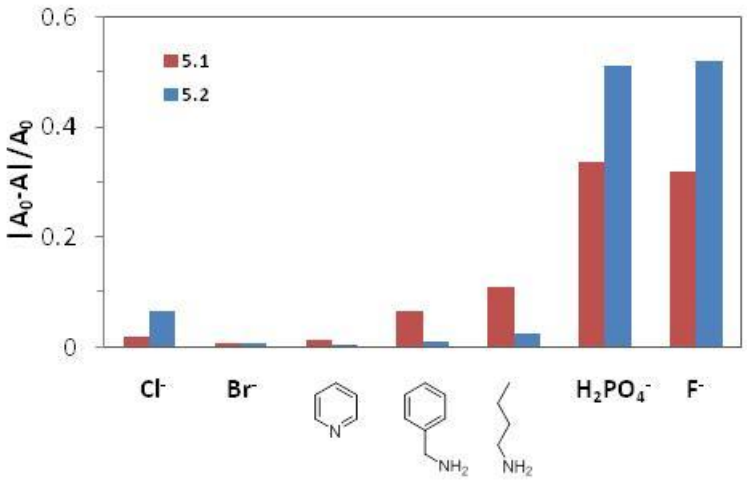

Figure 5.7 Degree of the absorbance response of borole **5.1** and **5.2** (2×10^{-5} M) upon the addition of Lewis bases (10^{-4} M) in CH_2Cl_2.

5.2 CONCLUSION

In summary, a new family of D-π-A boroles was preliminarily developed. The representative di- and poly- boroles were synthesized by dehydration reactions and characterized. The absorption studies indicated the extended π-conjugation of polyborole. The computational results of dimer predicted the optical and sensing properties of boroles. Polyborole showed a solvatochromism by fluorescence, due to the intramolecular charge transfer from triphenylamino- tetra-ol to borole. The sensing applications of boroles were also explored. The binding between boroles and fluoride was sensitive, reversible and cross-reactive. These D-π-A boroles may provide insights to develop new sensory materials for Lewis base detection.

5.3 EXPERIMENTAL

5.3.1 MATERIALS

4-Iodo-1,2-dimethoxybenzene was purchased from Oakwood Products Inc.. 1,10-Phenanthroline, anhydrous magnesium sulfate, and ethyl acetate were purchased from Fisher Scientific Company. Potassium hydroxide flakes were purchased from Spectrum Chemical MFG Corp.. Pyridine hydrochloride and 1,4-benzenediboronic acid were purchased from Alfa Aesar. Phenylboronic acid was purchased from Acros. 9,9-Didodecylfluorene-2,7-diboronic acid was purchased from Sigma-Aldrich. All the chemicals were used without further purification. Toluene, methanol, hexane, ether, tetrahydrofuran and dichloromethane were obtained by using purification systems from Innovative Technologies.

5.3.2 INSTRUMENTATION

FT-IR spectra were performed on a PerkinElmer Spectrum 100 FT-IR Spectrometer. Sample (~0.5 mg) was put on a diamond/ZnSe crystal. The spectrometer scanned 4 times with a resolution of 4.00 cm^{-1} from 4000 cm^{-1} to 650 cm^{-1}. ^{1}H NMR and ^{13}C NMR spectra were obtained on a Varian Mercury/VX 300 MHz Spectrometer. Mass spectra were obtained on a VG 70S Mass Spectrometer. Absorbance data were recorded on a Beckman Coulter 640 DU Spectrophotometer. Fluorescence data were recorded on a Cary Eclipse Fluorescence Spectrophotometer.

5.3.3 SYNTHESIS

5.3.3.1 SYNTHESIS OF DI(3,4-DIMETHOXYPHENYL)PHENYLAMINE

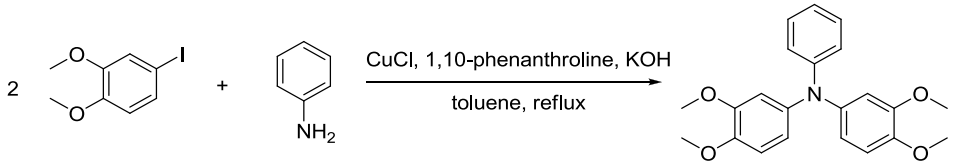

The protected tetra-ol was synthesized according to the literature with some modifications.[1] 40 mL of toluene, 480 μL (4.9273 mmol) of aniline, 2.6403 g (9.9989 mmol) of 4-iodo-1,2-dimethoxybenzene, 32.8 mg (0.1820 mmol) of 1,10-phenanthroline, 18.2 mg (0.1835 mmol) of cuprous chloride and 2.1987 g (39.1855 mmol) of potassium hydroxide flakes were sequentially added to a 100 mL round-bottom flask equipped with a Dean-Stark trap under a nitrogen purge. The starting materials were heated to reflux for 48 hours and cooled down to 80 ^{o}C. The mixture was poured into a separatory funnel containing 14 mL of toluene and 11 mL of water. The product was extracted with toluene twice. The combined organic layers were dried with anhydrous magnesium sulfate. Then toluene was removed by reduced pressure distillation to give the crude product, further purified by recrystallization using ethanol. The product was a pink solid (1.0668 g, 59.3 %). ^{1}H NMR (300 MHz, $CDCl_3$, δ): 7.20 (t, J = 9.0 Hz, 2H, Ar *m*-N), 6.99 (d, J = 7.8 Hz, 2H, Ar *o*-N), 6.89 (t, J = 7.2 Hz, 1H, Ar *p*-N), 6.76 (d, J = 8.7 Hz, 2H, ArOMe), 6.69 (s, 2H, ArOMe *o*-N), 6.64 (d, J = 8,7 Hz, 2H, ArOMe), 3.87 (s, 6H, OMe), 3.75 (s, 6H, OMe). ^{13}C NMR (75 MHz, $CDCl_3$, δ): 149.68, 148.70, 145.52, 141.57, 129.15, 121.66, 121.16, 117.31, 111.96, 109.42, 56.31 (OMe), 56.13 (OMe). GC/MS (EI) m/z (relatively intensity): 365 (100), 350 (49), 183 (9), 167 (5), 77 (4); MS calcd for $C_{22}H_{23}NO_4$: 365.42. FT-IR: 3002, 2965, 2839, 1587, 1508, 1463, 1441, 1300, 1232, 1127, 1025, 752.

5.3.3.2 SYNTHESIS OF DI(3,4-DIHYDROXYPHENYL)PHENYLAMINE

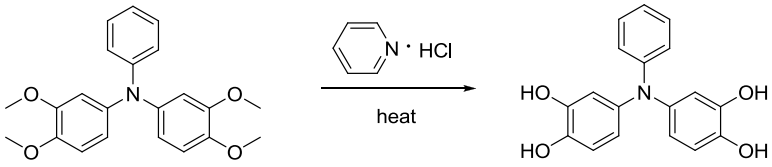

The tetra-ol was synthesized according to the literature with some modifications.[1] 548.3 mg (1.5000 mmol) of previously synthesized di(3,4-dimethoxyphenyl)phenylamine and 5352.8 mg (46.3205 mmol) of pyridine hydrochloride were added to a 50 mL round-bottom flask. The mixture was heated to 160°C for 2 hours under a nitrogen purge. The mixture was cooled down to room temperature, and transferred into a separatory funnel containing 15 mL of ethyl acetate and 15 mL of water. The product was extracted with ethyl acetate twice. The combined organic layers were dried with anhydrous magnesium sulfate. Then ethyl acetate was removed by reduced pressure distillation to give the crude product (403.6 mg, 87.0 %). ^{1}H NMR (300 MHz, acetone-d_6, δ): 7.14 (t, J = 7.2 Hz, 2H, Ar *m*-N), 6.87 (d, J = 8.7 Hz, 2H, Ar *o*-N), 6.80 (d, J = 7.2 Hz, 1H, Ar *p*-N), 6.74 (d, J = 8.4 Hz, 2H, ArOMe), 6.58 (s, 2H, ArOMe *o*-N), 6.45 (m, 2H, ArOMe). ^{13}C NMR (75 MHz, acetone-d_6, δ): 150.11, 146.47, 142.50, 141.50, 129.63, 121.31, 120.85, 117.89, 116.55, 113.98. MS (direct probe): 309; MS calcd for $C_{18}H_{15}NO_4$: 309.32. FT-IR: 3348, 1592, 1511, 1489, 1368, 1325, 1248, 1176, 1098, 779,750.

*5.3.3.3 SYNTHESIS OF DIBOROLE **5.1***

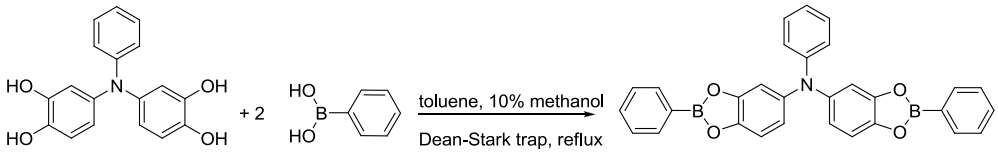

To a 100 mL round-bottom flask equipped with a Dean-Stark trap and a condenser 30 mL of toluene, 3 mL methanol, 30.7 mg (0.0992 mmol) of di(3,4-dihydroxyphenyl)phenylamine and 25.9 mg phenylboronic acid (0.2124 mmol) were added. Under a nitrogen purge, the starting materials were heated to reflux for 5.5 hours and cooled to room temperature. Then toluene was removed by reduced pressure distillation to yield the pure product (35.0 mg, 73.4 %). ^{1}H NMR (300 MHz, $CDCl_3$, δ): 8.06 (d, J = 6.6 Hz, 4H, *o*-B), 7.57 (d, J = 7.5 Hz, 2H, *p*-B), 7.51 (d, J = 7.5 Hz, 4H, *m*-B), 7.45 (s, 2H, Ar), 7.21 (d, J = 3.6 Hz, 2H, Ar), 7.11 (d, J = 2.1 Hz, 2H, Ar), 7.07 (d, J = 9.0 Hz, 2H, Ar), 6.98 (t, J = 6.9 Hz, 1H), 6.91 (m, 2H, Ar). ^{13}C NMR (75 MHz, $CDCl_3$, δ): 149.42, 144.89, 143.93, 135.70, 135.15, 132.60, 129.45, 128.47, 122.90, 122.27, 119.76, 112.75, 110.20. MS (direct probe): 481; MS calcd for $C_{30}H_{21}B_2NO_4$: 481.11. FT-IR: 3047, 1603, 1477, 1356, 1232, 1198, 1068, 1025, 692, 662.

5.3.3.4 SYTHESIS OF POLYBOROLE ***5.2***

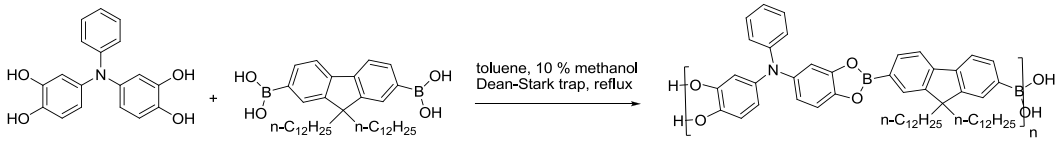

To a 50 mL round-bottom flask equipped with a Dean-Stark trap and a condenser, 30 mL of toluene, 3 mL methanol, 61.8 mg (0.1998 mmol) of di(3,4-dihydroxyphenyl)phenylamine and 118.1 mg 9,9-didodecylfluorene-2,7-diboronic acid (0.2003 mmol) were added. Under a nitrogen purge, the starting materials were heated to reflux for 5 hours and cooled to room temperature. The mixture was filtered under the reduced pressure. Then toluene was removed by reduced pressure distillation to yield a yellow product (173.5 mg, quantitative). ^{1}H NMR (300 MHz, $CDCl_3$, δ): 8.05 (m, 4H, *o*-

B), 7.89 (d, J = 7.8 Hz, 2H, *m*-B), 7.24 (m, 4H, Ar), 7.15 (s, 2H, Ar), 7.09 (d, J = 7.8 Hz, 2H, Ar), 7.00 (m, 1H, Ar), 6.93 (d, J = 9.3 Hz, 2H, Ar). ^{13}C NMR (75 MHz, $CDCl_3$, δ): 151.69, 149.89, 149.06, 145.36, 144.35, 134.36, 129.76, 129.53, 128.72, 125.80, 123.23, 120.80, 112.95, 110.42, 55.90, 40.71, 32.43, 30.48, 30.14, 29.85, 29.81, 24.38, 23.23, 14.44. FT-IR: 2922, 2851, 1608, 1473, 1421, 1352, 1229, 1184, 1064, 806, 749, 693, 663.

5.3.4 COMPUTATIONAL CALCULATIONS

Computational study was performed on Spartan 08 software. The geometries of diborole **5.1** and its fluoride complex were first optimized by using semi-empirical AM1 calculation. Then, molecular orbitals and band gap energies were calculated by using DFT B3LYP with a 6-31G* basis set.

5.3.5 OPTICAL TITRATIONS

Dichloromethane was used as a solvent and stock solutions were made in volumetric flasks. The solution of boroles **5.1**-**5.2** (2 mL in a quartz cuvette) was titrated with the incremental amounts (3-5 μL) of a TBAF solution by a microinjector. Then the absorbance data were recorded on an absorption spectrophotometer and the fluorescence intensity was recorded on a fluorescence spectrophotometer.

[1] (a) Hudson, Z. M.; Wang, S. Impact of donor-acceptor geometry and metal chelation on photophysical properties and applications of triarylboranes. *Acc. Chem. Res.*, **2009**, *42*(10): 1584-1596. (b) Jäkle, F. Advances in the synthesis of organoborane polymers for optical, electronic, and sensory applications. *Chem. Rev.*, **2010**, *110*(7), 3985-4022. (c) Mou, X.; Liu, S. J.; Dai, C. L.; Ma, T. C.; Zhao, Q.; Ling, Q. D.; Huang, W. A class of fascinating optoelectronic materials: triarylboron compounds. *Sci. China Chem.*, **2010**, *53*(6): 1235-1245. (d) Hudnall, T. W.; Chiu, C.-W.; Gabbai, F. P. Fluoride ion recognition by chelating and cationic boranes. *Acc. Chem. Res.*, **2009**, *42*(2): 388-397. (e) Wade, C. R.; Broomsgrove, A. E. J.; Aldridge, S.; Gabbai, F. P. Fluoride ion complexation and sensing using organoboron compounds. *Chem. Rev.*, **2010**, *110*(7), 3958-3984. (f) Galbraith, E.; James, T. D. Boron based anion receptors as sensor. *Chem. Soc. Rev.*, **2010**, *39*, 3831-3842. (g) Hudson, Z. M.; Wang, S. Metal-containing triarylboron compounds for optoelectronic applications. *Dalton Trans.*, **2011**, *40*: 7805-7816.

[2] Zengin, H.; Zengin, G.; Smith, D. W. *J. Polym. Sci. Part A: Polym. Chem.*, **2006**, *44*, 6988.

[3] Rambo, B. M.; Lavigne, J. J., Defining self-assembling linear oligo(dioxaborole)s. *Chem. Mater.* **2007,** 19, (15), 3732-3739.

[4] (a) Anslyn, E. V.; Dougherty, D. A. Solutions and non-covalent binding forces. *Modern physical organic chemistry*; University Science Books, 2004; p 147. (b) Reichardt, C. Solvatochromic dyes as solvent polarity indicators. *Chem. Rev.*, **1994**, *94*, 2319-2358.

[5] Dong, D. C.; Winnik, M. A. The Py scale of solvent polarities. *Can. J. Chem.*, **1984**, *62*, 2560-2565.

[6] Kamlet, M. J.; Abboud, J. L.; Taft, R. W. The solvatochromic comparison method. 6. The π* scale of solvent polarities. *J. Am. Chem. Soc*., **1977**, *99*(18): 6027-6038.

[7] Lavigne, J. J. Molecular recognition and molecular sensing: single analyte analysis and multi-component sensor arrays for the simultaneous detection of a plethora of analytes. Ph.D. Thesis, The University of Texas at Austin, Austin, TX, August 2000.

[8] (a) Hargrove, A. E.; Zhong, Z.; Sessler, J. L.; Anslyn, E. V. Algorithms for the determination of binding constants and enantiomeric excess in complex host:guest equilibria using optical measurements. *New J. Chem.*, **2010**, *34*, 348-354. (b) Absorption titration worksheet (guest:host of 2:1) was used, with permission of Dr. Ken D. Shimizu in University of South Carolina, Columbia. The worksheet was found at http://www.chem.sc.edu/faculty/shimizu/Site/Group%20Stuff.html.

[9] Hall, H. K., Jr. Correlation of the base strengths of amines. *J. Am. Chem. Soc.*, **1957**, *79*(20), 5441-5444.

CHAPTER 6

SUMMARY AND OUTLOOK OF BORONATE-LINKED MATERIALS IN CHEMICAL SENSORS

6.0 INTRODUCTION

Boronate ester formation, with its covalent but reversible feature, provides the advantages of facile synthesis, tunable optical properties, enhanced stability and planar geometry. Thus, boronate esters, especially dioxaboroles, were proposed as alternatives of boranes to design better sensors for Lewis bases. In previous chapters, several series of boronate ester-linked materials were designed, synthesized and characterized to study binding mechanism and sensing applications of Lewis bases.

Based on the previously intensive investigation of fluorenyl dioxaboroles by our group, this series of boronate esters were first studied. The fluorenyl bis(dioxaborole) and poly(dioxaborole) based sensors for Lewis bases were discussed in Chapter 2. The binding between boroles and Lewis bases was tunable, sensitive, reversible and cross-reactive. In addition, the fluorenyl bis(dioxaborole)-based cross-reactive sensor arrays for anions was shown in Chapter 3.

Inspired by the research of donor-π-acceptor (D-π-A) boranes, an amine was attached to a boron moiety to form two families of D-π-A boroles. Their synthesis, characterization, structure and opto/electronic property relationship for sensing

applications were studied in Chapter 4 and 5. These boronate esters showed an intramolecular charge transfer and a turn-off optical sensing mode for fluoride. Based on the previous studies, the future direction of boronate ester-linked materials in sensors will be predicted herein.

6.1 Summary and Outlook

6.1.1 Bisdioxa- and bisdiaza- boroles

Chapter 2 showed that introduction of different substituents on the catechol moiety of bis(dioxaborole)s could easily tune the optical properties and boron Lewis acidity, thereby impacting binding sensitivity and selectivity. For instance, the electron-withdrawing nitro groups on catechol increase the Lewis acidity of boron centers, leading to a more sensitive binding to fluoride. In addition, the binding makes the colorless solution turn yellow, allowing for an interesting colorimetric fluoride sensor.

In the future, similar bisdioxa- and bisdiaza- boroles with electron-withdrawing groups can be designed to further explore the interesting optical properties and sensing applications. As shown in **Figure 6.1**, other electron-withdrawing groups, such as ester, cyano or ammonium groups can be attached to either catechol or diamine moiety. Other π-systems, such as phenyl, biphenyl, groups or diphenylacetylene, can also be attached to diboronic acid.

The starting materials of substituted catechol **6.1**-**6.2**, diamine **6.4** and diboronic acid **6.5**-**6.7** are all commercially-available. Substituted catechol **6.3**[1] and diboronic acid **6.8**[2] can both be synthesized according to literary procedures. The diol or diamine can be combined with any diboronic acid to synthesize new boroles. Their synthesis,

characterization, optical properties and sensing studies can be performed according to the methods established in Chapter 2. It is anticipated that those boroles are interesting colorimetric sensors for Lewis bases with tunable optical properties.

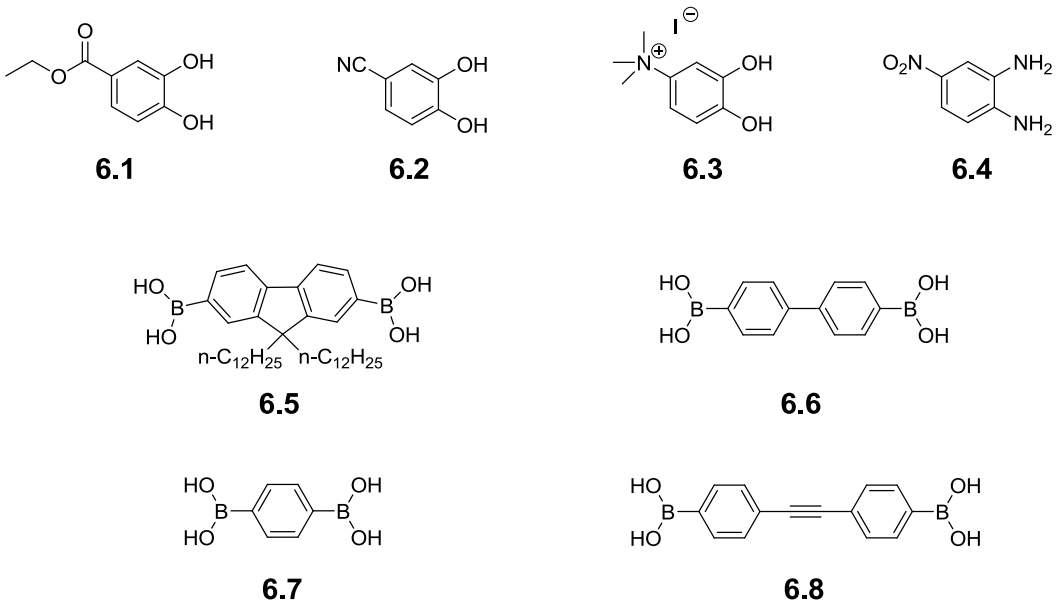

Figure 6.1 Proposed starting materials to synthesize new boroles.

In addition to sensing mechanism study, the bisdioxa- and bisdiaza- boroles can be used to design cross-reactive sensor arrays. The sensor array for anions or amines can be studied according to the methods described in Chapter 3. Anions are important species in environment, industry, and biology[3], but they are difficult to sense and discriminate.[4] Besides, amines are used as biomarkers.[5]

6.1.2 D-Π-A BOROLE-BASED POLYMER

In Chapter 4, a series of D-π-A triphenylaminoboroles were designed, synthesized and characterized. Those boroles showed tunable optical properties and

solvatochromism, resulting from the charge transfer from an amine group to a borole moiety. Boroles showed a turned-off sensing mode for fluoride. Those D-π-A boroles might have promising applications for sensing Lewis bases, such as anions and amines.

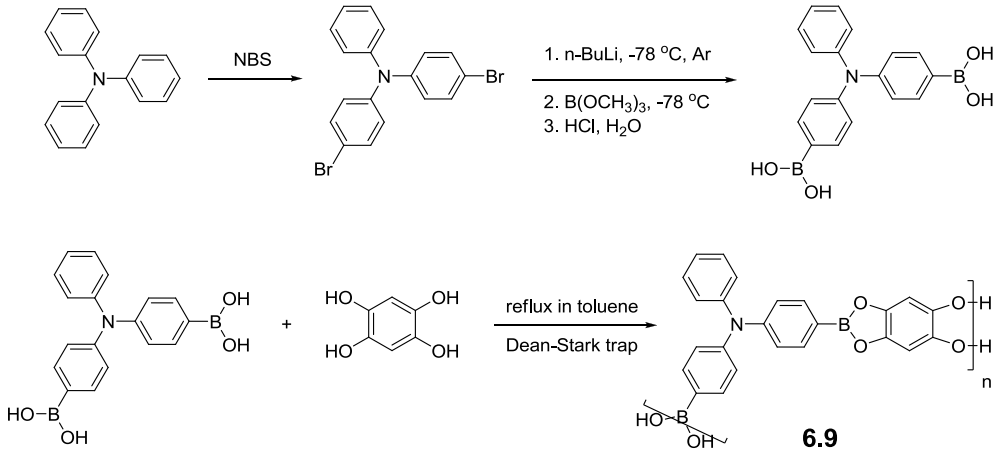

Figure 6.2 Synthesis of D-π-A polymer from triphenylamine diboronic acid and THB.

The future work can be extended to explore D-π-A borole-based polymer. As shown in **Figure 6.2**, synthesis of polymer **6.9** can start with the commercially-available triphenylamine, which can be brominated by NBS to form N,N-bis(4-bromophenyl)aniline. The resultant bromide will be borylated and hydrolyzed to generate triphenylamine diboronic acid.[6] A polymer will be formed via a condensation polymerization using diboronic acid and 1,2,4,5-tetrahydroxybenzene (THB). The optical property and sensing studies can be performed according to the methods described in Chapter 4. Due to the amplification effect of conjugated polymers[7], polymer **6.9** is expected have an enhanced sensitivity to Lewis bases than dimer.

6.1.3 D-π-A BIS(DIOXABOROLE)S

In Chapter 5, another family of D-π-A boroles was synthesized and characterized using triphenylaminotetra-ol and boronic acid building blocks. The computational calculations of diborole predicted the optical and sensing properties. Polyborole showed solvatochromism, due to the charge transfer from tetra-ol to borole. Binding between boroles and fluoride was sensitive, reversible and cross-reactive. These D-π-A di- and poly- boroles provide the insights to develop new sensory materials for sensing Lewis bases.

The future research can focus on studying structure and opto/electronic property relationship. Two sets of D-π-A boroles can be designed by modification of either phenylboronic acid (**6.10-6.14**) or phenylamine moiety (**6.15-6.19**). The synthetic process is similar to the method described in Chapter 5 (**Figure 6.3**). Substituted triphenylaminotetra-ol can be synthesized by Ullmann reaction between 4-iodo-1,2-dimethoxybenzene and substituted aniline, followed by deprotection using pyridine hydrochloride. The resultant tetral-ol will react with commercially-available substituted phenylboronic acid to form D-π-A boroles.

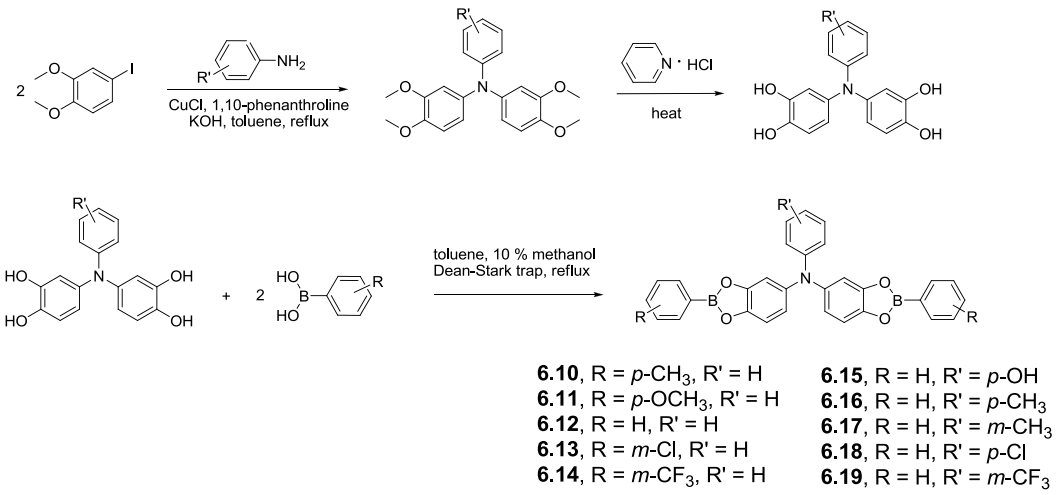

6.10, R = *p*-CH_3, R' = H
6.11, R = *p*-OCH_3, R' = H
6.12, R = H, R' = H
6.13, R = *m*-Cl, R' = H
6.14, R = *m*-CF_3, R' = H
6.15, R = H, R' = *p*-OH
6.16, R = H, R' = *p*-CH_3
6.17, R = H, R' = *m*-CH_3
6.18, R = H, R' = *p*-Cl
6.19, R = H, R' = *m*-CF_3

Figure 6.3 Synthesis of D-π-A boroles.

To provide the theoretical information about the electronic properties, computational calculations for D-π-A borole **6.10-6.19** were performed using the DFT package (B3LYP-6-31G*) in software Spartan 08. The calculated orbital geometries and energies are listed in **Table 6.1-6.2**. The HOMO of boroles is generally located on the central triphenylaminotetra-ol moiety, while the LUMO is mainly located on the terminal phenyl borole motif, where boron atoms make a larger contribution. It is expected that the charge transfer may occur from the HOMO to the LUMO, which can be confirmed by fluorescence study of boroles in solvents with different polarities.

Table 6.1 Computed orbitals and energies of borole **6.10-6.14** with modification of phenylborole motif

Compound	HOMO	LUMO
6.10 (*p*-CH_3)	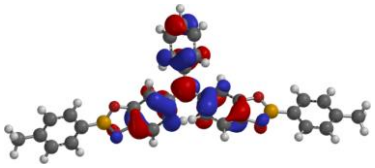	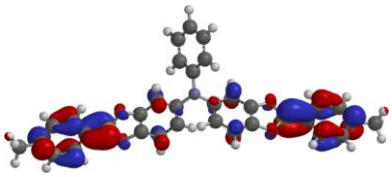
	-4.89 eV	-0.95eV
6.11 (*p*-OCH_3)	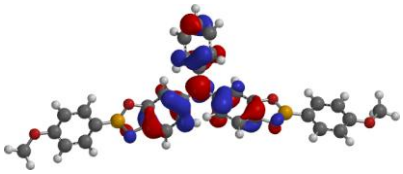	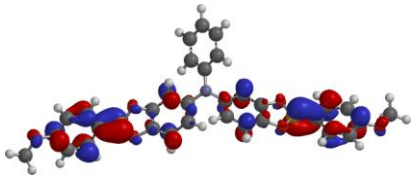
	-4.84 eV	-0.77 eV
6.12 (H)	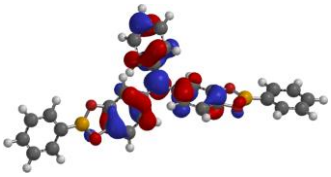	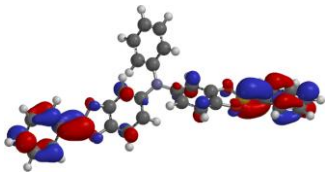
	-4.95 eV	-1.03 eV
6.13 (*m*-Cl)	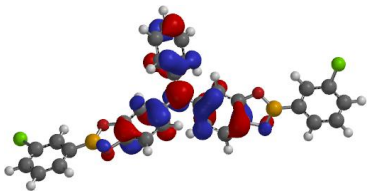	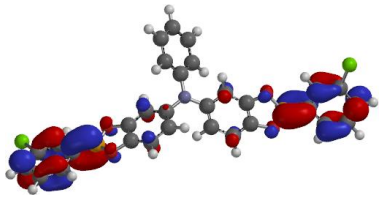
	-5.09 eV	-1.09 eV
6.14 (*m*-CF_3)	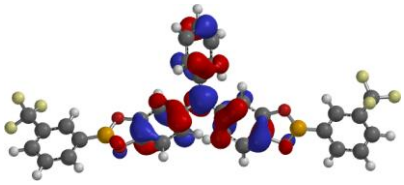	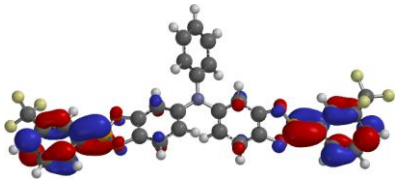
	-5.12 eV	-1.43 eV

Table 6.2 Computed orbitals and energies of borole **6.15-6.19** with modification of triphenylaminotetra-ol moiety

Compound	HOMO	LUMO
6.15 (*p*-OH)	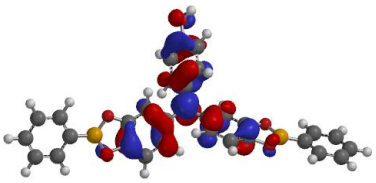	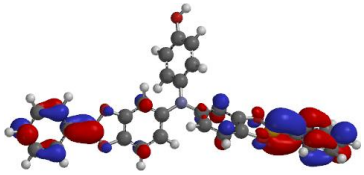
	-4.80 eV	-1.00 eV
6.16 (*p*-CH_3)	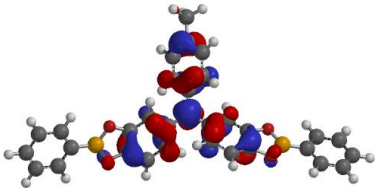	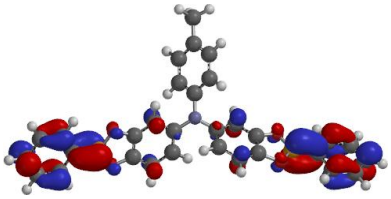
	-4.87 eV	-1.01 eV
6.17 (*m*-CH_3)	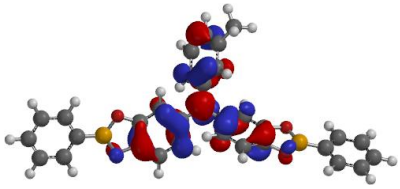	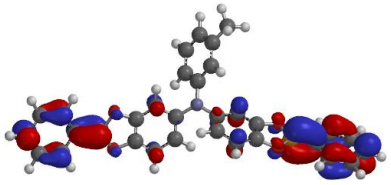
	-4.91 eV	-1.02 eV
6.18 (*p*-Cl)	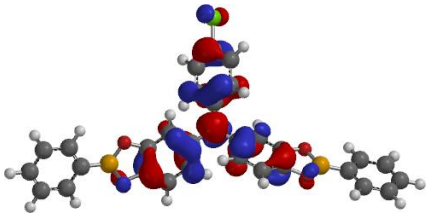	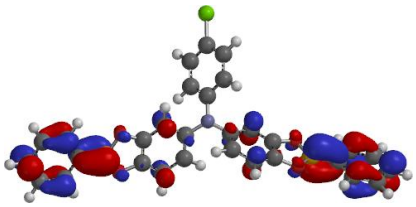
	-5.09 eV	-1.12 eV
6.19 (*m*-CF_3)	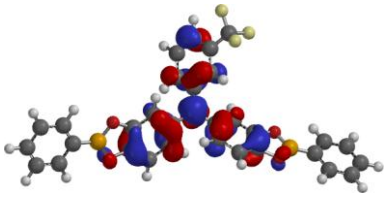	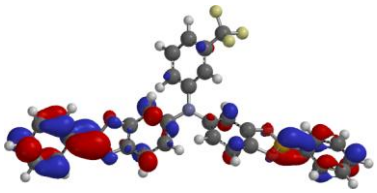
	-5.18 eV	-1.13 eV

The LUMO of boroles is located on the terminal phenylborole motif, which can be motified to tune the electronic properties. For instance, the incorporation of electron-donating groups of *p*-CH_3 (**6.10**) and *p*-OCH_3 (**6.11**) will raise the LUMO energy, thereby increasing the band gap. The introduction of electron-withdrawing groups of *m*-Cl (**6.13**) and *m*-CF_3 (**6.14**) will lower the LUMO energy, thereby effectively decreasing the band gap.

The HOMO focuses on the central triphenylaminotetra-ol moiety, which can also be used to modify the electronic properties. For example, the incorporation of electron-donating groups of *p*-OH (**6.15**), *p*-CH_3 (**6.16**) and *m*-CH_3 (**6.17**) will raise the HOMO energy and decrease band gap, while the introduction of electron-withdrawing groups of *p*-Cl (**6.18**) and *m*-CF_3 (**6.19**) will lower the HOMO energy and increase band gap.

Table 6.3 Hammett sigma constant and computed band gap of D-π-A borole **6.10-6.19**

Compound	Hammett sigma constant	Band gap eV	Compound	Hammett sigma constant	Band gap eV
6.10 (*p*-CH_3)	-0.14	3.94	**6.15 (*p*-OH)**	-0.38	3.80
6.11 (*p*-OCH_3)	-0.12	4.07	**6.16 (*p*-CH_3)**	-0.14	3.86
6.12 (H)	0	3.92	**6.17 (*m*-CH_3)**	-0.06	3.89
6.13 (*m*-Cl)	0.37	3.75	**6.12 (H)**	0	3.92
6.14 (*m*-CF_3)	0.46	3.69	**6.18 (*p*-Cl)**	0.24	3.97
			6.19 (*m*-CF_3)	0.46	4.05

Hammett sigma constant[8] and computed band gap for boroles are listed in **Table 6.3**. The computed band gap has a linear regression with Hammett sigma constant (**Figure 6.4**). This result indicates that band gap can be predicted when a substituent is employed to the triphenylaminotetra-ol or phenylborole moiety. The optical property and sensing studies can be performed according to the methods in Chapter 5.

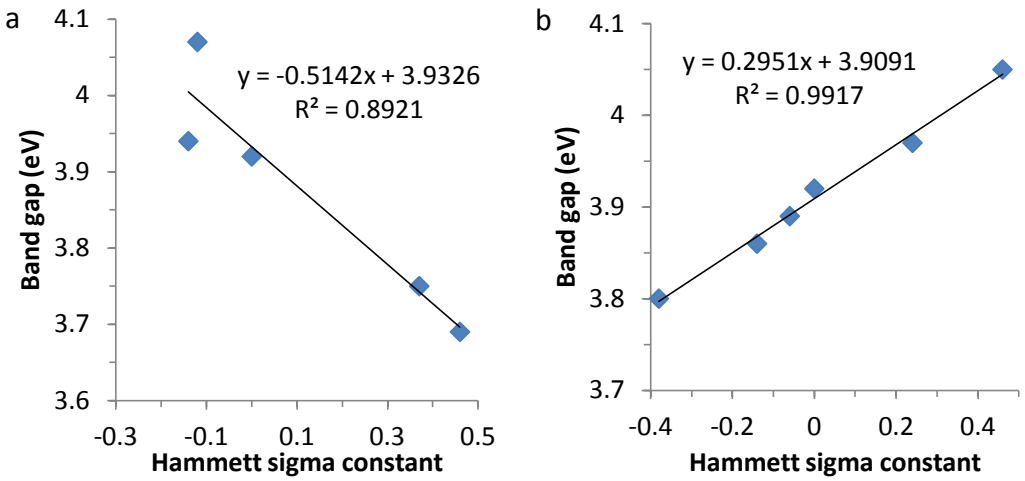

Figure 6.4 Plots of computed band gap vesus Hammett sigma constant for borole (a) **6.10-6.14** and (b) **6.12**, **6.15-6.19**.

6.1.4 CRUCIFORM BIS(DIOXABOROLE)S

Due to the interesting optical and sensing properties, cruciforms have recently been developed as promising sensory materials. Since they possess the spatially separated molecular obitals, either the HOMO or the LUMO will be changed when analytes bind. Thus, the optical properties especially fluorescence are modified.[9]

Nitrogen-boron is a good electron donor-accepter pair, thus, the LUMO located boron moiety and the HOMO located amine motif have been put in a perpendicular position to form cruciform-type D-π-A boranes.[10] However, boranes including cruciform boranes suffer from several disadvantages including difficult synthesis, unstability toward water and oxygen, and bulky subtituents, which hinder their sensing applications.

Compared to boranes, boronate esters including bis(dioxaborole)s have the relating advantages, thus, cruciform boronate esters can be developed in the future. For example, chloro-, bromo- and nitro- substituted THB (**6.20-6.21**)[11] and ester substituted THB (**6.23**) [12] can be synthesized according to the methods described in literature

(**Figure 6.5**). These substituted THB can react with phenylboronic acid or diboronic acids (**6.5-6.8**) to form diboroles or polyboroles.

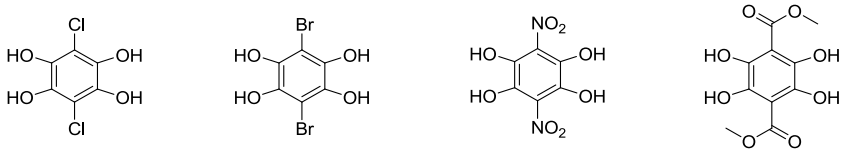

6.20 **6.21** **6.22** **6.23**

Figure 6.5 Structures of substituted THB used to synthesize cruciform boroles.

Computational calculations can be used to confirm the HOMO and the LUMO geometries. It is anticipated that the LUMO locates on the electron-withdrawing substituents while the HOMO focuses on the borole moiety. The optical property and sensing studies can be performed according to the methods described in Chapter 2. It is expected that the fluoride binding to cruciform boroles will change the HOMO geometry and energy, leading to the optical change.

6.1.5 METAL CHELATED D-π-A BOROLES

The fluoride sensing mode of boranes can easily be tuned by incorporation of metal ligands. For example, the Wang group[13] developed the Pt(II)-borane complex with a 2,2'-bipy linker as a colorimetric sensor for fluoride. Inspired by their work, the metal-borole complex (**6.24-6.25**) can be developed in the future.

As shown in **Figure 6.6**, the synthesis starts with 2,2'-bipyridyl, which undergoes oxidation and nitration to give 4-nitro-2,2'-bipyridyl N-oxide.[14] After bromination and borylation, 4-nitro-2,2'-bipyridyl N-oxide transforms to 2,2'-bipyridine-4-boronic acid.[15]

The resultant boronic acid then reacts with catechol to generate 2,2'-bipyridylborole, chelating Cu(I) and Pt(II)[13a]. Computational calculations, optical properties and sensing studies can be performed according to the methods described in Chapter 2. It is expected that the binding of fluoride to metal-chelated boroles will change the optical or/and electronic properties, leading to interesting fluoride sensors.

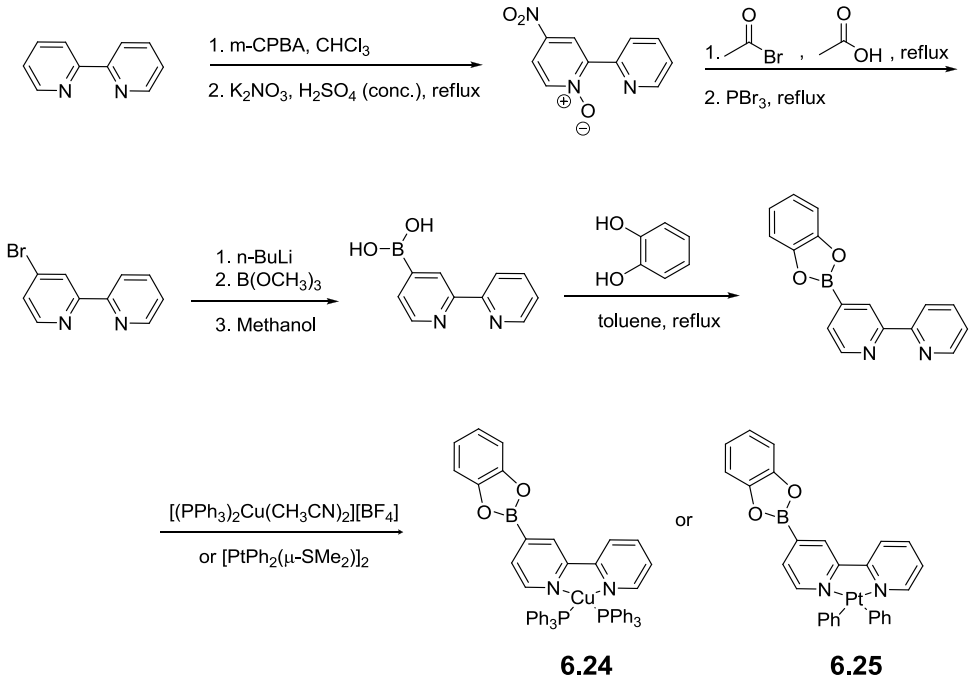

Figure 6.6 Synthesis of metal chelated boroles.

6.2 CONCLUSION

In summary, the future directions of boronate ester-linked materials in chemical sensors were predicted. The electron-withdrawing groups can be attached to catechol or diamine moiety to form new bisdioxa- and bisdiaza- boroles. New D-π-A triphenylaminoborole-based polymer and dimers can also be developed. Moreover,

cruciform and metal chelated boroles can be designed to develop interesting sensors or sensor arrays for Lewis bases.

6.3 REFERENCES

[1] Sheriff, T. S. Production of hydrogen peroxide from dioxygen and hydroxylamine or hydrazine catalysed by manganese complexes. J. *Chem. Soc. Dalton Trans.*, **1992**, 1051-1058.

[2] Maly, K. E.; Maris, T; and Wuest, J. D. Two-dimensional hydrogen-bonded networks in crystals of diboronic acids. *CrystEngComm*, **2006**, *8*, 33-35.

[3] Feng, L.; Li, H.; Li, X.; Chen, L.; Shen, Z.; Guan, Y. Colorimetric sensing of anions in water using ratiometric indicator-displacement assay. *Anal. Chim. Acta*, **2012**, *743*, 1-8.

[4] Nishiyabu, R.; Palacios, M. A.; Dehaen, W.; Anzenbacher, Jr. P. Synthesis, structure, anion binding, and sensing by calix[4]pyrrole isomers. *J. Am. Chem. Soc.*, **2006**, *128*, 11496-11504.

[5] Li, X. Development of conjugated boronate ester-linked materials for optical sensing applications targeting small molecules. Ph.D. Thesis, University of South Carolina, Columbia, SC, 2012.

[6] Xiao, H.; Leng, B.; Tian, H. Hole transport triphenylamine-spirosilabifluorene alternating copolymer: synthesis and optical, electrochemical and electroluminescent properties. *Polymer*, **2005**, *46*, 5707-5713.

[7] Zhou, Q.; Swager, T. M. Fluorescent chemosensors based on energy migration in conjugated polymers: the molecular wire approach to increased sensitivity. *J. Am. Chem. Soc.*, **1995**, *117*(50), 12593-12602.

[8] Anslyn, E. V.; Dougherty, D. A. Experiments related to the thermodynamics and kinetics. *Modern physical organic chemistry*; University Science Books, 2004; p 446.

[9] Zucchero, A. J.; Mcgrier, P. L.; Bunz, U. H. F. Cross-conjugated cruciform fluorophores. *Acc. Chem. Res.*, **2010**, *43*(3): 397-408.

[10] Zhao, Y.-H.; Pan, H.; Fu, G.-L.; Lin, J.-M.; Zhao, C.-H. A highly emissive cruciform triarylborane as a ratiometric and solid state fluorescence sensor for fluoride ions. *Tetrahedron Lett.*, **2011**, *52*, 3832-3835.

[11] Weider, P. R.; Hegedus, L. S.; Asada, H.; D'Andreq, S. V. Oxidative cyclization of unsaturated aminoquinones. Synthesis of quinolinoquinones. Palladium-catalyzed synthesis of pyrroloindoloquinones. *J. Org. Chem.* **1985**, *50*(22), 4276-4281.

[12] Tilford, R. W. Self-assembled cross-linked poly(boronate ester)s: facile methods for the construction of nanometer-size pores in crystalline and amorphous solides. Ph.D. Thesis, University of South Carolina, Columbia, SC, 2008.

[13] (a) Sun, Y.; Ross, N.; Zhao, S.-B.; Huszarik, K.; Jia, W.-L.; Wang, R.-Y.; Macartney, D.; Wang, S. Enhancing electron accepting ability of triarylboron via π-conjugation with 2,2'-bipy and metal chelation: 5,5'-bis($BMes_2$)-2,2'-bipy and its metal complexes. *J. Am. Chem. Soc.*, **2007**, *129*(24), 7510-7511. (b) Sun, Y.; Wang, S. Conjugated triarylboryl donor-acceptor systems supported by 2,2'-bipyridine: metal chelation impact on intraligand charge transfer emission, electron accepting ability, and "turn-on" fluoride sensing. *Inorg. Chem.*, **2009**, *48*(9), 3755-3767.

[14] Wenkert, D.; Woodward, R. B. Studies of 2,2'-bipyridyl N,N'-dioxides. *J. Org. Chem.*, **1983**, *48*(3), 283-289.

[15] Mizuno, T.; Takeuchi, M.; Hamachi, I.; Nakashima, K.; Shinkai, S. *J. Chem. Soc., Perkin Trans. 2*, **1998**, 2281-2288.

BIBLIOGRAPHY

Absorption titration worksheet (guest:host of 2:1) was used, with permission of Dr. Ken D. Shimizu in University of South Carolina, Columbia. The worksheet was found at http://www.chem.sc.edu/faculty/shimizu/Site/Group%20Stuff.html.

Anslyn, E. V.; Dougherty, D. A. Solutions and non-covalent binding forces. *Modern physical organic chemistry*; University Science Books, 2004; p 147.

Arimori, S.; Davidson, M. G.; Fyles, T. M.; Hibbert, T. G.; James, T. D.; Kociok-Köhn, G. I. Synthesis and structural characterization of the first bis(bora)calixarene: a selective, bidentate, fluorescent fluoride sensor. *Chem. Commun.*, **2004**, 1640-1641.

Bai, D.-R.; Liu, X.-Y.; Wang, S. Charge-transfer emission involving three-coordinate organoboron: V-shape versus U-shape and impact of the spacer on dual emission and fluorescent sensing. *Chem. Eur. J.*, **2007**, *13*, 5713-5723.

Beebe, K. R.; Pell, R. J.; Seasholtz, M. B. *Chemometrics: A Practical Guide*, Wiley, 1998.

Bonifácio, V. D. B.; Morgado, J.; Scherf, U. Polyfluorenes with on-chain dibenzoborole units-synthesis and anion-induced photoluminescence quenching. *J. Polym. Sci., Part A: Polym. Chem.*, **2008**, *46*, 2878-2883.

Brombosz, S. M.; Zucchero, A. J.; Phillips, R. L.; Vazquez, D.; Wilson, A.; Bunz, U. H. F. Terpyridine-based cruciform-Zn^{2+} complexes as anion-responsive fluorophores. *Org. Lett.*, **2007**, *9*(22), 4519-4522.

Cai, M.; Daniel, S. L.; Lavigne, J. J. Conjugated bis and poly(dioxaborole)s for optical sensing of Lewis bases based on main-chain perturbations. *Chem. Commun.*, **2013**, *49*, 6504-6506.

Cao, D.; Liu, Z.; Zhang, G.; Li, G. The synthesis, photophysical properties and fluoride anion recognition of a novel branched organoboron compound. *Dyes Pigm.*, **2009**, *81*, 193-196.

Carroll, C. N.; Coombs, B. A.; McClintock, S. P.; Johnson II, C. A.; Berryman, O. B.; Johnson, D. W.; Haley, M. M. Anion-dependent fluorescence in bis(anilinoethynyl)pyridine derivatives: switchable ON-OFF and OFF-ON responses. *Chem. Commun.*, **2011**, *47*, 5539-5541.

Christinat, N.; Croisier, E.; Scopelliti, R.; Cascella, M.; Röthlisberger, U.; Severin, K. Formation of boronate ester polymers with efficient intrastrand charge-transfer transitions by three-component reactions. *Eur. J. Inorg. Chem.*, **2007**, 5177-5181.

Côté, A. P.; Benin, A. I.; Ockwig, N. W.; Matzger, A. J.; O'Keeffe, M.; Yaghi, O. M. Porous, crystalline, covalent organic frameworks, *Science*, **2005**, *310*, 1166-1170.

Davey, E. A.; Zucchero, A. J.; Trapp, O.; Bunz, U. H. F. Discrimination of organic acids using a three molecule array based upon cruciform fluorophores. *J. Am. Chem. Soc.*, **2011**, *133*, 7716-7718.

Dong, D. C.; Winnik, M. A. The Py scale of solvent polarities. *Can. J. Chem.*, **1984**, *62*, 2560-2565.

Feng, L.; Li, H.; Li, X.; Chen, L.; Shen, Z.; Guan, Y. Colorimetric sensing of anions in water using ratiometric indicator-displacement assay. *Anal. Chim. Acta*, **2012**, *743*, 1-8.

Galbraith, E.; James, T. D. Boron based anion receptors as sensor. *Chem. Soc. Rev.*, **2010**, *39*, 3831-3842.

Hall, H. K., Jr. Correlation of the base strengths of amines. *J. Am. Chem. Soc.*, **1957**, *79*(20), 5441-5444.

Hargrove, A. E.; Zhong, Z.; Sessler, J. L.; Anslyn, E. V. Algorithms for the determination of binding constants and enantiomeric excess in complex host:guest equilibria using optical measurements. *New J. Chem.*, **2010**, *34*, 348-354.

Hauck, M.; Schönhaber, J.; Zucchero, A. J.; Hardcastle, K. I.; Müller, T. J. J.; Bunz, U. H. F. Phenothiazine cruciforms: synthesis and metallochromic properties. *J. Org. Chem.*, **2007**, *72*(18), 6714-6725.

Hudnall, T. W.; Chiu, C.-W.; Gabbai, F. P. Fluoride ion recognition by chelating and cationic boranes. *Acc. Chem. Res.*, **2009**, *42*(2): 388-397.

Hudson, Z. M.; Wang, S. Impact of donor-acceptor geometry and metal chelation on photophysical properties and applications of triarylboranes. *Acc. Chem. Res.*, **2009**, *42*(10): 1584-1596.

Hudson, Z. M.; Wang, S. Metal-containing triarylboron compounds for optoelectronic applications. *Dalton Trans.*, **2011**, *40*: 7805-7816.

Hulanicki, A.; Glab, S.; Ingman, F. Chemical sensors definitions and classification. *Pure & App. Chem.*, **1991**, *63* (9), 1247-1250.

Jäkle, F. Advances in the synthesis of organoborane polymers for optical, electronic, and sensory applications. *Chem. Rev.*, **2010**, *110*(7), 3985-4022.

Jia, W. L.; Feng, X. Dong.; Bai, D. R.; Lu, Z. H.; Wang, S.; Vamvounis, G. Mes_2B(*p*-4,4'-biphenyl-NPh(1-naphthyl)): a multifunctional molecule for electroluminescent devices. *Chem. Mater.*, **2005**, *17*(1), 164-170.

Kabalka, G. W.; Reddy, N. K.; Narayana, C. Sodium percarbonate: a convenient reagent for the Dakin reaction. *Tetrahedron Lett.* **1992**, *33*, 865-866.

Kamlet, M. J.; Abboud, J. L.; Taft, R. W. The solvatochromic comparison method. 6. The π* scale of solvent polarities. *J. Am. Chem. Soc*., **1977**, *99*(18): 6027-6038.

Kubo, Y.; Yamamoto, M.; Ikeda, M.; Takeuchi, M.; Shinkai, S.; Yamaguchi, S.; Tamao, K. A colorimetric and ratiometric fluorescent chemosensor with three emission changes: fluoride ion sensing by a triarylborane-porphyrin conjugate. *Angew. Chem. Int. Ed.*, **2003**, *42*, 2036-2040.

Lanni, L. M.; Tilford, R. W.; Bharathy, M.; Lavigne J. J. Enhanced hydrolytic stability of self-assembling alkylated 2-dimensional covalent organic frameworks. *J. Am. Chem. Soc*. **2011**, *133(35)*, 13975-13983.

Lavigne, J. J. Molecular recognition and molecular sensing: single analyte analysis and multi-component sensor arrays for the simultaneous detection of a plethora of analytes. Ph.D. Thesis, The University of Texas at Austin, Austin, TX, August 2000.

Lee, J. W.; Lee, J.-S.; Kang, M.; Su, A. I.; Chang, Y.-T. Visual artificial tongue for quantitative metal-cation analysis by an off-the-shelf dye array. *Chem. Eur. J.*, **2006**, *12*, 5691-5696.

Lee, K.; Povlich, L. K.; Kim, J. Recent advances in fluorescent and colorimetric conjugated polymer-based biosensors. *Analyst*, **2010**, *135*, 2179-2189.

Li, H.; Jäkle, F. Donor-π-acceptor polymer with alternating triarylborane and triphenylamine moieties. *Macromol. Rapid Commun.*, **2010**, 915-920.

Li, H.; Jäkle, F. Universal scaffold for fluorescent conjugated organoborane polymers. *Angew. Chem., Int. Ed*., **2009**, *48*, 2313-2316.

Li, J.; Zhang, G.; Zhang, D.; Zheng, R.; Shi, Q.; Zhu, D. Boron-containing monopyrrolo-annelated tetratriafulvalene compounds: synthesis and absorption spectral/electrochemical responsiveness toward fluoride ion. *J. Org. Chem.*, **2010**, *75*(15), 5330-5333.

Li, X. Development of conjugated boronate ester-linked materials for optical sensing applications targeting small molecules. Ph.D. Thesis, University of South Carolina, Columbia, SC, 2012.

Lim, J.; Nam, D.; Miljanić, O. Š. Identification of carboxylic and organoboronic acids and phenols with a single benzobisoxazole fluorophore. *Chem. Sci.*, **2012**, *3*, 559-563.
Liu, W.; Pink, M.; Lee, D. Conjugated polymer sensors built on π-extended borasiloxane cages. *J. Am. Chem. Soc.*, **2009**, *131*(24), 8703-8707.

Liu, X. Y.; Bai, D. R.; Wang, S. Charge-transfer emission in nonplanar three-coordinate organoboron compounds for fluorescent sensing of fluoride. *Angew. Chem. Int. Ed.*, **2006**, *45*, 5475-5478.

Liu, Y.; Ogawa, K.; Schanze K. S. Conjugated polyelectrolytes as fluorescent sensors. *J. Photochem. Photobiol. C: Photochem. Rev.*, **2009**, *10*, 173-190.

Liu, Z.-Q.; Shi, M.; Li, F.-Y.; Fang, Q.; Chen, Z.-H.; Yi, T.; Huang, C.-H. Highly selective two-photon chemosensor for fluoride derived from organic boranes. *Org. Lett.*, **2005**, *7*(24), 5481-5484.

Maly, K. E.; Maris, T; and Wuest, J. D. Two-dimensional hydrogen-bonded networks in crystals of diboronic acids. *CrystEngComm*, **2006**, *8*, 33-35.

Maynor, M. S.; Deason, T. K.; Nelson, T. L.; Lavigne, J. J. Multidimensional response analysis towards the detection and identification of soft divalent metal ions. *Supramolecular Chemistry*, **2009**, *21*(3-4), 310-315.

Maynor, M. S.; Nelson, T. L.; O'Sullivan C.; Lavigne, J. J. A food freshness sensor using the multistate response from analyte-induced aggregation of a cross-reactive poly(thiophene). *Org. Lett.*, **2007**, *9*(17), 3217-3220.

McDonagh, C.; Burke, C. S.; MacCraith B. D. Optical chemical sensors. *Chem. Rev.*, **2008**, *108* (2), 400-422.

McGrier, P. L.; Solntsev, K. M.; Miao, S.; Tolbert, L. M.; Miranda, O. R.; Rotello, V. M.; Bunz, U. H. F. Hydroxycruciforms: amine-responsive fluorophores. *Chem. Eur. J.*, **2008**, *14*, 4503-4510.

McGrier, P. L.; Solntsev, K. M.; Schönhaber, J.; Brombosz, S. M.; Tolbert, L. M.; Bunz, U. H. F. Hydroxy-cruciforms. *Chem. Commun.*, **2007**, 2127-2129.

Miyata, M.; Chujo, Y. π-Conjugated organoboron polymer as an anion sensor. *Polym. J.*, **2002**, *34*(12), 967-969.

Mizuno, T.; Takeuchi, M.; Hamachi, I.; Nakashima, K.; Shinkai, S. *J. Chem. Soc., Perkin Trans. 2*, **1998**, 2281-2288.

Mohammed, O. F.; Vauthey, E. Excited-state dynamics of nitroperylene in solution: solvent and excitation wavelength dependence. *J. Phy. Chem. A.* **2008,** *112*(17), 3823-3830.

Mou, X.; Liu, S. J.; Dai, C. L.; Ma, T. C.; Zhao, Q.; Ling, Q. D.; Huang, W. A class of fascinating optoelectronic materials: triarylboron compounds. *Sci. China Chem.*, **2010**, *53*(6): 1235-1245.

Nelson, T. L.; O'Sullivan C.; Greene, N. T.; Maynor, M. S.; Lavigne, J. J. Cross-reactive conjugated polymers: analyte-specific aggregative response for structurally similar diamines. *J. Am. Chem. Soc.*, **2006**, *128*(17), 5640-5641.

Nelson, T. L.; Tran, I.; Ingallinera, T. G.; Maynor, M. S.; Lavigne, J. J. Multi-layered analyses using directed partitioning to identify and discriminate between biogenic amines. *Analyst*, **2007**, *132*, 1024-1030.

Neumann, T.; Dienes, Y.; Baumgartner, T. Highly sensitive sensory materials for fluoride ions based on the dithieno[3,2-b:2',3'-d]phosphole system. *Org. Lett.*, **2006**, *8*(3), 495-497.

Nishiyabu, R.; Palacios, M. A.; Dehaen, W.; Anzenbacher, Jr. P. Synthesis, structure, anion binding, and sensing by calix[4]pyrrole isomers. *J. Am. Chem. Soc.*, **2006**, *128*, 11496-11504.

Niu, W.; O'Sullivan, C.; Rambo, B. M.; Smith, M. D.; Lavigne, J. J. Self-repairing polymers: poly(dioxaborole)s containing trigonal planar boron. *Chem. Commun.*, **2005**, 4342-4344.

Niu, W.; Rambo, B. M.; Smith, M. D.; Lavigne, J. J., Self-assembling polymeric and oligomeric borole materials. *Polym. Mater. Sci. Eng.* **2005**, *91*, 147-148.

Niu, W.; Smith, M. D.; Lavigne, J. J. Self-assembling poly(dioxaborole)s as blue-emissive materials. *J. Am. Chem. Soc.*, **2006**, *128*(51), 16466-16467.

Niu, W. J.; Rambo, B.; Smith, M. D.; Lavigne, J. J., Substituent effects on the structure and supramolecular assembly of bis(dioxaborole)s. *Chem. Commun.* **2005**, (41), 5166-5168.

Niu, W. J.; Smith, M. D.; Lavigne, J. J., Substituent effects on the structure and supramolecular assembly of bis(dioxaborole)s derived from 1,2,4,5-tetrahydroxybenzene. *Cryst. Growth & Des.* **2006**, *6*(6), 1274-1277.

Pan, H.; Fu, G.-L.; Zhao, Y.-H.; Zhao, C.-H. Through-space charge-transfer emitting biphenyls containing a boryl and an amino group at the o,o'-positions. *Org. Lett.*, **2011**, *13*(18), 4830-4833.

Rambo, B. M.; Lavigne, J. J., Defining self-assembling linear oligo(dioxaborole)s. *Chem. Mater.* **2007**, *19*(15), 3732-3739.

Reichardt, C. Solvatochromic dyes as solvent polarity indicators. *Chem. Rev.*, **1994**, *94*, 2319-2358.

Sanchez, J. C.; Trogler, W. C. Polymerization of a boronate-functionalized fluorophore by double transferification: applications to fluorescence detection of hydrogen peroxide vapor. *J. Mater. Chem.*, **2008**, *18*, 5134-5141.

See Chapter 2 for details.

Severin, K. Boronic acids as building blocks for molecular nanostructures and polymeric materials. *Dalton Trans.*, **2009**, 5254-5264.

Sheriff, T. S. Production of hydrogen peroxide from dioxygen and hydroxylamine or hydrazine catalysed by manganese complexes. *J. Chem. Soc. Dalton Trans.*, **1992**, 1051-1058.

Silverstein, R. M.; Webster, F. X.; Kiemle D. J. Infrared spectrometry. *Spectrometric identification of organic compounds*, 7th ed.; Wiley & Sons: Hoboken, NJ, 2005; p 101.

SMART Version 5.630, SAINT+ Version 6.45. Bruker Analytical X-ray Systems, Inc., Madison, Wisconsin, USA, 2003. (b) Sheldrick, G. M. A short history of SHELX. *Acta Cryst.*, **2008**, *A64*, 112-122.

Sundararaman, A.; Victor, M.; Varughese, R.; Jäkle, F. A family of main-chain polymeric Lewis acids: synthesis and fluorescent sensing properties of boron-modified polythiophene. *J. Am. Chem. Soc.*, **2005**, *127*(40), 13748-13749.

Sun, Y.; Ross, N.; Zhao, S.-B.; Huszarik, K.; Jia, W.-L.; Wang, R.-Y.; Macartney, D.; Wang, S. Enhancing electron accepting ability of triarylboron via π-conjugation with 2,2'-bipy and metal chelation: 5,5'-bis($BMes_2$)-2,2'-bipy and its metal complexes. *J. Am. Chem. Soc.*, **2007**, *129*(24), 7510-7511.

Sun, Y.; Wang, S. Conjugated triarylboryl donor-acceptor systems supported by 2,2'-bipyridine: metal chelation impact on intraligand charge transfer emission, electron accepting ability, and "turn-on" fluoride sensing. *Inorg. Chem.*, **2009**, *48*(9), 3755-3767.

Thomas III, S. W.; Joly, G. D.; Swager, T. M. Chemical sensors based on amplifying fluorescent conjugated polymers. *Chem. Rev.*, **2007**, *107* (4), 1339-1386.

Tilford, R. W.; Gemmill, W. R.; zur Loye, H.-C.; Lavigne, J. J. Facile synthesis of a highly crystalline, covalently linked porous boronate network. *Chem. Mater.*, **2006**, *18*(22), 5296-5301.

Tolosa, J.; Zucchero, A. J.; Bunz, U. H. F. Water-soluble cruciforms: response to protons and selected metal ions. *J. Am. Chem. Soc.*, **2008**, *130*(20), 6498-6506.

Vlasov, Yu. G.; Ermolenko, Yu. E.; Legin, A. V.; Rudnitskaya, A. M.; Kolodnikov,V. V. Chemical sensors and their systems. *J. Anal. Chem.*, **2010**, *65* (9), 880–898.

Wade, C. R.; Broomsgrove, A. E. J.; Aldridge, S.; Gabbai, F. P. Fluoride ion complexation and sensing using organoboron compounds. *Chem. Rev.*, **2010**, *110*(7), 3958-3984.

Wang, B.; Wasielewski, M. R. Design and synthesis of metal ion-recognition-induced conjugated polymers: an approach to metal ion sensory materials. *J. Am. Chem. Soc.*, **1997**, *119*(1), 12-21.

Weider, P. R.; Hegedus, L. S.; Asada, H.; D'Andreq, S. V. Oxidative cyclization of unsaturated aminoquinones. Synthesis of quinolinoquinones. Palladium-catalyzed synthesis of pyrroloindoloquinones. *J. Org. Chem.*, **1985**, *50*(22), 4276-4281.

Wenkert, D.; Woodward, R. B. Studies of 2,2'-bipyridyl N,N'-dioxides. *J. Org. Chem.*, **1983**, *48*(3), 283-289.

Wilson, J. N.; Bunz, U. H. F. Switching of intramolecular charge transfer in cruciforms: metal ion sensing, *J. Am. Chem. Soc.*, **2005**, *127*(12), 4124-4125.

Xiao, H.; Leng, B.; Tian, H. Hole transport triphenylamine-spirosilabifluorene alternating copolymer: synthesis and optical, electrochemical and electroluminescent properties. *Polymer*, **2005**, *46*, 5707-5713.

Yamaguchi, I.; Choi, B.-J.; Koizumi, T.; Kubota, K.; Yamamoto, T. π-Conjugated polyphenylenes with diazaborole side chains synthesized via 1,2-phenylenediamine polymer. *Macromolecules*, **2007**, *40*, 438-443.

Yamaguchi, S.; Akiyama, S.; Tamao, K. Colorimetric fluoride ion sensing by boron-containing π-electron systems. *J. Am. Chem. Soc.*, **2001**, *123*(46), 11372-11375.

Yamaguchi, S.; Akiyama, S.; Tamao, K. Tri-9-anthrylborane and its derivatives: new boron-containing π-electron systems with divergently extended π-conjugation through boron. *J. Am. Chem. Soc.*, **2000**, *122*(26), 6335-6336.

Yoon, J.; Czarnik, A. W. Fluorescent chemosensors of carbohydrates, a means of chemically communicating the binding of polyols in water based on chelation-enhanced quenching. *J. Am. Chem. Soc.*, **1992**, *114*, 5874-5875.

Yuan, M. J.; Li, Y. J.; Liu, H. B.; Li, Y. L. Chemical sensors based on π-conjugated organic molecules and gold nanoparticles. *Sci. China Ser. B Chem.*, **2009**, *52* (6), 715-730.

Zengin, H.; Zengin, G.; Smith, D. W. *J. Polym. Sci. Part A: Polym. Chem.*, **2006**, *44*, 6988.

Zhao, Y.-H.; Pan, H.; Fu, G.-L.; Lin, J.-M.; Zhao, C.-H. A highly emissive cruciform triarylborane as a ratiometric and solid state fluorescence sensor for fluoride ions. *Tetrahedron Lett.*, **2011**, *52*, 3832-3835.

Zhou, G.; Baumgarten, M.; Müllen, K. Mesitylboron-substituted ladder-type pentaphenylenes: charge-transfer, electronic communication, and sensing properties. *J. Am. Chem. Soc.*, **2008**, *130*(37), 12477-12484.

Zhou, Q.; Swager, T. M. Fluorescent chemosensors based on energy migration in conjugated polymers: the molecular wire approach to increased sensitivity. *J. Am. Chem. Soc.*, **1995**, *117*(50), 12593-12602.

Zucchero, A. J.; Mcgrier, P. L.; Bunz, U. H. F. Cross-conjugated cruciform fluorophores. *Acc. Chem. Res.*, **2010**, *43*(3): 397-408.

Zucchero, A. J.; Wilson, J. N.; Bunz, U. H. F. Cruciforms as functional fluorophores: response to protons and selected metal ions. *J. Am. Chem. Soc.*, **2006**, *128*(36), 11872-11881.